

DISS. ETH NO. 16838

**PREDICTING THE CONSEQUENCES OF RIVER
REHABILITATION MEASURES ON MORPHOLOGY,
HYDRAULICS, PERIPHYTON AND ON INVERTEBRATES**

A dissertation submitted to the
Swiss Federal Institute of Technology ZÜRICH (ETHZ)

for the degree of
Doctor of Sciences

presented by

STEFFEN PATRICK SCHWEIZER
Masters of Geoecology, Technical University of Karlsruhe (Germany)
Bachelor of Hydrology, University of Freiburg (Germany)

born 11.01.1973
citizen of Germany

accepted on the recommendation of

Prof. Dr. Peter Reichert, examiner
Prof. Dr. Mark Borsuk, co-examiner
Dr. habil. Nicolas Lamouroux
Prof. Dr. Bernhard Wehrli, co-examiner

Zürich, Switzerland 2007

Contents

1	INTRODUCTION	10
1.1	Background and Motivation	10
1.2	Goals and Research Questions.....	11
1.3	Contents and Structure of the Thesis	12
1.4	References.....	12
2	PREDICTING JOINT FREQUENCY DISTRIBUTIONS OF DEPTH AND VELOCITY FOR INSTREAM HABITAT ASSESSMENT	14
2.1	Abstract.....	14
2.2	Introduction.....	15
2.3	Methods.....	18
2.3.1	Data Description	18
2.3.2	Modeling.....	20
2.4	Results.....	24
2.4.1	Distributional Parameter Estimates.....	24
2.4.2	Predicting the Mixture Parameter.....	28
2.5	Discussion.....	31
2.6	Conclusions.....	35
2.7	References.....	37
3	PREDICTING THE MORPHOLOGICAL AND HYDRAULIC CONSEQUENCES OF RIVER REHABILITATION	41
3.1	Abstract.....	41
3.2	Introduction.....	42
3.3	Model Description	44
3.3.1	Channel Morphology	45
3.3.1.1	Natural Morphology.....	47
3.3.1.2	Width-Constrained Morphology Assuming Sufficient Gravel Supply.....	48
3.3.1.3	Final Width-Constrained Morphology under Actual Gravel Supply....	50
3.3.2	Flooding.....	52
3.3.3	Velocity and Depth Distribution.....	53
3.3.4	Riverbed Siltation	55
3.3.5	Model Implementation.....	57
3.4	A Case Study.....	59
3.4.1	Inputs.....	59
3.4.2	Results.....	61
3.5	Discussion and Conclusions	67
3.6	References.....	70
4	PREDICTING THE BIOMASS OF PERIPHYTON AND MACROINVERTEBRATE FUNCTIONAL FEEDING GROUPS IN STREAM REACHES	74
4.1	Abstract.....	74
4.2	Introduction.....	75
4.3	Study Sites and Data.....	78

4.4	Modelling Methods	82
4.4.1	Preliminary Analysis of the Significance of Influence Factors	82
4.4.2	Formulation of Nonlinear Model	83
4.4.3	Parameter Estimation	85
4.4.4	Sensitivity Analysis	86
4.4.5	Model Structure Selection.....	86
4.4.6	Uncertainty Analysis.....	86
4.5	Results.....	87
4.6	Discussion.....	94
4.7	Summary and Conclusions	96
4.8	References.....	98
4.9	Appendix.....	101
5	GENERAL DISCUSSION	103
5.1	The hydraulic-morphological submodel.....	103
5.2	The benthic submodel.....	108
5.3	The IRRM.....	111
5.4	Future Research Questions	113
5.5	References.....	114
	Acknowledgements.....	118

Summary

Decisions about reach-scale river rehabilitation for the purposes of flood protection and ecological enhancement require prediction of the possible consequences of management alternatives. To provide such predictions, an integrative river rehabilitation model is necessary that represents the principal cause-effect relations between rehabilitation options and morphological, hydraulic, and ecological consequences. In 2000, the interdisciplinary “Rhone/Thur River Rehabilitation Project” was initiated to improve the understanding of the ecological and socio-economic consequences of river rehabilitation projects and to supply advice for future efforts. One subproject of this research program is the development of an integrative river rehabilitation model (IRRM) to predict the hydraulic-morphological situation after river management actions and the resulting changes in the terrestrial and aquatic ecosystems. The focus is on reach-scale rehabilitation actions that primarily involve widening the stream corridor and allowing the river to take a more natural course. Therefore, the primary decision is how much space to give the river so that an optimal trade-off between benefits and costs is obtained. Although developed for Midland rivers in Switzerland, the IRRM is intended to be as generally applicable as possible by using quantities that are either readily available or easily predictable even for a changed channel morphology.

The development of an integrative model usually requires scientific knowledge in a variety of forms including literature review, experimental and field results, other models, and, in the absence of other information, expert judgment. Implementing the IRRM as a probability network makes it relatively simple to combine different sources of information to represent cause-effect relations, to simultaneously consider different spatial and temporal scales, and to explicitly include uncertainties in model inputs, structure and outcomes.

Within this thesis the hydraulic-morphological sub-model (I) and the benthic sub-model (II) of the IRRM have been developed. Other sub-models describing fish, riparian vegetation, shoreline fauna and economics are being developed and reported separately by the Eawag-SIAM research group.

Because all biotic endpoints of interest are influenced by hydraulics and river morphology, sub-model I is focused on predicting variables that are required as inputs for the economic and biotic sub-models (riparian vegetation and fauna, Benthos, Fish). This sub-model I is further subdivided into four modules predicting: (1) channel morphology, (2) flooding (dike overtopping, floodplain flooding, and bed moving floods), (3) bivariate (joint) velocity and depth distribution, and (4) riverbed siltation.

For the modules (2) and (4) the major task was to compile results provided in the literature, estimate input and model structural uncertainty, and integrate the resulting model formulations in the probability network.

The prediction of channel morphology (module 1) is based on published formulae to determine the river form with and without width constraints. To identify possible width constraints an additional data analyses on 127 unconstrained gravel-bed rivers has been conducted to estimate a river's natural (unconstrained) width. Finally the gravel budget is considered in the model. The model presented in this thesis combines all key factors controlling channel morphology.

For module (3) work on univariate velocity and depth distributions was found in the literature, as well as indication of the ecological significance of the joint distribution. A derivation of a joint distribution (for a changed channel geometry) could, however, not be found. To close this gap, velocity-depth data from 92 relatively natural stream reaches in New Zealand and from 5 channelized Swiss river reaches was analyzed and a bivariate distribution could be found that describes these observations. For each reach, the bivariate distribution of relative velocity and relative depth can be described by a mixture of two end-member distributions, one bivariate normal and the other bivariate log-normal, each with fixed parameters. The relative contribution of each shape for a particular reach at a particular discharge can then be related to the reach mean Froude number, the reach mean relative roughness, and the ratio of the survey discharge to the mean discharge which can be easily estimated (even for a changed channel morphology) by applying sub-model I.

Considering all sources of uncertainty (in model inputs and model parameters) explicitly allows us to compute probabilistic model results which support decision making under uncertainty.

An application of the hydraulic morphological sub-model to a reach of the Thur River in Switzerland is described and demonstrates its utility for predicting morphological and hydraulic consequences of a planned river widening: Widening the Thur river from 30m (straight) to 200m will alter the morphology with a probability of 84% (28% probability for a braided form and 56% for the development of alternating gravel bars) and will increase the variability of the bivariate velocity-depth distribution significantly and thus augment habitat variability (rising the proportion of pools and riffles from approximately 5% to 50% at the expense of runs). Increasing the river widths leads generally to lower water depths and thus to a lower frequency of bed moving floods. Hence, a higher mean siltation of the river bed is predicted. However, a widened river is expected to be much more variable with respect to depth (controlling the distribution of bottom shear force) and contains 20 to 30 % more riffles which remain clear of fine particles due to their hydraulic conditions compared to a constrained river. Both of these phenomena will result in a mosaic of silted and clean riverbed sections in a widened river, rather than the spatial uniformity expected for a channelized river.

The second sub-model (II) of the IRRM has been developed to predict the biomass of periphyton and functional feeding groups of invertebrates which play an important role in

lotic ecosystems due to their ability to produce organic material, to decompose detritus and to serve as a food source for higher trophic levels (e.g. fish). To derive the periphyton model, data from 8 sites (3 different rivers, total sample size 286) have been used whereas the development of the invertebrate model is based on data from one river (2 sites, sample size 86). Performing linear and non-linear regression computations revealed that periphyton is most strongly influenced by the time since the last bed-moving flood occurred and from hydraulic conditions (in particular velocity), whereas invertebrate functional groups are predominantly dependent on seasonality. For total invertebrates, collector-gatherers, and predators, regression models could be developed with R^2 values between 0.52 and 0.71. The representation of scrapers was somewhat less satisfying. Shredders and filterers were significantly less abundant in our data set and were therefore not modelled.

Having the diversity of the data sets and the simplicity of the model in mind, the models lead to a remarkably good agreement even with time series of measurements of periphyton, total macrozoobenthos, collector-gatherers and predators. The small number and simple nature of considered influence factors makes the model to a useful tool for predicting the effect of rehabilitation measures on the benthic community. Despite the model was derived with as many data sets as possible (available); a better support by data from additional rivers is necessary to test and improve its universality

The full integrative model (IRRM), including ecological endpoints, shall be used together with quantitative assessments of stakeholder preferences to support rehabilitation decisions for a number of Swiss rivers.

Zusammenfassung

Entscheide über grossräumige Flussrevitalisierungen zur Verbesserung des Hochwasserschutzes und der ökologischen Lebensraumbedingungen erfordern Vorhersagen über die möglichen Konsequenzen verschiedener Alternativen. Dafür ist ein integratives Flussrevitalisierungsmodell nötig, das die wichtigsten Ursache-Wirkungs-Beziehungen von Flussaufweitungen auf die Flussmorphologie, Hydraulik und Ökologie abbildet. Innerhalb des interdisziplinären Forschungsprojekts „Rhone-Thur“ wurde ein solches integratives Flussrevitalisierungsmodell (IFRM) zur Vorhersage der hydraulisch-morphologischen Bedingungen nach einer Aufweitung und den daraus resultierenden Änderungen in den terrestrischen und aquatischen Ökosystemen entwickelt. Das IFRM konzentriert sich dabei auf grossräumige Massnahmen wie Flussaufweitungen, die wieder Raum für einen natürlicheren Flusslauf geben. Dabei ist entscheidend, wie viel Raum (welche Breite) einem Fluss (wieder) gegeben werden soll, um einen optimalen Kompromiss zwischen ökologischen und sozio-ökonomischen Verbesserungen und Kosten zu erreichen. Das IFRM wurde für schweizerische Mittelland-Flüsse entwickelt und als Modelleingabewerte werden nur leicht zugängliche (vor einer Aufweitung) oder auch für eine veränderte Flussmorphologie vorhersagbare Grössen berücksichtigt.

Die Entwicklung eines integrativen Modells basiert in der Regel auf verschiedenen Quellen wissenschaftlicher Erkenntnisse: Publikationen, Labor- und Feldversuche, anderer Modelle und auf die Beurteilung durch Experten. Das IFRM wurde als Wahrscheinlichkeitsnetzwerk implementiert, da dieser Ansatz auf eine relativ einfache Art die Verbindung verschiedener wissenschaftlicher Quellen (i), die simultane Betrachtung verschiedener räumlicher und zeitlicher Skalen (ii) und die explizite Berücksichtigung der Unsicherheit in den Modelleingangsgrössen, der Modellstruktur und den Modellergebnissen (iii) erlaubt.

Innerhalb dieser Doktorarbeit wurden die Teilmodelle „Hydraulik & Morphologie“ (I) und „Benthos“ (II) entwickelt.

Das Teilmodell „Hydraulik & Morphologie (I)“ konzentriert sich dabei auf die Vorhersage von Variablen, die von den biologischen Teilmodellen als Eingangsgrössen benötigt werden. Es ist in vier weitere Module unterteilt, die die sich einstellende Morphologie (1), die Häufigkeiten von Extremereignissen (Aufreissen des Flussbetts, Vorland- und Dammüberflutung) (2), die bivariate (gemeinsame) Verteilung von Fliessgeschwindigkeit und Abflusstiefe (3) sowie die innere Kolmation des Flussbetts (4) prognostizieren.

Die entscheidenden Aufgaben zur Entwicklung der Module (2) und (4) waren eine umfassende Zusammenstellung und Verknüpfung bereits bestehender Ansätze, die Berücksichtigung der Unsicherheit in Modelleingangsgrössen und Modellparametern sowie die Implementierung der Module in einem Wahrscheinlichkeitsnetz.

Für das Modul (3) konnten verschiedene Ansätze, die die univariate Verteilung von Fließgeschwindigkeit oder Abflusstiefe beschreiben, gefunden werden. Allerdings wurde in verschiedenen Publikationen die gemeinsame (bivariate) Verteilung dieser beiden Größen als ökologisch relevant betrachtet. In der wissenschaftlichen Literatur fehlt bisher ein Ansatz, der die bivariate Verteilung von Tiefe und Geschwindigkeit für eine sich ändernde Flussgeometrie (z.B. nach einer Aufweitung) vorhersagt. Um diese Lücke zu schliessen, wurden Geschwindigkeits-Tiefen Daten von 92 relativ natürlichen neuseeländischen Flüssen und von fünf kanalisierten schweizerischen Flüssen analysiert und es konnte eine bivariate Verteilung, die die Messdaten gut beschreibt, hergeleitet werden. Für jeden betrachteten Flussabschnitt kann eine bivariate Verteilung der relativen Geschwindigkeit und Tiefe durch eine Kombination von zwei bivariaten Verteilungen (bivariate Normalverteilung und bivariate Log-Normalverteilung) mit fixen Verteilungsparametern beschrieben werden. Der jeweilige relative Anteil dieser beiden fixen bivariaten Verteilungen kann dann für einen bestimmten Abfluss aus der mittleren Froude Zahl, der mittleren relativen Rauigkeit und dem Verhältnis von aktuellem zu mittlerem Abfluss hergeleitet werden. Diese Größen können mit dem Teilmodell „Hydraulik & Morphologie“ (auch für eine veränderte Flussmorphologie) berechnet werden.

Die Vorhersage der Flussmorphologie (Modul 1) basiert auf veröffentlichten Ansätzen zur Bestimmung der Morphologie mit und ohne seitliche Begrenzungen. Um mögliche seitliche Begrenzungen zu erkennen, wurde eine zusätzliche Datenanalyse von 127 seitlich unbegrenzten (natürlichen) Kiesbettflüsse durchgeführt, womit die natürliche Breite eines Flusses berechnet werden kann. Schliesslich wird auch der Geschiebehalt (Geschiebeeintrag vs. Transportkapazität in einem Flussabschnitt) berücksichtigt. Das in dieser Dissertation präsentierte Modul berücksichtigt alle entscheidenden Einflussfaktoren, die die Flussmorphologie bestimmen.

In einer Fallstudie an der Thur (zwischen Bürglen und Weinfeldern) werden der Einsatz und die Möglichkeiten des hydraulisch-morphologischen Teilmodells demonstriert. Wenn die Thur von aktuell 30m (kanalisiert, gerade) auf 200m aufgeweitet wird, beträgt die Wahrscheinlichkeit für eine Änderung der Flussmorphologie 84% (28% für ein verzweigtes Gerinne, 56% für die Entstehung alternierender Kiesbänke). Dies würde die Variabilität der bivariaten Tiefen-Geschwindigkeits Verteilung und damit die Variabilität benthischer Habitate signifikant erhöhen (der Anteil von „Pools“ und „Riffeln“ würde von 5% (Ist-Zustand) auf 50% ansteigen - auf Kosten der „Runs“). Eine grössere Flussbreite führt allgemein zu niedrigeren Abflusstiefen und daher zu einer verringerten Häufigkeit von bettaufreissenden Hochwässern. Daher ist für eine mögliche Aufweitung eine höhere mittlere Kolmation des Flussbetts (im Vergleich zum Ist-Zustand) prognostiziert. Allerdings kann bei einem aufgeweiteten Fluss eine höhere Variabilität der Abflusstiefe und ein höherer Anteil an Riffeln (20-30%) erwartet werden. Aufgrund ihrer hydraulischen Bedingungen kolmatieren Riffel in der Regel nicht. Dies führt zu

einem Mosaik von kolmatierten und unkolmatierten Bereichen in einem aufgeweiteten Fluss - im Gegensatz zu einem gleichmässig kolmatierten Bett eines kanalisierten Flusses.

Das Teilmodell „Benthos“ (II) wurde entwickelt, um die Entwicklung der Biomasse des Periphytons (Algen) und der funktionellen Ernährungsgruppen der Wirbellosen vorherzusagen. Diese spielen eine wichtige Rolle in Fließgewässern, da sie Nährstoffe aus der fließenden Welle und dem Sediment aufnehmen und daraus lebende organische Substanz bilden, abgestorbenes organisches Material wieder abbauen und als Futter für höhere trophische Stufen (z.B. Fische) dienen. Zur Entwicklung des Periphyton Modells wurden Daten von 8 unterschiedlichen Stellen (an 3 verschiedenen Flüssen, Gesamtprobenzahl = 286) verwendet, für das Invertebratenmodell zwei Stellen von einem Fluss (n=86). Lineare und nicht-lineare Regressionsrechnungen zeigen, dass die Algenbiomasse massgeblich von der Zeit seit dem letzten bettaufreissenden Hochwasser und von hydraulischen Bedingungen (v.a. Fließgeschwindigkeit) bestimmt wird. Saisonale Effekte bestimmen massgeblich die Gesamtbiomasse der Invertebraten und ihrer Ernährungsgruppen. Während für die Gesamtbiomasse der Invertebraten sowie für die Biomasse der Sammler und der Räuber gute Regressionsmodelle mit R^2 zwischen 0.52 und 0.71 entwickelt werden können, erzielen die besten Modelle für Weidegänger $R^2 = 0.31$. Die Ernährungsgruppen der Zerkleinerer und Filterer wurden aufgrund sehr geringer Biomassen in den Datensätzen nicht modelliert.

Die Modellentwicklung und -komplexität werden durch die relativ kleine Anzahl an kompletten Datensätzen limitiert. Zusätzliche Datensätze mit längeren Zeitreihen der Biomassen von Algen und Wirbellosen sowie Daten über die entscheidenden Einflussfaktoren wären für die Weiterentwicklung dieser einfachen Modelle äusserst hilfreich.

Das fertig gestellte IFRM soll gemeinsam mit einer quantitativen Abschätzung der Präferenzen aller Interessensvertreter (stakeholder) den Prozess der Entscheidungsfindung bei Flussrevitalisierungen unterstützen.

1 INTRODUCTION

1.1 Background and Motivation

In the last 200 years, many river systems throughout the world have been regulated and channelized (Petts, 1989). These alterations have been conducted mainly to extend agricultural and urban areas, enable or facilitate river navigation, and reduce flooding risk. This has resulted in a dramatic reduction of river floodplain area and loss of hydraulic and morphological variability (Ward et al, 2001). These changes decrease the habitat quality for organisms living in or near a regulated river. Thus, the abundance, biomass and diversity of aquatic and terrestrial organisms are affected, leading to a functional alteration of the river ecosystem (Peter, 1998).

In Switzerland, only about 10% of all rivers remain in a natural or near natural state (BUWAL, 1997). Therefore, there is a need for ecological rehabilitation. Although historically most funding for river construction has been granted for the purposes of additional flood control, a recent federal requirement to include ecological rehabilitation measures in flood control projects has provided new opportunities (Peter et al, 2005).

To improve the understanding of the ecological and socio-economic consequences of river rehabilitation projects and provide advice for future efforts, the interdisciplinary “Rhone/Thur River Rehabilitation Project” was recently initiated (Peter et al., 2005, <http://www.rivermanagement.ch>). One subproject of this research program is the development of an integrative river rehabilitation model (IRRM) to predict the hydraulic-morphological situation after river management actions and the resulting changes in the terrestrial (shoreline fauna and riparian vegetation) and aquatic ecosystems (algae, invertebrates, fish). The focus is on reach-scale rehabilitation actions that primarily involve widening the stream corridor and allowing the river to take a more natural course. Therefore, the primary decision is how much space to give the river so that an optimal trade-off between benefits and costs is obtained. Although developed to apply for Swiss mid-land rivers, the model is intended to be as generally applicable as possible.

The development of an integrative model usually requires scientific knowledge in a variety of forms including literature review, experimental and field results, other models, and, in the absence of other information, expert judgment. Implementing the IRRM as a probability network (Pearl, 1988) makes it relatively simple to combine different sources of information to represent cause-effect relations, to simultaneously consider different spatial and temporal scales, and to explicitly include uncertainties in model inputs, structure (model parameters) and outcomes.

The IRRM represents the relevant cause-effect-relations within and among the important biotic and abiotic factors, leading to attributes (model endpoints) of concern to river system stakeholders. Together with a model of the preference structure for different levels of these attributes (Hostmann et al, 2005), the IRRM is intended to provide a comprehensive basis for supporting river rehabilitation decisions (Reichert et al., 2007).

The IRRM comprises of the six sub-models Hydraulics & Morphology (I), Benthos (II), Fish (III) (Borsuk et al 2006), Riparian Vegetation (IV), Shoreline Fauna (V) and Economics (VI) (Spörri et al 2006) which are linked within the IRRM (e.g., total invertebrate biomass is an input to the fish sub-model; see also Fig.3.1, chapter 3). The sub-model Hydraulics & Morphology (I), which has an influence on all other sub-models as well as the Benthos sub-model (II) have been developed within this dissertation while the other sub-models are being developed and reported separately by this research group (Eawag-SIAM).

1.2 Goals and Research Questions

The first goal of this dissertation was to develop the overall structure of an integrative river rehabilitation model (IRRM) accounting for all relevant cause-effect relations within and among the important biotic and abiotic factors (Fig. 3.1, chapter 3). After the IRRM was subdivided into six sub-models, it was decided that within this dissertation the two sub-models “Hydraulics & Morphology” (I) and “Benthos” (II) were to be developed.

A second goal was to combine as much information as possible from all sources (literature review, experimental and field results, other models, expert judgment and new data evaluations) into the quantification of morphological, hydraulic and benthic development.

As a third goal, the model formulation should contain explicit description and quantification of the uncertainty in model inputs, structure and predictions.

The fourth goal was to apply the model to a reach of the Thur River (between the towns of Bürglen and Weinfelden) to test its usefulness as a contribution to river rehabilitation decision support.

Within this dissertation the major research questions are:

- How can the different approaches to determine channel morphology and river hydraulics be combined accounting for different temporal and spatial scales and including uncertainty estimates of model predictions?

- Which knowledge gaps for ecology-relevant hydraulic-morphological river modelling exist and how can they be closed?
- How can we estimate the biomass of functional feeding groups of the benthic community based on simple indicators applying external influence factors and considering uncertainty in model inputs and structure?
- How can hydraulic-morphological and benthic river community models be combined to form part of an integrated river rehabilitation model?

1.3 Contents and Structure of the Thesis

This thesis consists of three main sections describing

- the approach to predicting the bivariate distribution of flow velocity and water depth (chapter 2)
- the hydraulic-morphological sub-model (chapter 3)
- the periphyton and invertebrate models (chapter 4)

These sections are followed by a general discussion of the overall model.

1.4 References

- Borsuk M E, Reichert P, Peter A, Schager E, Burkhardt-Holm P. 2006. Assessing the decline of brown trout (*Salmo trutta*) in Swiss rivers using a Bayesian probability network. *Ecological Modelling* **192**: 224-244.
- BUWAL (Swiss Agency for the Environment, Forests and Landscape). 1997. *Umwelt in der Schweiz (The Environment of Switzerland)*. Bern, Switzerland.
- Hostmann M, Borsuk M, Reichert P, Truffer B. 2005. Stakeholder values in decision support for river rehabilitation. *Large Rivers* **15(1-4) Arch.Hydrobiol.Suppl.155/1-4**, P. 491-505.
- Pearl J. 1988. *Probabilistic Reasoning in Intelligent Systems*. Morgan Kaufmann, San Mateo, CA,.

- Peter A. 1998. Interruption of the river continuum by barriers and the consequences for migratory fish. - In: Jungwirth M, Schmutz S & Weiss S (eds.): *Fish migration and fish bypasses*: 99-112. Fishing News Books, Oxford.
- Peter A, Kienast F, and Nutter S. 2005. The Rhone-Thur River project: a comprehensive river rehabilitation project in Switzerland. *Large Rivers* **15**: 643-656.
- Petts G E. 1989. Perspectives for ecological management of regulated rivers. In: Gore J A & Petts G E (Editors), *Alternatives in Regulated River Management*. CRC Press, Boca Raton, Fla., pp. 3-24.
- Reichert P, Borsuk M, Hostmann M, Schweizer S, Spörri C, Tockner K and Truffer B. 2007. Concepts of decision support for river rehabilitation. *Environmental Modelling and Software* **22**: 188-201.
- Spörri, C, C. Borsuk M, Peters I, Reichert P. 2006. The economic impacts of river rehabilitation: a regional input-output analysis. *Ecological Economics*, in press.
- Ward J V, Tockner K, Uehlinger U, and Malard F. 2001. Understanding natural patterns and processes in river corridors as the basis for effective river restoration. *Regulated Rivers: Research & Management* **17**: 311-323.

2 PREDICTING JOINT FREQUENCY DISTRIBUTIONS OF DEPTH AND VELOCITY FOR INSTREAM HABITAT ASSESSMENT

Steffen Schweizer¹, Mark E. Borsuk², Ian Jowett³, and Peter Reichert¹

¹*Swiss Federal Institute of Aquatic Science and Technology (Eawag), Dübendorf, and
ETH Zürich, Switzerland*

²*Department of Biological Sciences, Dartmouth College, Hanover, NH, USA*

³*National Institute of Water and Atmospheric Research Limited, Hamilton, New Zealand*

2.1 Abstract

Stream ecosystem structure and function are strongly influenced by patterns of velocity and depth. Simple methods for predicting the spatial distributions of these two variables, as functions of one-dimensional reach and discharge characteristics, have been recently reported in the literature. These studies have provided valuable insight into the fundamental factors influencing stream behavior and represent a practical alternative to multi-dimensional hydrodynamic models. However, these previous studies have handled velocity and depth separately, while there is evidence that meso-habitats and stream biota are associated with distinct combinations of the two variables. Therefore, we used survey data from 92 stream reaches in New Zealand to develop a model for the joint distribution of depth and velocity. We found that, for each reach, the bivariate distribution of relative velocity and relative depth could be described by a mixture of two end-member distributions, one bivariate normal and the other bivariate log-normal, each with fixed parameters. The relative contribution of each shape for a particular reach at a particular discharge could then be related to the reach mean Froude number, the reach mean relative roughness, and the ratio of the survey discharge to the mean discharge. As these inputs can be readily estimated for changed channel morphology, our model should provide a useful approach for linking river rehabilitation strategies to hydraulics and ecology.

2.2 Introduction

Spatial variation in velocity and depth over a stream reach is one of the most important factors regulating stream ecosystem structure and function (Allan 1995). The distribution of benthic plants and invertebrates is strongly influenced by these variables (Jowett 2003, Quinn and Hickey 1994) and by the resulting distribution of shear stress (Lamouroux et al. 1992). Fish have also shown distinct preferences for certain values of depth and velocity (Bovee 1982, Thomas and Bovee 1993, Jowett 2002). Human-induced change in velocity and depth distributions, resulting from modifications of discharge and river bed morphology, is therefore altering local habitat suitability. Reach-scale efforts to rehabilitate streams are being undertaken (Peter et al. 2005) but should be guided by scientific predictions of the morphologic, hydraulic and ecosystem consequences (Reichert et al. 2007).

Mechanistic hydrodynamic modeling is becoming increasingly common for predicting velocity and depth patterns in rivers from detailed information on the topography of the river bed (Clifford et al. 2002, Emery et al. 2003, Wheaton et al. 2004). This approach is particularly useful for assessing the effect of local river rehabilitation measures, such as in-stream bed form design, bank reconstruction, or local habitat improvement. However, for predicting the effect of reach-scale rehabilitation measures that can alter stream morphology, such as extensive widenings, mechanistic approaches are difficult to apply. For these applications, the prediction of river hydrodynamics must be preceded by a prediction of the form of the river bed. Because this is difficult, and because predictive ecology is not sufficiently advanced to benefit from the detailed, spatially-explicit information provided by hydrodynamic simulations, simpler, empirical approaches for predicting the distributions of velocity and depth in rivers are often appropriate.

Empirical approaches attempt to relate the form and the shape of velocity and depth distributions to predictor variables that are relatively easy to determine (Lamouroux et al. 1995, Lamouroux 1998). Such studies have shown that both depth and velocity distributions tend to shift from a positively skewed (exponential) to a symmetric (Gaussian) distributional shape with increasing discharge. Additionally, the higher the relative roughness and the lower the average Froude number of a reach, the more likely the velocity distribution is to have a skewed form (Lamouroux et al. 1995).

Such empirical approaches are conceptually valuable because of the insight they provide into the primary controls on hydraulic variation across a variety of rivers. They are also

practically valuable because they provide an alternative to numerical solutions of equations of motion, which, as mentioned above, require detailed data on channel geometry and high computational cost. The empirical approach is particularly appropriate for preliminary screening of rehabilitation alternatives or for evaluating future rehabilitation actions, such as river widening, that are so dramatic that measurements made of the presently existing conditions are no longer relevant. In such cases, the goal is to determine what the hydraulic habitat would be if the river were to be allowed to assume a natural form, relatively free of human-imposed constraints.

To date, most of the empirical approaches have yielded separate distributions for depth and velocity, implying independence of the two. Yet, we know that spatial patterns of depth and velocity in a stream reach are intimately linked. Furthermore, habitat structure and stream biota have been shown to be associated with distinct combinations of depth and velocity, rather than with depth and velocity independently (Kemp et al. 1999, Statzner et al. 1988). Therefore, the univariate distributions of these variables developed in previous studies are not fully informative for habitat characterization or prediction.

Stewardson and McMahon (2002) attempted to overcome this problem by transforming velocity and depth into two more nearly independent variables, one with a strong cross-channel component and the other with a strong along-channel component. The univariate distributions of these transformed variables were then independently fitted to data from 149 reaches, and the resulting parameters were related to measurable channel geometry characteristics. Unfortunately, as recognized by Stewardson and McMahon (2002), the transformations they chose do not lead to entirely independent variables. Additionally, the geometric characteristics used to predict the values of distributional parameters are measurable, but not readily predictable for changed channel morphology, such as that resulting from rehabilitation measures. This is the case for the standard deviation of the Froude number and the coefficients of variation of both depth and surface width, all three of which are used as predictor variables by Stewardson and McMahon (2002). In fact, the first two of these are related to quantities that one would like to predict with the model (i.e., descriptions of the variation in velocity and depth) and therefore should not be used as model inputs. Further, the use of transformed variables makes it difficult to visualize and interpret the distributions of velocity and depth directly.

It is not necessary to transform depth and velocity to independent variables prior to analysis, as long as the dependence between the two is explicitly modeled. In fact, Stewardson and McMahon (2002) concluded their analysis by hypothesizing the existence of two fundamental bivariate distributions, each with a significant correlation between depth and velocity (Figure 2.1). They suggested that one is characterized by a

centered form with a positive correlation resulting from significant cross-channel effects and weak along-channel effects, while the other has a skewed “banana-shape” resulting from longitudinal bed undulations (e.g., pool-riffle sequences) and minimal lateral variation. Most channels, they state, can be expected to be a mixture of these two forms.

In the present chapter, we attempt to test the hypothesis of Stewardson and McMahon (2002) by fitting their two proposed distributional forms directly and relating the relative dominance of each form to reach and discharge characteristics. Our goal is to examine the universality of the end-member distributions as well as the factors controlling their degree of mixture at a particular reach and discharge. Additionally, to make the results of our analysis useful for predicting the consequences of reach-scale river rehabilitation, we focus on characteristics that can be readily estimated for changed channel morphology.

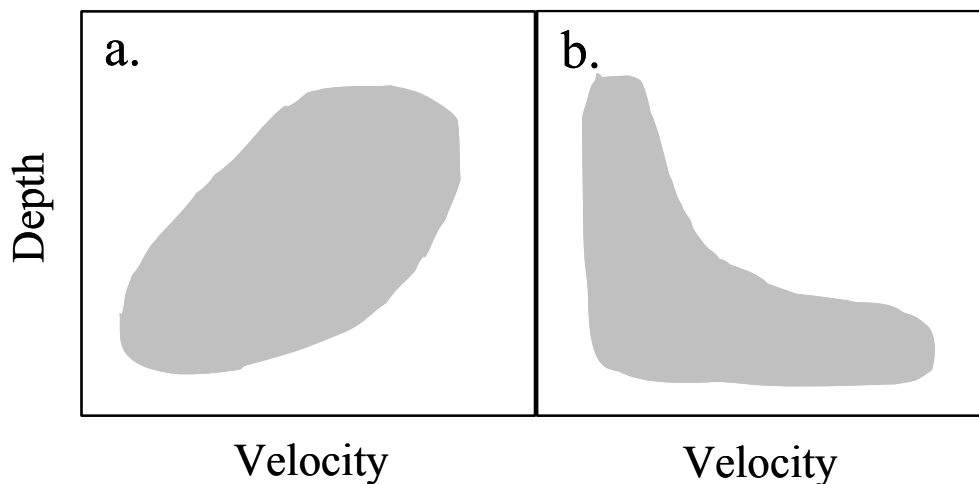


Figure 2.1: Two proposed shapes for the joint distribution of depth-averaged velocity and water depth: (a) a positive association with a centered form resulting from strong bank effects, (b) a negative association with a skewed form resulting from strong pool-riffle effects (adapted from Stewardson and McMahon 2002).

2.3 Methods

2.3.1 Data Description

This study uses in-stream survey data from 92 stream reaches in New Zealand (Table 2.1), most of which are described by Jowett (1998) and Lamouroux and Jowett (2005). The main channel and hydraulic properties (slope, velocity, depth, and width for mean flow conditions) were determined from data collected by government and regional authorities. The 92 studied river reaches range in mean discharge from 0.1 m³/s to 95 m³/s (mean 14 m³/s) and in channel slope from 0.8‰ to 2% (mean 0.5%). Streambeds include a variety of substrate sizes with median diameter ranging from 13 to 639 mm (mean 99 mm). Most rivers were without significant human disturbance. The studied river reaches are all single thread channels and contain gravel bars.

Table 2.1: General characteristics of investigated reaches

	Notation	Minimum	Mean	Median	Maximum
Length of reach [m]	L	12	338	278	1785
Slope [-]	J	0.0008	0.005	0.004	0.020
Width (at mean flow) [m]	w	2.3	25.9	22	76.4
Number of cross-sections per river reach [-]	-	9	23	21	47
Number of data points per river reach [-]	-	32	339	335	645
Mean discharge [m ³ /s]	MQ	0.1	9.4	13.8	95
Relative survey discharge [-]	q/MQ	0.05	0.46	0.46	1.08
Reach mean velocity (at mean discharge) [m/s]	\bar{v}	0.2	0.7	0.6	1.4
Reach mean depth (at mean discharge) [m]	\bar{h}	0.1	0.6	0.5	1.3
Reach mean Froude number (at mean discharge)[-]	Fr	0.1	0.3	0.3	0.7
Reach mean Reynold's number (at mean discharge) [-]	Re	3.36×10^4	5.86×10^5	4.00×10^5	3.27×10^6
Reach mean boundary Reynold's number (at mean discharge) [-]	Re_f	7.25×10^2	9.10×10^3	6.97×10^3	3.55×10^4
Median substrate size [mm]	d_{50}	13	99	84	639
Reach mean relative roughness (at mean discharge) [-]	Z	0.02	0.19	0.16	1.47

Each reach was surveyed once to obtain a set of velocity-depth pairs representing hydraulic conditions throughout the reach at the time of the survey. Measurements were made according to the procedures detailed by Jowett (1989). Habitat mapping was first undertaken to determine the presence of various habitat types (e.g., pools, riffles, runs). Reach length and survey site locations were then chosen to appropriately represent this range of habitat. On average, 23 cross-sections (range 9-47) were surveyed at each reach (Table 2.1). Velocity was measured at a depth below the water surface equal to 60% of the total depth or at 20% and 80% below the surface if the total depth exceeded one metre. Upstream currents (due to eddies or backwaters) were recorded as negative velocities. Multi-depth velocity measurements were averaged to derive the depth-averaged mean velocity. The modified Wentworth particle size scale (Bovee and Milhous 1978) was used for substrate characterization, except that gravel was further divided into fine gravel (2-10 mm) and gravel (10-64 mm). In total, seven substrate classes were distinguished: silt, sand, fine gravel, gravel, cobble, boulder, bedrock.

Measurements were usually made at regular 0.5–1m intervals across the stream, but extra measurements were made where the depth or velocity changed abruptly. For this reason, we assigned to each measurement a weight according to the width it represented. This width was calculated as the sum of the two half-distances to adjacent measurement points, except for points at the water's edge, for which the width interval was set to half the distance to the next instream point. All such width intervals were then divided by the total wetted width for the cross-section to obtain the relative width weight. In this way, the mean weight for each cross-section equals 1.0. Measured water velocities were weighted by the width that they represented. Because this process leads to width-weighted velocities, and not cross-sectional area-weighted, the weighted mean velocity will not equal the discharge divided by the cross-sectional area. This equality is not necessary in the context of this study, and width-weighted velocities are more appropriate because they correspond with the surface area of the stream - a quantity that is more relevant to habitat utilization than volume. Average reach characteristics were obtained by multiplying cross-section characteristics by the proportion of reach represented by each cross-section.

Most surveys were conducted at discharge conditions between the mean annual low flow and the mean flow. Data with a survey flow less than 5% of the mean flow were excluded from our analysis. After this exclusion, sample sizes ranged from 32 to 645 (mean 339) depth-velocity pairs for each river reach. In total, more than 31,000 depth-velocity measurements were analyzed.

2.3.2 Modeling

Similarly to Lamouroux et al. (1995) and Lamouroux (1998), who modeled velocity and depth independently, our analysis began by transforming the point data to relative values. This was done by dividing each velocity and depth measurement by the reach mean velocity, \bar{v} , and reach mean depth, \bar{h} , respectively (each calculated as the width-weighted average over all measurements for each survey). Exploratory plots of relative velocity and depth supported Stewardson and McMahon's (2002) suggestion that there appear to be two extreme shapes to the bivariate data clouds (Figure 2.1), with most reaches having shapes intermediate to these two. We chose to represent the centered, positively correlated distribution by a bivariate normal (Gaussian) form, consistent with the centered distributional form used by Lamouroux et al. (1995) and Lamouroux (1998). The distribution was truncated at $h/\bar{h} = 0$ and renormalized (by dividing by the integral of the remaining distribution) to preclude the possibility of obtaining negative values for depth. However, negative values for velocity (flow in upstream direction due to eddies) were maintained. While the truncation of negative depth values will slightly shift the mean of the distribution, this effect was insignificant for the distribution that was found to be the best fit (<3% of the distribution was truncated).

We chose to use a log-normal distributional form to represent the skewed distribution. Lamouroux et al. (1995) used exponential models for the positively skewed shapes, but our exploratory analysis indicated the presence of a non-zero mode for both depth and velocity, consistent with a log-normal distribution. Later testing of the final model, by replacing the log-normal distribution with the exponential, confirmed that the log-normal provides a superior fit to our data.

Mean values of both bivariate distributions were fixed at (1, 1) which, by definition, are the mean values of relative velocity, v/\bar{v} , and relative depth, h/\bar{h} . Two standard deviations and one correlation coefficient are then needed to define each bivariate distribution. These were assumed to be constant across all reaches, but were treated as free parameters, to be estimated from the data. A parameter, s_{mix} , describing the relative contribution of the normal and log-normal forms was assumed to be reach-specific and ranged from 0 (entirely centered) to 1 (entirely skewed), similar to Lamouroux et al. (1995). Therefore, for each river reach, the joint distribution of velocity and depth was of the form,

$$f\left(x = \frac{v}{v}, y = \frac{h}{h}\right) = (1 - s_{mix}) \cdot N_{y>0}(\mu_{xN} = 1, \mu_{yN} = 1, \sigma_{xN}, \sigma_{yN}, \rho_N) + s_{mix} \cdot LN(\mu_{xLN} = 1, \mu_{yLN} = 1, \sigma_{xLN}, \sigma_{yLN}, \rho_{LN}) \quad (1)$$

where N represents the normal distributional component and LN the log-normal component, the subscript $y>0$ indicates that the normal distribution was truncated and renormalized as described above, the μ represent the means of the relative velocity and depth of the normal and log-normal distributions, the σ represent the corresponding standard deviations, and the ρ are the correlation coefficients. The six reach-constant parameters (four standard deviations and two correlation coefficients) were estimated together with the reach-specific parameter, s_{mix} , for all reaches simultaneously. This was done by maximizing the log-likelihood function,

$$\log[L(\mathbf{x}, \mathbf{y}, \sigma_{xN}, \sigma_{yN}, \rho_N, \sigma_{xLN}, \sigma_{yLN}, \rho_{LN}, \mathbf{s}_{mix})] = \sum_i \sum_j w_{ij} \log[f(x_{ij}, y_{ij}, \sigma_{xN}, \sigma_{yN}, \rho_N, \sigma_{xLN}, \sigma_{yLN}, \rho_{LN}, s_{mix,i})] \quad (2)$$

where the model function, f , of equation (1) is now written as an explicit function of both the data and the distributional parameters. The data are designated by $\mathbf{x} = \{x_{ij}\}$ and $\mathbf{y} = \{y_{ij}\}$, which are vectors of the measured relative velocities and depths, respectively (indexed according to the river reach, i , and the data point within the reach, j), w_{ij} is the relative width weight associated with the data point (i, j) as described in the data description section above, and $s_{mix} = \{s_{mix,i}\}$ is a vector of reach-specific mixing parameters. The sums in equation (2) extend over all 92 reaches and all data points within each reach (a total of 31188 data points). Maximization was performed using a Newton-type algorithm according to Dennis and Schnabel (1983) and Schnabel et al. (1985) as implemented in the non-linear minimization routine *nlm* supplied with the statistical programming language and computing environment R (Ihaka and Gentleman 1996, <http://www.r-project.org>). A total of 98 parameters were fitted: 6 parameters characterizing the two bivariate end-member distributions, and 92 reach-specific mixing parameters, s_{mix} . Standard errors of the parameter estimates were calculated from the Hessian matrix, which is an optional additional result of the *nlm* routine. Compared to the optimization methods of Lamouroux et al. (1995) and Stewardson and McMahon (2002), ours does not require discretization (or “binning”) of the data; all data points were used and distributions were fitted in their continuous form.

The goodness of fit of the model distributions to the data was examined quantitatively using the Kolmogorov-Smirnov statistic. In one dimension, this is measured by the largest difference between the cumulative distribution function of the data and that of the model. In two or more dimensions however, the definition of this statistic is ambiguous because the direction in which one can perform the cumulation is not unique. To overcome this problem, Peacock (1983) suggested using the largest difference between the empirical and modeled cumulative distribution functions when all possible ways to cumulate the data and model along the directions of the coordinate axes are considered. In two dimensions with n data points, this corresponds to calculating probabilities for the data and model in each of the four quadrants around the n^2 locations defined by all combinations of the x and y coordinates of the data. This procedure is computationally expensive for large numbers of data and a faster approximation was proposed by Fasano and Franceschini (1987). This approximation only considers the n locations where data points actually lie as suitable locations around which to define the quadrants used for cumulation. We implemented this approximation in R, following the method given by Press et al. (1992, pp. 645-649). Our version included a modification to allow for weighting of the data points.

To make the model predictive, we next attempted to relate the distributional mixture parameter, s_{mix} , to variables that could be derived from simple field measurements and one-dimensional hydraulic modeling. We used a procedure in which s_{mix} was used as the response variable in a weighted regression for which the predictor variables included all possible subsets, of size one through three, of a set of candidate variables. These candidate predictor variables included the reach characteristics d_{50} and J (see notation at the end of the chapter for the meaning of the variables), the flow-dependent characteristics q , w , h , and v , as well as the dimensionless quantities q/MQ , Fr , Re , Re_f , Y , Z , and θ . The flow-dependent variables were determined for both survey and mean flow conditions. The latter may be necessary to account for systematic effects of river size and/or geometry. Dimensionless quantities (e.g. Fr , Re) were calculated by using reach mean values of velocity and depth. This is because such quantities are significantly simpler to predict for changed conditions using one-dimensional modeling. Natural logarithmic, square root, square, and inverse transformations of these possible predictors were also considered, as were interaction terms. The numbers of measured velocity and depth pairs recorded for each reach were used as the weights in this regression procedure.

Because the response variable, s_{mix} , can only assume values between 0 and 1, we applied a logit transformation to linearize the model and allow it to better meet the assumptions of regression analysis (Dobson 1999). This leads to the model form,

$$\ln\left(\frac{s_{mix}}{1-s_{mix}}\right) = \beta_0 + \beta_1 x \quad (3)$$

where β_0 represents the model intercept term, x represents the vector of one or more predictor variables, and β_1 represents the vector of one or more regression coefficients. This process is similar to logistic regression (Dobson 1999) except that s_{mix} is not interpreted as a probability. After performing the linear regression, Eq. (3) can be re-transformed to solve for s_{mix} , yielding

$$s_{mix} = \frac{\exp(\beta_0 + \beta_1 x)}{1 + \exp(\beta_0 + \beta_1 x)} \quad (4).$$

We recognize that the consideration of candidate models with so many combinations of predictors invalidates strict interpretation of hypothesis test statistics, such as p -values. However, our primary purpose in this study was to find a useful predictive relationship for s_{mix} and not necessarily to test hypotheses. Therefore, to ensure that the final resulting model did not simply arise as a result of our broad search strategy, we used a K -fold cross-validation procedure for model evaluation (Efron and Tibshirani 1984). This involves first dividing the data randomly into K groups. Each group is then sequentially omitted and the linear regression is performed on the remaining data. The results are then used to generate predicted values of the response variable in the omitted group. All predictions are compared to all observations and the total prediction error variance is calculated. This statistic provides a useful criterion for model selection because it controls for overfitting. When K is chosen to be less than the number of observations, some bias is introduced in the prediction error, but this can be corrected using the adjustment of Davison and Hinkley (1997). We chose to use four groups in our cross-validation procedure, which we implemented using the `cv.glm` routine supplied with the “boot” package for R (Davison and Hinkley 1997). The *Akaike information criterion (AIC)* and the *Bayesian information criterion (BIC)* were also considered, but did not lead to significant differences in the final ranking of models, relative to the cross-validation procedure.

The bivariate distributions that result from our analysis can be used to predict the relative frequency of pool, run, and riffle habitat, given a quantitative definition of these hydraulic units in terms of depth and velocity. For example, Jowett (1993) found that pool habitat was associated with values of the Froude number less than 0.18, riffle habitat with values greater than 0.41, and run habitat with intermediate values. These thresholds can be compared with our velocity/depth distributions and the fraction of the distribution within each range can be calculated through appropriate integration of the joint density function. Because our distribution diagrams represent relative (and not absolute) velocity and depth, the position of each threshold on the diagram is reach-specific and can be shown to depend on the reach mean Froude number (Fr_{reach}) according to the expression,

$$\frac{h}{\bar{h}} = \left(\frac{Fr_{reach}}{Fr^*} \right)^2 \left(\frac{v}{\bar{v}} \right)^2 \quad (5)$$

where Fr^* is the threshold Froude number used to distinguish the various hydraulic units (e.g., 0.18 and 0.41 of Jowett 1993).

2.4 Results

2.4.1 Distributional Parameter Estimates

Estimates of the six model parameters (four standard deviations and two correlation coefficients) of the bivariate normal and log-normal distributions comprising Eq. (1) are given in Table 2.2. Figure 2.2 shows the shapes of the two end-member distributions (corresponding to s_{mix} values of 0 and 1) with the estimated parameter values, as well as an intermediate mixture with $s_{mix}=0.5$. Estimated values for the parameter s_{mix} spanned the entire range across the set of stream reaches from 0 to 1 with an average of 0.40. The standard errors of s_{mix} ranged from 0.02 to 0.15 with a mean of 0.05 and generally scaled inversely with the number of measurements made at the corresponding reach.

Figure 2.3 presents the modeled and observed distributions for four representative stream reaches that span the range of possible values for s_{mix} . The visual aspect of such figures reveals a very good agreement between the parametric models and the measured data.

Table 2.2: Parameter estimates (with standard errors in parentheses) of the bivariate normal and log-normal distributions in equation (1). (Note: mean values of relative velocity and relative depth were not estimated but set to 1 prior to parameter estimation.)

Normal Distribution				
μ_{vN}	μ_{hN}	σ_{vN}	σ_{hN}	ρ_N
1	1	0.52 (± 0.004)	0.52 (± 0.005)	0.12 (± 0.011)
Log-normal Distribution				
μ_{vLN}	μ_{hLN}	σ_{vLN}	σ_{hLN}	ρ_{LN}
1	1	1.19 (± 0.031)	1.09 (± 0.026)	0.01 (± 0.007)

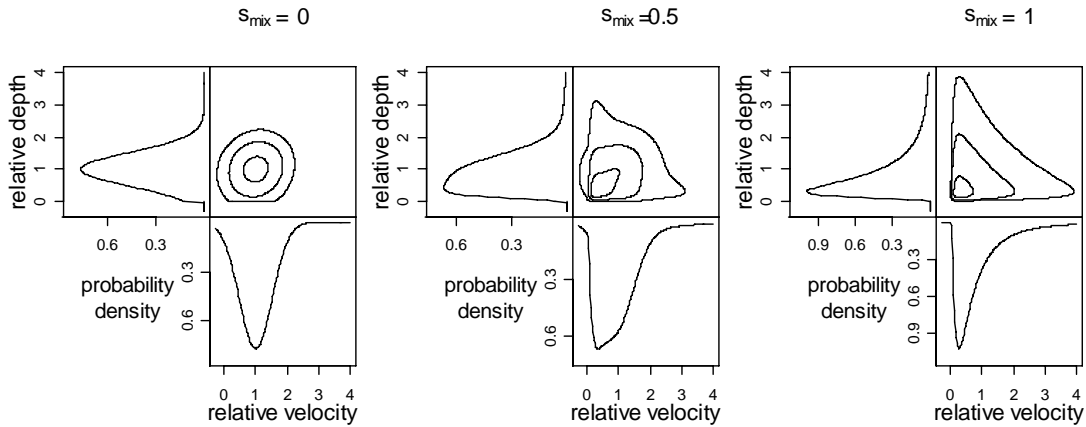


Figure 2.2: Modeled bivariate distributions (joint and marginal densities for relative velocity and relative depth) for $s_{mix}=0$ (normal), $s_{mix}=0.5$ (intermediate mixture) and $s_{mix}=1$ (log-normal). Contour lines in the joint plots indicate the regions containing 25, 75, and 95% of the probability mass.

The Kolmogorov-Smirnov goodness-of-fit statistics indicate that the model distributions fit the data on relative velocity and relative depth equally well (Figure 2.4). Lower values of the K-S statistic represent a better fit than high values, and, for the one-dimensional marginal distributions of relative velocity and depth, values for the statistic ranged from 0.04 to 0.23 and from 0.03 and 0.32, respectively. The values of the third quartile for both variables indicate that, for 75% of the river reaches, the maximum difference between the cumulative probability function of the model and that of the data is 0.13. This means that, for most of the reaches, the cumulative probabilities are never wrong by more than 13%.

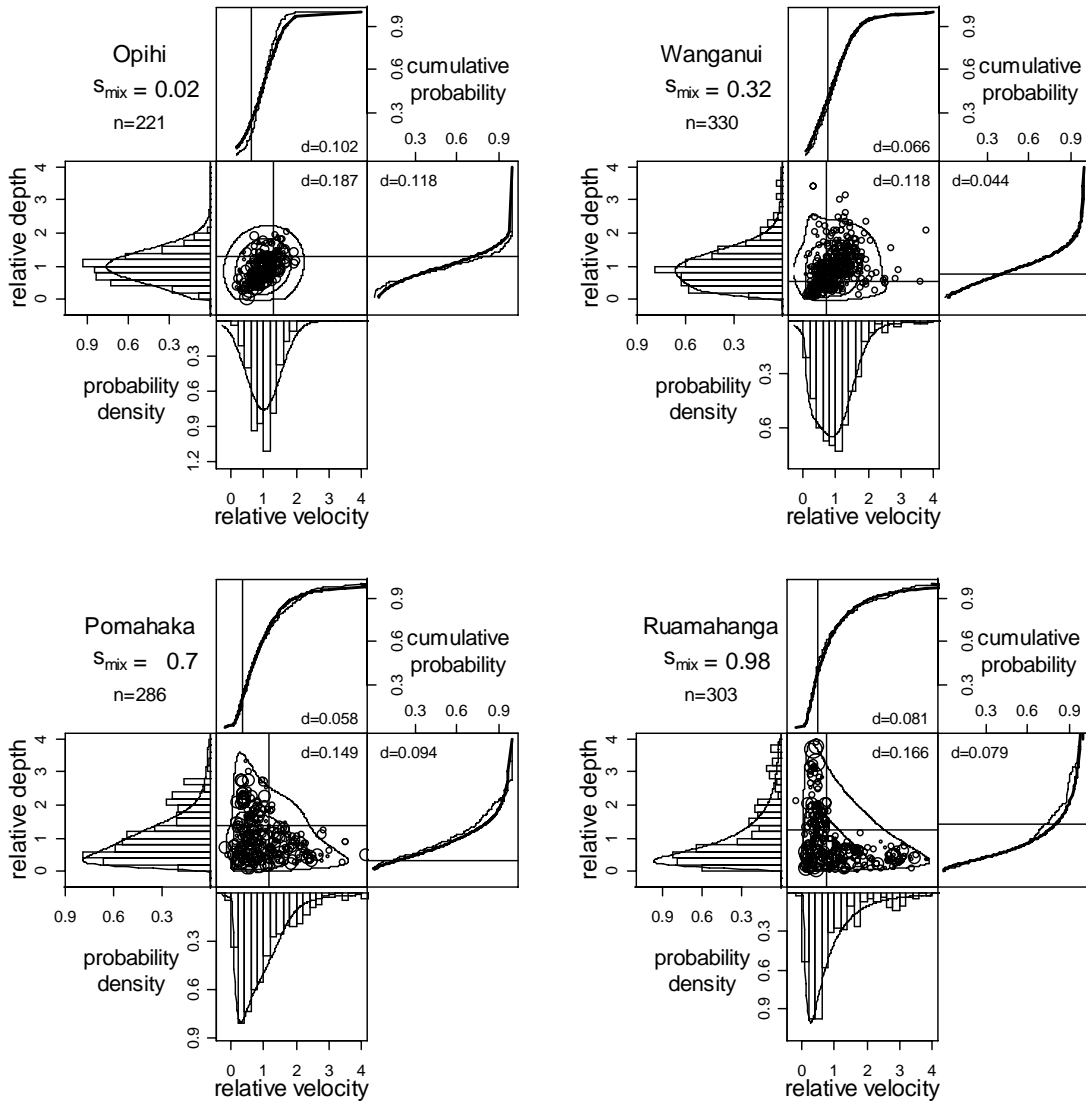


Figure 2.3: Comparison of modeled and observed distributions for four stream reaches with a wide range of values for s_{mix} . Plots show joint and marginal densities and marginal cumulative probabilities for relative velocity and relative depth. Points (with size proportional to relative width weights), histograms and thin cumulative probability lines correspond to the data; contour plots, continuous density lines, and thick cumulative distribution lines correspond to the model. Values of the mixture parameter, s_{mix} , and the number of data points, n , are given under the name of each river reach. Values for the Kolmogorov-Smirnov (K-S) statistic, d , are given in the corners of the corresponding marginal cumulative and joint density plots. Straight lines indicate the positions at which the K-S statistic is located (which may be different between the joint and marginal distribution plots). The representativeness of the K-S statistics for these four reaches can be gauged through comparison with the K-S values shown in Figure 2.4.

The reaches with the worst fit (shown as outliers in Figure 2.4) are those with relatively few measurements, and there was, in general, a negative relationship between the size of the K-S statistic and the number of measurements taken at a reach.

For the two-dimensional joint distribution, the test statistic is larger than for the one-dimensional cases because it is calculated as the largest difference between the empirical and modeled cumulative distribution functions in all four directions along the coordinate axes. Values ranged from 0.07 to 0.33 with a third quartile of 0.19. Again, those with the worst fit tended to be those with relatively few data.

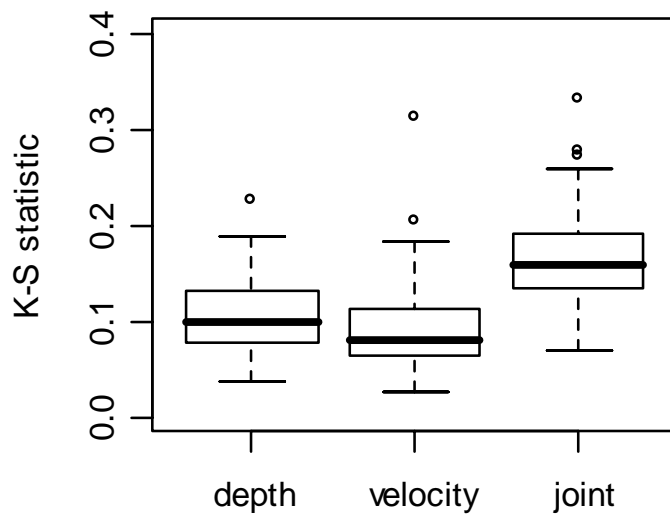


Figure 2.4: Box-and-whisker plots of the K-S statistic for the marginal distributions of relative depth and relative velocity and the joint distribution of both variables. The lower and upper edges of each box represent the first and third quartiles, respectively, and the horizontal line in the middle represents the median. The whiskers extend to the most extreme data point that is no further from the box than 1.5 times the interquartile range. Data that are more extreme are shown as points.

2.4.2 Predicting the Mixture Parameter

After fitting the normal and log-normal bivariate distributional parameters, we next attempted to predict the mixture parameter, s_{mix} , from reach characteristics. After trying all combinations of predictor variables, we found that the natural logarithm of the Froude number, $\ln(Fr)$, calculated for survey flow conditions was the best single predictor of s_{mix} and that the square root of the relative survey discharge, $(q/MQ)^{0.5}$, was the best second predictor. Adding the inverse of relative roughness, Z^{-1} (also calculated for survey flow conditions), as a third predictor further reduced the cross-validation prediction error. Models with four predictors did not lead to further improvements, demonstrating the ability of the cross-validation procedure to discourage overfitting. The regression equations (with parameter standard errors given in brackets) are:

$$\ln\left(\frac{s_{mix}}{1-s_{mix}}\right) = -4.72[\pm 0.44] - 2.84[\pm 0.29] \cdot \ln(Fr) \quad (6a)$$

$$R_{adj,smix}^2 = 0.54$$

$$\ln\left(\frac{s_{mix}}{1-s_{mix}}\right) = -2.75[\pm 0.79] - 2.38[\pm 0.32] \cdot \ln(Fr) - 2.08[\pm 0.71] \cdot \left(\frac{q}{MQ}\right)^{0.5} \quad (6b)$$

$$R_{adj,smix}^2 = 0.59$$

$$\ln\left(\frac{s_{mix}}{1-s_{mix}}\right) = -2.34[\pm 0.79] - 2.27[\pm 0.31] \cdot \ln(Fr) - 2.03[\pm 0.69] \cdot \left(\frac{q}{MQ}\right)^{0.5} - 0.04[\pm 0.02] \cdot Z^{-1} \quad (6c)$$

$$R_{adj,smix}^2 = 0.62$$

No significant collinearities were observed between the three explanatory variables $\ln(Fr)$, $(q/MQ)^{0.5}$ and Z^{-1} (Table 2.3). Thus, the influence of each explanatory variable on the value of s_{mix} can be considered separately. The linear forms of eqs. (6a-c) lead to curvilinear relationships when the re-transformation in eq. (4) is applied (Figure 2.5), but

the direction of each influence remains the same: s_{mix} decreases in close relation with $\ln(Fr)$, with the inverse of the relative roughness Z^{-1} , and with the square root of relative discharge $(q/MQ)^{0.5}$. The relative errors (standard error divided by mean estimate) of the parameter estimates in eq. (6c) indicate that uncertainty increases in the following order:

$$\ln(Fr) (0.31/2.27 \approx 14\%) < (q/MQ)^{0.5} (0.69/2.03 \approx 34\%) < Z^{-1} (0.02/0.04 \approx 39\%).$$

Table 2.3: Matrix of correlation coefficients between the three predictors of equations 4a-c ($n = 92$)

	$(q/MQ)^{0.5}$	$\ln(Fr)$
$\ln(Fr)$	0.43	
Z^{-1}	0.18	0.09

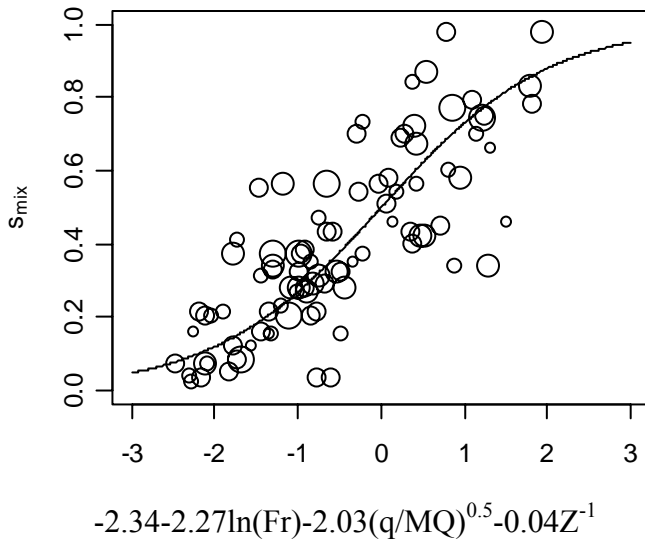


Figure 2.5: Plot of relation between s_{mix} and the right-hand side of eq. (4c), representing the influence of reach mean Froude number (Fr), relative survey discharge (q/MQ), and reach mean relative roughness (Z). Points represent reach-specific estimates of s_{mix} with point size proportional to the number of measured velocity-depth pairs. Line represents the regression fit given by eq. (6c).

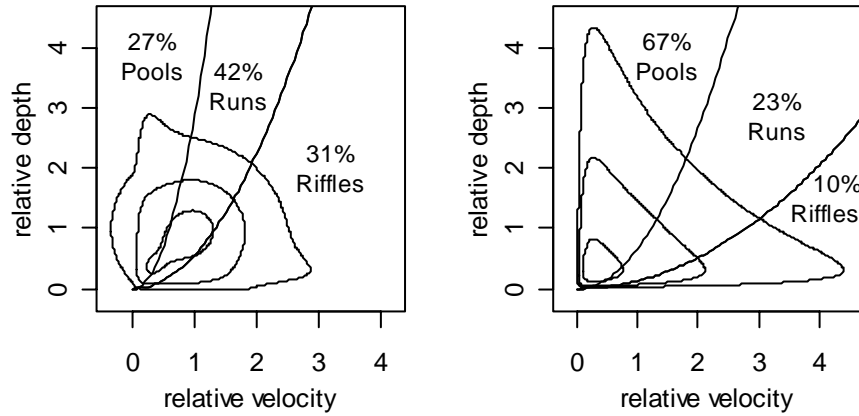


Figure 2.6: Estimates of pool, run, and riffle habitat for two of the river reaches shown in Figure 2.3. Left: Wanganui ($s_{mix}=0.32$, $Fr_{reach}=0.31$). Right: Ruamahanga ($s_{mix}=0.98$, $Fr_{reach}=0.15$). The threshold between pool and run habitat corresponds to $Fr_{point} = 0.18$, and between run and riffle habitat $Fr_{point} = 0.41$.

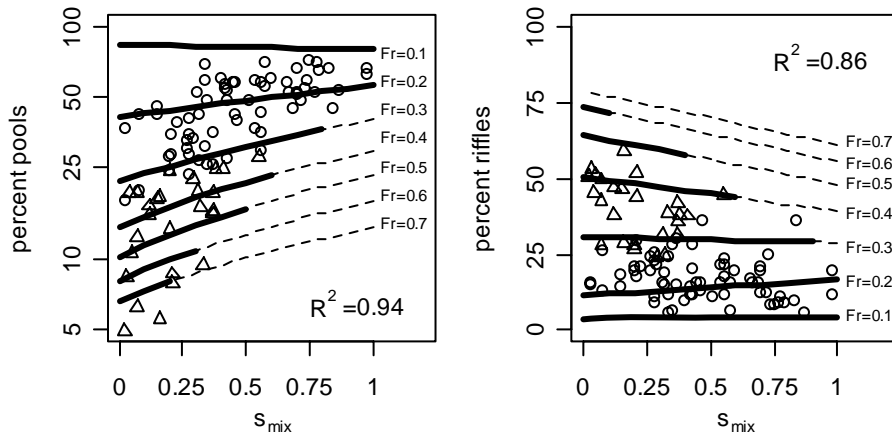


Figure 2.7: The relationship between s_{mix} , Fr_{reach} (labeled as Fr in the figure), and the predicted percent pool (left) and riffle (right) habitats. Points indicate estimated reach-specific values and are shown only to demonstrate the range of our data. Triangles are those points with Fr_{reach} greater than 0.3 and circles are those with Fr_{reach} less than 0.3. Dashed lines indicate extrapolations beyond the data range. Note that the vertical axis for the left plot uses a logarithmic scale for ease of presentation, while the right plot uses a linear scale.

In terms of predicting hydraulic units (Figure 2.6), over 94% of the point-wise variation in the percent pool habitat and 86% of the variation in the percent riffle habitat (using the quantitative definitions of Jowett (1993)) across the 92 stream reaches we studied can be accounted for by the predicted bivariate distributions. To aid future application of this part of the model, the predicted relative frequency of each unit has been plotted against Fr_{reach} and the s_{mix} value resulting from eq. (6c) (Figure 2.7). Such a plot eliminates the need for users of our model to integrate the joint density function.

2.5 Discussion

Our results show that the joint frequency distribution of velocity and depth can be predicted for a wide variety of stream reaches using a simple mixture of two end-member distributions with fixed parameters. This finding suggests that there is some degree of “universality” in the two extreme distributions, at least for the type of gravel bed rivers examined in this study. One of these end-members is a normal distribution centered at (1, 1) with equal standard deviations for relative depth and velocity and a positive correlation coefficient (see Table 2.2). The small standard errors of the parameter estimates indicate that the parameters are well-identified by the data and that the correlation coefficient is significantly different from zero. The other end-member is a log-normal distribution, also with mean (1, 1) and a slightly wider marginal distribution for velocity than for depth. The correlation coefficient is positive, but very small and not significantly different from zero. For this reason the skewed shape of the bivariate log-normal still leads to a visually negative relationship between the two variables (see Figure 2.2), as anticipated by Stewardson and McMahon (2002). As also expected by Stewardson and McMahon (2002), the relative contribution of each end-member distribution, indicated by the value of s_{mix} , spans the range from 0 to 1, with most river reaches having some contribution of each distributional form. The small standard errors indicate that these mixture parameters are also well-identified by the data.

Lamouroux et al. (1995) and Lamouroux (1998) also used mixture parameters to describe the relative contribution of skewed (exponential) and symmetric (Gaussian) distributional forms to observed velocity and depth distributions separately. In our study, we chose to represent the positively skewed form with a joint log-normal distribution, rather than an exponential. Nevertheless, regarding the prediction of s_{mix} , the qualitative results of the two approaches are comparable. A higher reach mean Froude number led, in Lamouroux’s velocity model and in our joint velocity-depth model, to a more

symmetric/normal distributional shape. Additionally, the mixture parameter s_{mix} responds to relative roughness consistently in the two approaches: a shift from a symmetric to a skewed shape with increasing relative roughness. This is because a stream bed with larger roughness elements will produce more spatial variation in velocity and depth than one with lower roughness.

Lamouroux et al. (1995) used the coefficient of variation (standard deviation divided by mean) of river width as their third predictor. However, one cannot expect to predict the value of this variable for a reach which will be rehabilitated in the future, and so we did not include it as a candidate predictor variable. Instead, we found that the square root of relative survey discharge, $(q/MQ)^{0.5}$, was an appropriate additional predictor, and the distributional response to this variable is as anticipated by Stewardson and McMahon (2002) - an increasingly centered shape with increasing discharge. This is because for a fixed streambed and channel geometry, increases in discharge will tend to smooth out variations between riffles and pools. Changes in discharge also have an indirect effect, by influencing the stage and therefore the relative importance of roughness elements. Consequently, with increasing discharge, the influence of roughness elements on flow pattern will decrease and the variability in velocity and depth will be reduced. This effect is captured by the relative roughness term in equation 6c. The explicit representation of the direct and indirect influences of flow on spatial patterns of velocity and depth may make our model useful for assessing the biological effects of variations in discharge.

The consistency between our results and those of previous authors are reassuring, considering that the analyses were based on independent data sets from different continents. This similarity shows that empirical analyses can reveal the general patterns that govern river morphology and hydraulics worldwide, even for rivers of very different size (see Table 2.1). This is a type of finding which could not come from detailed, hydrodynamic model applications that are generally site-specific.

While our results are qualitatively similar to those of previous studies, our representation of velocity and depth jointly, rather than independently, is a significant advancement. Not only does this lead to a more realistic description of hydraulic conditions, but it should also lead to improved ecological assessments. Both living and non-living elements of streams are clearly influenced by these two variables simultaneously, and methods for analyzing survey data are beginning to reflect this (e.g., Kemp et al. 1999, Jowett 2003). Using “occurrence matrices” to identify the depth and velocity combinations at which various meso-habitats are most likely to be found, Kemp et al. (1999) distinguished some distinct sets of conditions. For example, cobbles, mosses, and submerged fine-leaved macrophytes were most often found in the fastest water at low

depths. Silt, submerged broad-leaved macrophytes, and floating leaved macrophytes were found in the slowest water at high depths. Marginal plants were associated with the slowest and shallowest water. These findings could not be addressed by a model that considers velocity and depth independently.

The interactions between velocity and depth in determining habitat quality and preferences are also beginning to be explicitly considered in predictive ecological models (e.g., Schneider 2001). We believe this to be the most comprehensive and appropriate use of our model results and hope that this paper will stimulate such efforts. However, many other published studies have related the occurrence of stream-dwelling organisms to hydraulic units, such as pools, runs, and riffles (e.g., Logan and Brooker 1983, Pridmore and Roper 1985), and this categorization continues to be employed by some ecological models (Fausch et al. 1988). We have shown how the joint frequency distributions we have developed here are compatible with such approaches. However, it should be kept in mind that classification of pool, run, and riffle habitats may be river-specific and with different threshold definitions. Jowett (1993) found that the velocity:depth ratio was nearly as good a discriminant between the hydraulic units as the Froude number. Allen (1951) also used the Froude number and the velocity:depth ratio, but with lower threshold values than Jowett (1993). In any case, the definition that is deemed most appropriate for a studied reach can be used as the boundaries for integrating the joint density function to yield the relative frequencies of each hydraulic unit.

Other researchers have attempted to capture the interactive effects of velocity and depth on instream fauna by using dimensionless transformations that combine the two variables. The Froude number and boundary Reynold's number are common choices (Orth and Maughan 1983, Quinn and Hickey 1994, Brooks et al. 2005). Our predicted joint distribution can easily be transformed to distributions on these derived quantities. These distributions will usually not have a convenient closed-form expression such as eq. (1) but can be determined straightforwardly using Monte Carlo sampling on eq. (1) and subsequent propagation of the Monte Carlo samples through the expressions for Fr or Re . Another option would be to predict a joint distribution of Fr and Re directly, using a method similar to the one we presented here. However, as velocity and depth are the fundamental quantities that are measured in the field and directly experienced by aquatic organisms, we feel that their use as response variables is more convenient and direct.

While we have detailed the compatibility of our joint distributional approach with approaches employing discrete hydraulic units or derived dimensionless quantities, we believe that full consideration of the joint distribution is the most informative way forward for modelling and data analysis. Each of the other approaches loses some

information content, as is apparent through consideration of the results of Kemp et al. (1999), described above. While the particular habitat containing cobbles, mosses, and submerged fine-leaved macrophytes could be classified as “riffles” and that containing silt, submerged broad-leaved macrophytes, and floating leaved macrophytes could be classified as “pools” (with high and low Froude numbers, respectively), the distinct habitat of marginal plants (slow and shallow) would not be identified by a system only using pools, runs, and riffles. Therefore, we encourage more studies of the type of Kemp et al. (1999) and Jowett (2003), which consider depth, velocity, and their interaction explicitly.

Our purpose in undertaking the present study was to provide support for reach-scale river rehabilitation decisions of the type described by Hostmann et al. (2005). These include conversion of an entire river reach from a channelized form to a natural form by relieving lateral width constraints and/or restoring natural flow and gravel input patterns. Assessments of what the hydraulic habitat will be after such re-naturalization efforts can be informed by empirical studies of existing natural rivers, such as we describe here. In terms of the notation we employ, greater ecological benefits can be expected when the value of s_{mix} is predicted to be relatively high. This is an indication of diverse velocity-depth pairs (see Figure 2.2), and a relatively high proportion of pools and riffles relative to runs, although the exact combination of hydraulic units will also depend on the reach average Froude number (see Figure 2.6). Channelized rivers are predominated by runs (see chapter 3), and a common goal of rehabilitation is to increase diversity by creating pools and riffles. Although the values of s_{mix} and Fr for a re-naturalized river reach (i.e. without width constraints) will be primarily determined by the discharge regime, valley topography, gravel balance and river bed composition (all of which may not be affected by most rehabilitation measures), river managers can influence these parameters through appropriate gravel entrainment and discharge regulation strategies.

Hydraulic habitat assessment is the first step towards predicting the anticipated ecological response to management actions (Hardy 1998). Hydraulic model results can be combined with preference curves or, better yet, “occurrence matrices” for meso-habitats or biota, leading to predictions of the suitability of conditions after rehabilitation. Additionally, the results of our model can be used as inputs for other types of ecological models, such as population or individual-based models, which predict biomass, abundance and/or functional groups of species. Such ecological predictions can improve a project’s financial and public support, as well as help guide selection of the most appropriate stream reaches and site-specific rehabilitation measures (see Hostmann et al. 2005 for an example).

2.6 Conclusions

Among the most important influences on organisms living in a watercourse are depth and velocity patterns. Our model allows for prediction of these patterns in the form of a joint frequency distribution, without requiring detailed knowledge of the river geometry. This is particularly important when the model is to be used to predict conditions resulting from future reach-scale rehabilitation. To apply our model, the following information is required (see eqs. 6a-c):

Reach mean depth and velocity as a function of discharge, used to calculate reach mean Froude number and to convert the predicted values of relative velocity and depth to absolute values. These quantities can be estimated for a future channel profile using slope and roughness according to Manning (1891) or Strickler (1923). As our model employs width-weighted velocity, and not the area-weighted velocity that results from one-dimensional modelling, a translation between the two must be employed, as demonstrated in chapter 3.

Substrate size characterization, including the median grain size, can be determined according to Bovee and Milhous (1978) and can generally be assumed to be unaffected by the type of rehabilitation measures we describe.

Mean flow and survey (or ‘representative’) flow. Mean flow can be determined from historical records. Survey flow should be set to a value of interest which will depend on the inputs required for any subsequent ecological assessments.

Equations to estimate the variables in the first bullet above, as a function of various rehabilitation measures such as the removal of along-channel width constraints, have been implemented in the form of a probability network model (see chapter 3). Ecological response models will soon also be added to this framework to facilitate integrated assessment (Reichert et al. 2007).

Applications of the model with the parameters given in equation (6a-c) should be limited to rivers of size and slope similar to those included in our data set (see Table 2.1) and those which have a relatively natural flow regime. Since only rivers with sufficient gravel supply to form gravel bars were included in our analysis, the model should only be applied to rivers of this morphological type and not to rivers that are expected to be highly braided or channelized after rehabilitation. The presence of artificial constructions, such as weirs or groynes, should also preclude the application of the model with the parameters derived in this chapter. However, reach-scale rehabilitation projects usually target the removal of such artificial constructions. Further, because the model was derived for intermediate flow conditions (at survey flows between 5% and 100% of MQ), it should not be applied to flows outside of this range.

Acknowledgements

We thank Nicolas Lamouroux and Michael J. Stewardson, who contributed to this chapter through stimulating discussions, comments, and suggestions and provided a valuable data set that was used for exploratory purposes in the early stages of this study. This project was supported by the multidisciplinary Rhone-Thur project for scientific support of river rehabilitation projects in Switzerland, initiated and funded by the Swiss Federal Office for Water and Geology (BWG), the Swiss Federal Institute for Environmental Science and Technology (EAWAG) and the Swiss Federal Institute for Forest, Snow and Landscape Research (WSL).

Notation

MQ	mean discharge, m^3/s
q	survey discharge, m^3/s
v	velocity, m/s
\bar{v}	reach mean velocity, m/s
h	water depth, m
\bar{h}	reach mean depth, m
w	reach mean width, m
d_{50}	median substrate size, m
J	slope, dimensionless
ν	kinematic viscosity, m^2/s
g	gravitational acceleration, m/s^2
Fr	Froude number, $v/(g \cdot h)^{0.5}$, dimensionless
Re	Reynold's number, $(v \cdot h) / \nu$, dimensionless
Re_f	boundary Reynold's number $(v \cdot d_{50}) / \nu$, dimensionless

θ	dimensionless bottom shear stress $(\bar{h} \cdot J) / [(s - 1) \cdot d_{50}]$, where s is the ratio of sediment density to water density ≈ 2.6 , dimensionless
s_{mix}	mixing factor of a bivariate log-normal distribution and a bivariate normal distribution, dimensionless
N	bivariate normal distribution
LN	bivariate log-normal distribution
μ	mean
σ	standard deviation
ρ	correlation coefficient
x	relative velocity, dimensionless
y	relative depth, dimensionless
Y	relative width w/h , dimensionless
Z	relative roughness d_{50}/h , dimensionless

2.7 References

- Allan J D. 1995. Stream Ecology: Structure and Function of Running Waters. Chapman & Hall: London.
- Allen K R. 1951. The Horokiwi Stream. Fisheries Bulletin 10, New Zealand Marine Department, Wellington. 231 pp.
- Bovee K D. 1982. A guide to stream habitat analysis using the in-stream flow incremental methodology. Instream Flow Information Paper **12**, U.S. Fish and Wildlife Service, Fort Collins, CO.
- Bovee K D and Milhous R. 1978. Hydraulic simulation in instream flow studies: theory and techniques. Instream Flow Information Paper **5**, United States Fish and Wildlife Service, Fort Collins, Colorado.

- Brooks A J, Haeusler T, Reinfelds I, and Williams S. 2005. Hydraulic microhabitats and the distribution of macroinvertebrate assemblages in riffles. *Freshwater Biology* **50**: 331-344.
- Clifford N J, Soar P J, Petts G E, Gurnell A M and Emery J C. 2002. Numerical flow modelling for eco-hydraulic and river rehabilitation applications: a case study of the River Cole, Birmingham, UK. In: Bousmar D and Zech Y (eds.) *River Flow 2002 - Proceedings of the International Conference on Fluvial Hydraulics*, 4-6 September 2002, Louvain-le-Neuve, Belgium, Lisse: Swets & Zeitlinger/Balema. 1195-1204.
- Davison A C and Hinkley D V. 1997. *Bootstrap Methods and Their Application*. Cambridge University Press, Cambridge, UK.
- Dennis, J E and Schnabel, R . 1983. *Numerical Methods for Unconstrained Optimization and Nonlinear Equations*. Prentice-Hall, Englewood Cliffs, NJ.
- Dobson A J. 1999. *An Introduction to Generalized Linear Models*. CRC Press, Boca Raton, FL. 174 pp.
- Efron B and Tibshirani R J. 1983. *An Introduction to the Bootstrap*. Chapman and Hall, New York, NY. 436 pp.
- Emery J C, Gurnell A M, Clifford N J, Petts G E and Soar P S. 2003. Classifying the performance of riffle-pool bedforms for habitat assessment and river rehabilitation design. *River Research and Applications* **19**: 533-549.
- Fasano G and Franceschini A. 1987. A multidimensional version of the Kolmogorov - Smirnov test. *Monthly Notices of the Royal Astronomical Society* **225**: 155-170.
- Fausch K D, Hawkes C L, and Parsons M G. 1988. Models that predict standing crop of stream fish from habitat variables, 1950-85. Gen. Tech. Rep. PNW-GTR-213. Portland, OR, U.S. Department of Agriculture, Forest Service, Pacific Northwest Research Station. 52 pp.
- Hardy T B. 1998. The future of habitat modeling and instream flow assessment techniques. *Regulated Rivers: Research & Management* **14**: 405-420.
- Hostmann M, Borsuk M, Reichert P, Truffer B. 2005. Stakeholder values in decision support for river rehabilitation. *Large Rivers* **15**(1-4). *Arch. Hydrobiol. Suppl.* **155**/1-4: 491-505.
- Ihaka R and Gentleman R. 1996. R: A language for data analysis and graphics. *Journal of Computational and Graphical Statistics* **5**: 299-314.
- Jowett I G. 1989. River hydraulic and habitat simulation, RHYHABSIM computer manual. New Zealand Fisheries Miscellaneous Report **49**. Ministry of Agriculture and Fisheries, Christchurch 39 pp.

- Jowett I G. 1993. A method for objectively identifying pool, run, and riffle habitats from physical measurements. *New Zealand Journal of Marine and Freshwater Research* **27**: 241-248.
- Jowett I G. 1998. Hydraulic geometry of New Zealand rivers and its use as a preliminary method of habitat assessment. *Regulated Rivers: Research and Management* **14**: 451-466.
- Jowett I G. 2002. In-stream habitat suitability criteria for feeding inanga (*Galaxias maculatus*). *New Zealand Journal of Marine and Freshwater Research* **36**: 399-407.
- Jowett I G. 2003. Hydraulic constraints on habitat suitability for benthic invertebrates in gravel-bed rivers. *River Research and Applications* **19**: 495-507.
- Kemp J L, Harper D M and Crosa G A. 1999. Use of 'functional habitats' to link ecology with morphology and hydrology in river rehabilitation. *Aquatic Conservation: Marine and Freshwater Ecosystems* **9**: 159-178.
- Lamouroux N, Statzner B, Fuchs U, Kohmann F, Schmedtje U. 1992. An unconventional approach to modeling spatial and temporal variability of local shear stress in stream segments. *Water Resources Research* **28**: 3251-3258.
- Lamouroux N, Souchon Y, Herouin E. 1995. Predicting velocity frequency distributions in stream reaches. *Water Resources Research* **31**: 2367-2375.
- Lamouroux N. 1998. Depth probability distributions in stream reaches. *Journal of Hydraulic Engineering* **124**: 224-227.
- Lamouroux N and Jowett I G. 2005. Generalized instream habitat models. *Canadian Journal of Fisheries and Aquatic Sciences* **62**: 7-14.
- Logan P and Brooker M P. 1983. The macroinvertebrate faunas of riffles and pools. *Water Research* **17**: 262-270.
- Manning R. 1891. On the flow of water in open channels and pipes. *Transactions of the Institution of Civil Engineers of Ireland* **20**: 161-207.
- Orth D J and Maughan O E. 1983. Microhabitat preferences of benthic fauna in a woodland stream. *Hydrobiologia* **106**: 157-168.
- Peacock J A. 1983. Two-dimensional goodness-of-fit testing in astronomy. *Monthly Notes of the Royal Astronomical Society* **202**: 615-627.
- Peter A, Kienast F, and Woolsey S. 2005. River rehabilitation in Switzerland: scope, challenges and research. *Archiv für Hydrobiologie, Supplement Volume* **155**: 643-656.
- Press W H, Flannery B P, Teukolsky S A, and Vetterling W T. 1992. *Numerical Recipes in C: The Art of Scientific Computing*. Cambridge University Press, Cambridge, UK. pp. 645-649.

- Pridmore R D and Roper D S. 1985. Comparison of the macroinvertebrate faunas of runs and riffles in three New Zealand streams. *New Zealand Journal of Marine and Freshwater Research* **19**: 283-291.
- Quinn J M and Hickey C W. 1994. Hydraulic parameters and benthic invertebrate distributions in two gravel-bed New Zealand rivers. *Freshwater Biology* **32**: 489-500.
- Reichert P, Borsuk M, Hostmann M, Schweizer S, Spörri C, Tockner K and Truffer B. 2007. Concepts of decision support for river rehabilitation. *Environmental Modelling and Software* **22**: 188-201.
- Schnabel R B, Koontz J E and Weiss B E. 1985. A modular system of algorithms for unconstrained minimization. *ACM Trans. Math. Software*, 11, 419-440.
- Schneider M. 2001. Habitat- und Abflussmodellierung für Fliessgewässer mit unschaften Berechnungsansätzen. Weiterentwicklung des Simulationsmodells CASiMiR. Ph.D., 146 pp., Institut für Wasserbau, Universität Stuttgart, Mitteilungen 106.
- Schweizer S, Borsuk M E, Reichert P. 2007. Predicting the hydraulic and morphological consequences of river rehabilitation. *River Research and Applications*. *In press*.
- Statzner B, Gore J A, Resh V H. 1988. Hydraulic stream ecology: observed patterns and potential applications. *Journal of the North American Benthological Society* **7**: 307-360.
- Stewardson M J and McMahon T A. 2002. A stochastic model of hydraulic variations within stream channels. *Water Resources Research* **38**: 1-14.
- Strickler A. 1923. Beiträge zur Frage der Geschwindigkeitsformel und der Rauigkeitszahlen für Ströme, Kanäle und geschlossene Leitungen, Mitteilung Nr. **16** des Amtes für Wasserwirtschaft; Eidg. Departement des Inneren, Bern.
- Thomas J A and Bovee K D. 1993. Application and testing of a procedure to evaluate transferability of habitat suitability criteria. *Regulated Rivers* **8**: 285-294.
- Wheaton J M, Pasternack G B, Merz J E. 2004. Spawning habitat rehabilitation - II. Using hypothesis development and testing in design, Mokelumne River, California, USA. *Intl. J. River Basin Management* Vol. **2**(1): 21-37.

3 PREDICTING THE MORPHOLOGICAL AND HYDRAULIC CONSEQUENCES OF RIVER REHABILITATION

S. Schweizer¹, M. E. Borsuk², and P. Reichert¹

¹ Swiss Federal Institute of Aquatic Science and Technology (Eawag),
P.O. Box 611, 8600 Dübendorf, Switzerland

² Department of Biological Sciences, Dartmouth College,
Hanover, New Hampshire, 03755 USA

3.1 Abstract:

Decisions about reach-scale river rehabilitation for the purposes of flood protection and ecological enhancement require prediction of the possible consequences of management alternatives. To provide such predictions, an integrative model is necessary that represents the cause-effect relations between rehabilitation options and morphological, hydraulic, and ecological consequences. This chapter describes the morphological and hydraulic submodel of such an integrative model. This submodel is further subdivided into four modules predicting: (1) channel morphology, (2) flooding (dike overtopping, floodplain flooding, and bed moving floods), (3) velocity and depth distribution, and (4) riverbed siltation. Model relationships come from results reported in the literature and new data analyses. By using quantities that are all either readily available or easily predictable for changed conditions, the model should be widely applicable, even for data-limited situations. The overall model is implemented as a probability network to facilitate estimation of uncertainties in model results. An application of the model to a reach of the Thur River in Switzerland demonstrates its utility for predicting morphological and hydraulic consequences of a planned river widening. The full integrative model, including ecological endpoints, will be used together with quantitative assessments of stakeholder preferences to support rehabilitation decisions for a number of Swiss rivers.

3.2 Introduction

In the last 200 years, many river systems throughout the world have been regulated and channelized (Petts, 1989). These alterations have been conducted mainly to extend agricultural and urban areas, enable or facilitate river navigation, and reduce flooding risk. This has resulted in a dramatic reduction of river floodplain area and loss of hydraulic and morphological variability (Ward et al, 2001). These changes decrease the habitat quality for organisms living in or near a regulated river. Thus, the abundance, biomass and diversity of aquatic and terrestrial organisms are affected, leading to a functional alteration of the river ecosystem (Peter, 1998).

In Switzerland, only about 10% of all rivers remain in a natural or near natural state (BUWAL, 1997). Therefore, there is a need for ecological rehabilitation. Although historically most funding for river construction has been granted for the purposes of additional flood control, a recent federal requirement to include ecological rehabilitation measures in flood control projects has provided new opportunities (Peter et al, 2005).

To improve our understanding of the ecological and socio-economic consequences of river rehabilitation projects and provide advice for future efforts, the interdisciplinary “Rhône/Thur River Rehabilitation Project” was recently initiated (Peter et al., 2005, <http://www.rivermanagement.ch>). One subproject of this research program is the development of an integrative river rehabilitation model (IRRM) to predict the hydraulic-morphological situation after river management actions and the resulting changes in the terrestrial and aquatic ecosystems. The focus is on reach-scale rehabilitation actions that primarily involve widening the stream corridor and allowing the river to take a more natural course. Therefore, the primary decision is how much space to give the river so that an optimal trade-off between benefits and costs is obtained. Although developed for use in Switzerland, the model is intended to be as generally applicable as possible.

The IRRM is formulated as a probability network model (Pearl, 1988) and represents the relevant cause-effect-relations within and among the important biotic and abiotic factors, leading to attributes (model endpoints) of concern to river system stakeholders. Together with a model of the preference structure for different levels of these attributes (Hostmann et al, 2005a), the IRRM is intended to provide a comprehensive basis for supporting river rehabilitation decisions (Reichert et al., 2007).

In this chapter, we describe the hydraulic and morphological submodel that provides the foundation for predicting all the biotic and abiotic attributes of interest (Figure 3.1). This submodel is based to a large degree on results already published in the literature by other research groups. The major goal of our effort is to combine such approaches into an overall picture of morphological and hydraulic river development (channel morphology, flooding, velocity and depth distribution, riverbed siltation) and to explicitly estimate

uncertainty in model predictions. A secondary goal is to fill remaining gaps through new data evaluations. Because endpoints were selected according to their relevance for ecological assessment, the submodel described here can be used as the basis for other submodels aimed at predicting ecological consequences of river rehabilitation, such as impacts on bankline vegetation and fauna, benthic water plants, macroinvertebrates, and fish. Such models are being developed and reported separately by our research group (e.g. Borsuk et al., 2006). An economic input-output model has also been developed to predict the effects of construction work and new recreational activity on the local economy (Spörri et al., 2006). Interactions between the submodels (e.g. the effect of bankline shading on water plants, the influence of macroinvertebrate biomass on fish, the effect of morphology on recreational use) are also being considered (see Fig.3.1).

We begin by outlining the approach taken to model morphology and hydraulics. We then describe the model equations and implementation, and finally demonstrate application to a section of the Thur River, Switzerland, for which rehabilitation is planned.

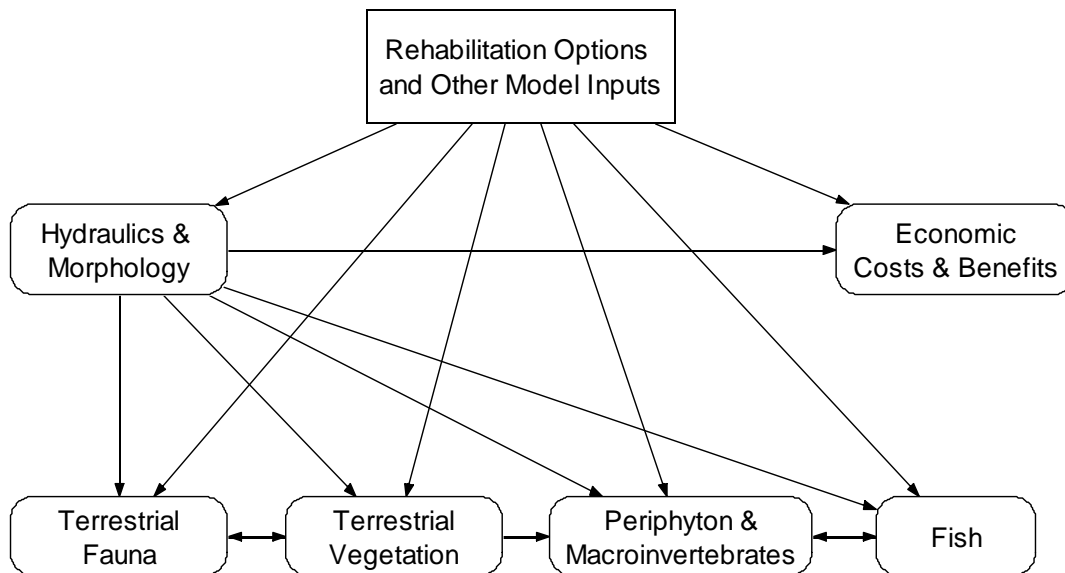


Figure 3.1: Structure of the integrative river rehabilitation model (IRRM). Rounded boxes represent submodels and the rectangular box denotes rehabilitation options (e.g., river width constraints, flood plain and dike height, distance between dikes) and other model inputs (e.g., slope, gravel size). Note that the submodel “Hydraulics & Morphology” has an influence on all other submodels.

3.3 Model Description

The development of an integrative model usually requires scientific knowledge in a variety of forms including literature review, experimental and field results, other models, and, in the absence of other information, expert judgment. For this reason, we chose to implement the IRRM as a probability network (Pearl, 1988). This approach makes it relatively simple to combine different sources of information to represent cause-effect relations, to simultaneously consider different spatial and temporal scales, and to explicitly include uncertainties in model inputs, structure and outcomes (Borsuk et al., 2004). The sources of information used to derive each submodel are described explicitly in the following sections.

Because all biotic endpoints of interest (including terrestrial fauna, riparian vegetation, aquatic benthos, and fish) are influenced by hydraulics and river morphology (see Figure 3.1), IRRM construction began with this abiotic submodel. The focus is on predicting variables that are required as inputs for the economic and biotic submodels. These include river morphology, flooding (dike overtopping, floodplain flooding, and bed moving floods), joint spatial patterns of depth and velocity, and degree of riverbed siltation. Modules to predict these attributes are described in the following subsections.

Table 3.1: Model parameter distributions

Variable	Equation	Distribution	Units	Median	Standard Deviation
ε_w	(2a-c)	Lognormal	-	1.0	0.71
A_{St}	(4)	Normal	$m^{0.5} \cdot s^{-1}$	23.5	2
ε_1	(5b)	Triangular [0.92, 1.08]	-	1	0.034
ε_2	(5c)	Triangular [0.69, 1.31]	-	1	0.126
ε_3	(5d)	Triangular [-0.37, 0.37]	-	0	0.15
ε_4	(6)	Normal	-	0	0.4
a	(9)	Uniform [4.5; 5.5]	-	5	0.289
b	(9)	Uniform [1.5; 1.6]	-	1.55	0.029
θ_{Cr}	(9)	Uniform [0.045; 0.050]	-	0.0475	0.001
ε_5	(11)	Normal	-	0	0.004
b_1	(14)	Normal	-	-2.34	0.79
b_2	(14)	Normal	-	-2.27	0.31
b_3	(14)	Normal	-	-0.04	0.02
b_4	(14)	Normal	-	2.03	0.69
e	(17)	Normal	$m \cdot kg^{-1}$	$1.2 \cdot 10^{12}$	$1.2 \cdot 10^{11}$
f	(20)	Normal	m^{-1}	$3.3 \cdot 10^{11}$	$1.7 \cdot 10^{10}$

3.3.1 Channel Morphology

River channel pattern is an important model endpoint on its own and is also a fundamental determinant of hydraulic habitat characteristics. Whether a river is single- or multi-threaded depends on the balance between stream power, bed composition, and external width constraints (van den Berg, 1995). While a number of researchers have developed diagrams separating channel patterns based on flow-related parameters (e.g. da Silva, 1991), these have generally been descriptive, in that they require advanced knowledge of the channel geometry, which is pattern-dependent. To overcome this difficulty, we start with a truly predictive method for distinguishing between multi- and single-thread rivers in the absence of width constraints (section 2.1.1). Next, we consider the effect of width constraints on this natural morphology (section 2.1.2). Finally, we check if the gravel supply from upstream is sufficient relative to the transport capacity within the reach to allow morphological structures to develop (section 2.1.3). Figure 3.2 summarizes the overall procedure for predicting channel morphology under a given set of conditions.

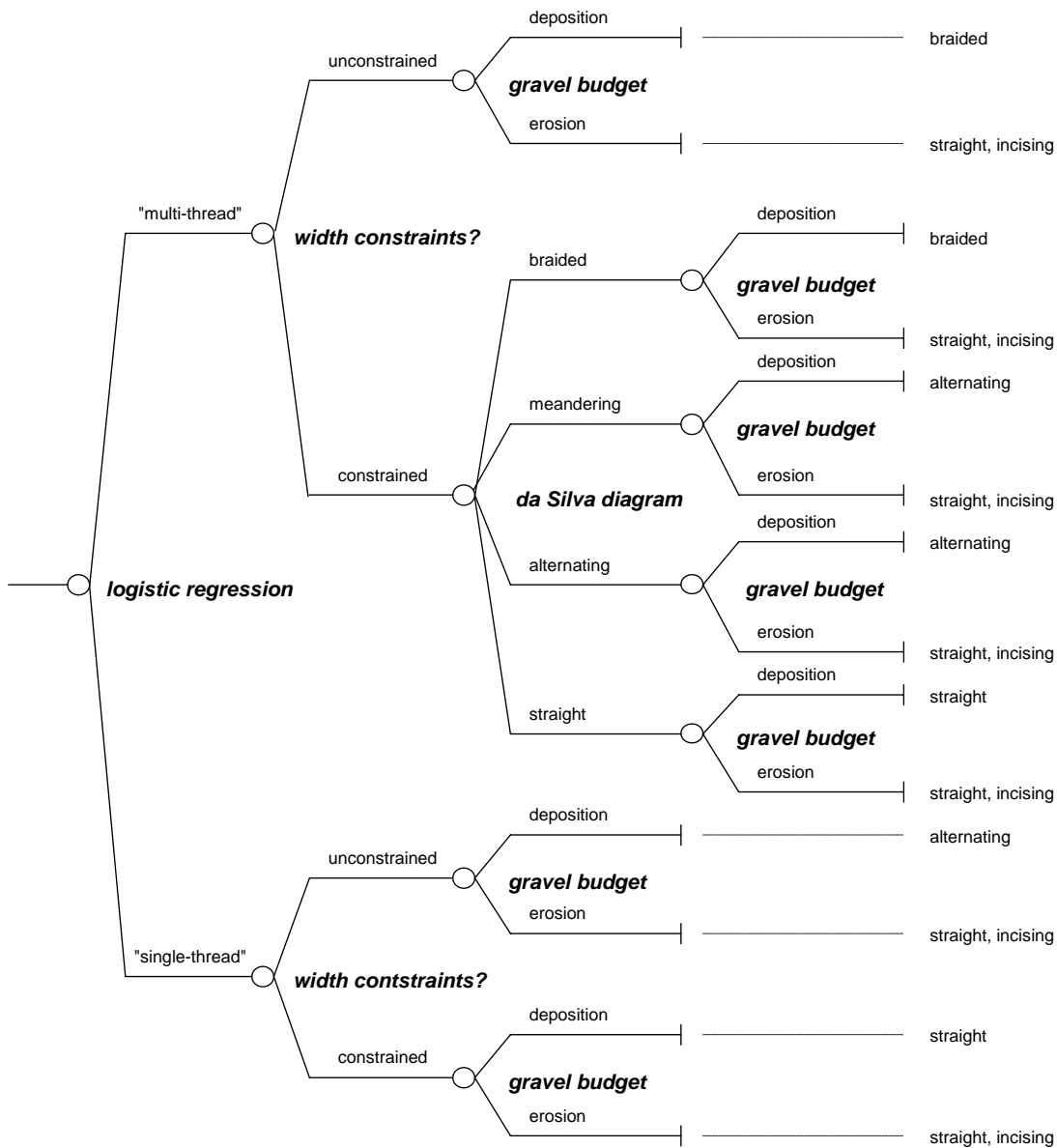


Figure 3.2: Event tree illustrating the procedure for predicting channel morphology based on: (1) the logistic regression of Bledsoe & Watson (2001), (2) consideration of width constraints (from the estimation of the natural width using equation 2a, 2b or 2c), (3) the pattern diagram of da Silva (1991), and (4) the gravel budget.

3.3.1.1 Natural Morphology

Van den Berg (1995) developed a predictive method for distinguishing between multi- and single-thread rivers that requires only the pattern-independent properties of mean annual flood discharge, gravel size, and valley slope. Bledsoe and Watson (2001) made this approach probabilistic by fitting a logistic regression model to data from 127 unconstrained, gravel-bed rivers. Of the several fitted relationships, we chose one which gives the probability, p_m , of a multi-thread pattern as,

$$p_m = \frac{\exp\left[3.00 + 5.71 \cdot \log_{10}\left(J_V \cdot \sqrt{Q_a}\right) - 2.45 \cdot \log_{10}(d_{50})\right]}{1 + \exp\left[3.00 + 5.71 \cdot \log_{10}\left(J_V \cdot \sqrt{Q_a}\right) - 2.45 \cdot \log_{10}(d_{50})\right]} \quad (1)$$

where J_V is valley slope, Q_a is mean annual flood discharge (m^3s^{-1}), and d_{50} is median gravel diameter (m) (Bledsoe and Watson, 2001). Equation (1) is formulated probabilistically, accounting for uncertainty in the predicted channel pattern. Therefore, it does not contain an error term, as later equations do.

Neither Van den Berg (1995) nor Bledsoe and Watson (2001) provide a means to estimate the width of the predicted natural river form. Therefore, we used their data set to derive regression estimates of width as functions of discharge, valley slope, and gravel size for three possible river patterns. These analyses yielded, for multi-thread rivers,

$$w_{bf} = 2.61 \cdot Q_a^{0.49} \cdot d_{50}^{-0.76} \cdot \varepsilon_w \quad (2a)$$

for single-thread meandering rivers,

$$w_{bf} = 4.86 \cdot Q_a^{0.49} \cdot \varepsilon_w \quad (2b)$$

and for single-thread straight rivers,

$$w_{bf} = 3.36 \cdot Q_a^{0.49} \cdot \varepsilon_w \quad (2c)$$

where w_{bf} is bankfull width (m), assumed to occur at the mean annual flood discharge, Q_a is mean annual flood discharge (m^3s^{-1}), d_{50} is median gravel diameter (m), and ε_w is a lognormally-distributed error term with median of 1.0 and standard deviation of 0.71 (Table 3.1), as estimated by the regression procedure. Valley slope was not a significant predictor for any river pattern, and gravel size was only significant for multi-thread rivers. The exponent on discharge was not significantly different for the three river patterns (all at the 0.01 significance level). The three equations accounted for 80% of the

variation in width across the studied rivers ($R^2=0.80$). The remaining unexplained variation is accounted for in the model by the error term, ε_w .

3.3.1.2 *Width-Constrained Morphology Assuming Sufficient Gravel Supply*

Single-thread rivers may be either straight, meandering, or sinuous with alternating side bars (da Silva, 1991, Jäggi, 1983). In most locations where rehabilitation is being considered, the space required to restore a meandering pattern is impractical given present land use. Therefore, we expect that, as long as there is sufficient gravel supply (see Section 2.1.3), rivers predicted to be single-threaded according to equation (1) will be sinuous with alternating side bars unless the constrained width is narrower than the natural width predicted by equation (2c), in which case the river will be straight.

Rivers predicted to be multi-threaded according to equation (1) might yet be single-threaded if width constraints are too severe. This can be checked using the pattern diagram of da Silva (1991) for a known gravel size, channel geometry, and mean depth at bankfull discharge (see Figure 3.6 in Section 3.4.2), which is assumed to equal the mean annual flood discharge (Van den Berg, 1995). Width at mean annual flood discharge is estimated from equation (2), accounting for any width constraints, and mean depth of single-thread rivers is estimated iteratively using the equation of Strickler (1923),

$$J = \frac{1}{k_{st}^2} \left(\frac{P}{A} \right)^{4/3} \left(\frac{Q}{A} \right)^2 \quad (3)$$

where J is channel slope (assumed here to equal valley slope, J_v), k_{st} is Strickler's coefficient ($\text{m}^{1/3}\text{s}^{-1}$), P is wetted perimeter (m), A is cross-sectional area (m^2), and Q is discharge (m^3s^{-1}). For single-thread meandering (alternating gravel bar) rivers, we assumed a triangular cross-section with an angle calculated from the estimated width and mean depth. For single-thread straight rivers, we assumed a trapezoidal cross-section with a fixed bank angle. In eq. (3), Strickler's coefficient, k_{st} , is estimated as,

$$k_{st} = \frac{A_{st}}{\sqrt[6]{d_{90}}} \quad (4)$$

where d_{90} is 90th percentile of gravel diameter (m) and A_{st} is a coefficient with probability distribution given in Table 3.1. This distribution accounts for values reported in the literature ranging from 21 to 26 $\text{m}^{1/3}\text{s}^{-1}$ (Strickler, 1923, Meyer-Peter & Müller, 1948, Schöberl, 1981).

To estimate the water depth for braided rivers, we used a method developed by Zarn (1997) based on the logarithmic flow law (Keulegan 1938) and on flume experiments.

His method employs a notional transformation of the braided reach into a theoretical, rectangular substitution-channel thereby accounting for a reduced wetted width B_w (m) (due to non-inundated gravel bars) and slope (-) (due to sinuosity S of the braids). When discharge Q (m^3/s), valley slope J_v (-), mean gravel size d_m (m) and width constraints w_{bf} (m) are given, the equations (5a)-(5g) can be solved iteratively to estimate mean water depth h (m):

$$Y = \frac{w_{bf}}{h} \quad (5a)$$

$$S = (1.081 - 0.087 \cdot e^{-0.011Y}) \cdot \varepsilon_1 \quad (5b)$$

$$B_w = (1.05 \cdot w_{bf} \cdot e^{-0.0016Y}) \cdot \varepsilon_2 \quad (5c)$$

$$A_K = \left(12.9 \cdot e^{1.041 \cdot \frac{h}{B_w}} - 1.78 \cdot e^{3.104 \cdot \frac{h}{B_w}} \right) + \varepsilon_3 \quad (5d)$$

$$c = 2.5 \cdot \ln \left(\frac{A_K \cdot R}{2 \cdot d_m} \right) \quad (5e)$$

$$v_m = c \cdot \sqrt{g \cdot R \cdot \frac{J_v}{S}} \quad (5f)$$

$$Q = v_m \cdot B_w \cdot h \quad (5g)$$

where Y is relative width (-), A_K is a constant of the logarithmic flow law (-), c is a coefficient of flow resistance (-), g is the gravitational acceleration (9.81 m/s^2), R is the hydraulic radius (m), v_m is mean flow velocity (m/s) and ε_1 , ε_2 , and ε_3 , are error terms describing uncertainty in equations (5b-d), as estimated from the figures of Zarn (1997) (see Table 3.1). Because these error terms can lead to values of S , B_w , and A_K that make the iteration procedure very slow to converge, we used a surrogate error model in the final implementation. To do this, we simulated results for equations (5a-g) for a wide range of values for w_{bf} , Q , J , and d_{50} . We then statistically estimated the dependence of the coefficient of variation of depth (CV_h) on these four predictor variables using a stepwise regression procedure. The resulting equation predicted CV_h with an R^2 value of 0.99 and can be written as,

$$CV_h = 0.098 - 0.013 * \log(w_{bf}) + 0.006 * \log(Q) - 0.073 \cdot J_v^{0.5} \quad (5h)$$

Predictions of h in the final model, h_{pred} , then consist of the deterministic prediction, h_d , as estimated by equations (5a-g) without the three error terms, multiplied by a lognormal error term with median of one and coefficient of variation equal to CV_h .

The number of channels expected in an unconstrained multi-thread river is predicted using the relation identified by Robertson-Rintoul and Richards (1993) in an analysis of 21 braided rivers,

$$n_b = \text{round}[1 + 5.52 \cdot (Q_a J_v)^{0.40} d_{84}^{-0.14} + \varepsilon_4] \quad (6)$$

where n_b is the number of braids, d_{84} (m) is the 84th percentile of gravel size, and ε_4 is an additive error term estimated from figure 4 in Robertson-Rintoul and Richards (1993) (see Table 3.1). To account for width constraints, we multiply the predicted number of channels by the ratio of the constrained width to the natural width predicted by equation (2). Developing vegetation on gravel bars may influence gravel movement during floods and thus reduce the number of predicted braids. This effect is not currently considered in the model.

3.3.1.3 Final Width-Constrained Morphology under Actual Gravel Supply

Regardless of predicted morphology, mid- or side-channel gravel bars will not develop unless there is a net deposition of gravel in the reach. Therefore, performing a comparison between the gravel supply from upstream and the estimated transport capacity within the study reach is a critical task for rehabilitation planning.

We assume the upstream input to be known, while the transport capacity within the reach, Q_b ($\text{m}^3 \text{s}^{-1}$), is calculated as the product of a specific transport capacity, q_b ($\text{m}^2 \text{s}^{-1}$), and the width, w (m),

$$Q_b = w \cdot q_b \quad (7)$$

The computation of the specific transport capacity is based on the method of Meyer-Peter and Müller (1948) who developed the following formula for Swiss rivers:

$$q_b = \Phi \sqrt{(s-1)g} d_m^3 \quad (8)$$

where Φ is a dimensionless transport capacity, s is the ratio of sediment to water density (-) and d_m is the mean gravel diameter (m).

In our model, the dimensionless transport capacity Φ is estimated from a modification of the bed load formula of Meyer-Peter and Müller (1948),

$$\Phi = a \cdot (\theta - \theta_{Cr})^b \quad (9)$$

where a and b are dimensionless empirical parameters (dimensionless), θ_{Cr} is the dimensionless bottom shear stress at the initiation of gravel movement (see Table 3.1), and θ is the actual dimensionless bottom shear stress, calculated as,

$$\theta = \frac{R \cdot J_v}{(s-1) \cdot d_m} \quad (10)$$

After analysing the original data of Meyer-Peter & Müller (1948), Wong & Parker (2006) found that the formula can mispredict transport capacity due to: (1) the application of an unnecessary bed roughness correction to cases of plane-bed morphodynamic equilibrium and (2) a flow resistance parameterisation in terms of the Nikuradse roughness height, which has been shown (after the publication date of Meyer-Peter & Müller's work) to be inappropriate for the characterisation of mobile bed conditions in rivers. Hunziker (1995), Hunziker & Jäggi (2002), Smart & Jäggi (1983) and Smart (1984) have also concluded that the relation of Meyer-Peter & Müller (1948) can mispredict bedload transport under plane-bed conditions. Thus, in contrast to conventional applications of equation (9), we consider uncertainty in the parameters a , b and θ_{Cr} (Table 3.1) which accounts for the combined findings of the authors cited in this paragraph.

In braided rivers, the flow (and thus the transport of gravel) is usually concentrated to only one or two main braids or channels (when the gravel bars are inundated). To account for higher shear stresses in these braids, Zarn (1997) proposes an augmentation of the dimensionless bottom shear stress calculated from equation (10) according to:

$$\theta_{Correction} = \theta_{Cr} \cdot (0.3 - e^{-0.005 \cdot (Y+211)}) + \varepsilon_5, \quad Y > 30 \quad (11a)$$

$$\theta_{Correction} = 0, \quad Y \leq 30 \quad (11b)$$

where ε_5 is an error term describing uncertainty in the derivation of this formula as estimated from the data of Zarn (1997).

The purpose of the gravel transport calculations is to predict whether the gravel supply into a river reach is sufficient for the development of morphological structures, given transport capacity within the reach, not to develop a detailed gravel budget. Therefore, annual gravel transport capacity (for both single and multi-thread morphologies) is calculated by cumulating the daily transport estimated using daily discharge. When there is net annual erosion, we assume that a straight, incising channel will result. When there is net deposition, we assume that the morphologies predicted in section 2.1.2 will

develop. Incision may be prevented by the installation of weirs and other bed stabilization measures or the reduction of upstream gravel retainment. These may be additional management options for a rehabilitation project. If an accurate gravel budget is needed prior to project implementation, we recommend the use of more sophisticated hydraulic models.

3.3.2 Flooding

Floods are a fundamental element of river ecosystems. Bed-moving floods affect the development of periphyton, macroinvertebrate and fish communities, floodplain and gravel bar flooding influences riparian flora and fauna, and dike overtopping exerts severe social and economic impacts. Besides the frequency of floods, the duration, timing, and magnitude are also important characteristics influencing biota.

In the IRRM, we calculate the critical discharges for these types of floods under the predicted morphological conditions (see section 2.1) and then use historical hydrograph data to determine the expected timing, frequency, and duration. To do this, we assume a rectangular cross section for flood conditions and translate the critical floodwater depth into discharge using Strickler's formula (equation 3) for single-thread rivers and Zarn's (1997) method (equation 5a-h) for braided rivers. Critical water depths for the different types of floods are determined as follows:

- **Bed moving floods** - We calculate the dimensionless bottom shear stress θ_D necessary for river bed delamination by applying the formula of Günther (1971).

$$\theta_D = \theta_{Cr} \cdot \left(\frac{d_{mD}}{d_m} \right)^{2/3} \quad (12)$$

where d_{mD} is the mean diameter of the armour layer (m), d_m is the mean diameter of bed material (m), and θ_{Cr} is the critical shear stress. We then use Equation (10) to determine the water depth corresponding to this value of shear stress.

- **Floodplain flooding** - Floodwater depth is equal to the floodplain height, which is determined by the rehabilitation design
- **Dike overtopping** - Dike height is another value determined by the rehabilitation design.

3.3.3 Velocity and Depth Distribution

The quality of habitat for aquatic biota is strongly influenced by velocity and depth characteristics. Previous authors have demonstrated the usefulness of describing point-wise variation in these hydraulic variables using frequency distributions and have related the form and shape of these distributions to easily obtained predictor variables (Lamouroux et al., 1995, Lamouroux, 1998). However, meso-habitats and stream biota have been shown to be associated with distinct combinations of these two variables, rather than responding to depth and velocity separately (Kemp et al., 1999, Statzner et al., 1988). Therefore, predictions of the univariate distributions of these variables are not sufficient for habitat characterization or prediction.

We developed a model for the joint distribution of depth and velocity using survey data from 92 stream reaches in New Zealand (Chapter 2, Schweizer et al., 2007). We found that, for each reach, the bivariate distribution of relative velocity and relative depth can be described by a mixture of two end-member distributions, one normal and the other lognormal, each with fixed parameters:

$$f\left(x = \frac{v}{v_m}, y = \frac{h}{h_m}\right) = (1 - s_{mix}) \cdot N_{y>0}(\mu_{xN} = 1, \mu_{yN} = 1, \sigma_{xN} = 0.52, \sigma_{yN} = 0.52, \rho_N = 0.12) + s_{mix} \cdot LN(\mu_{xLN} = 1, \mu_{yLN} = 1, \sigma_{xLN} = 1.19, \sigma_{yLN} = 1.09, \rho_{LN} = 0.01) \quad (13)$$

where v_m and h_m are the width-weighted mean velocity and depth, respectively, s_{mix} is a mixing parameter describing the relative contribution of each shape, N represents the normal distributional component and LN the lognormal component, the subscript $y>0$ indicates that the normal distribution was truncated to only include positive values of depth, the μ represent the means of the relative velocity and depth of the (non-truncated) normal and lognormal distributions, the σ represent the corresponding standard deviations, and the ρ are the correlation coefficients.

For a particular reach at a particular discharge, we found that the parameter s_{mix} can be predicted from the dimensionless characteristics: reach mean Froude number Fr , reach mean relative roughness Z (d_{50}/h), and relative discharge q/MQ (ratio of actual discharge to mean discharge), as follows:

$$\ln\left(\frac{s_{mix}}{1 - s_{mix}}\right) = b_1 + b_2 \cdot \ln(Fr) + b_3 \cdot Z^{-1} + b_4 \cdot \left(\frac{q}{MQ}\right)^{0.5} \quad (14)$$

where the values of the four parameters b_1 to b_4 (including their uncertainties) are given in Table 3.1. The three predictors of equation (14), as well as mean velocity, v_m , and

mean depth, h_m , for use in eq. (13) can be readily estimated, even for changed channel morphology, using one-dimensional hydraulic modelling based on Strickler's equation for single-thread rivers (eq. 3) and on Zarn's (1997) method for braided rivers (eq. 5 a-h). In the model, we assume that the two bivariate distributions of eq. (13) apply to both alternating gravel bar and braided morphologies. Additionally, we assume that the predictors included in eq. (14) will control the hydraulic patterns of the two morphologies in a similar way. We attempted to test these two assumptions for the braided rivers in the New Zealand data set (see chapter 2, Schweizer et al. 2007). We were able to confirm that the two end-member distributions of eq. (13) were as appropriate for braided rivers as for alternating gravel bar rivers. However, the braided rivers had estimated values of s_{mix} that did not span a very broad range, thus preventing us from rigorously testing eq. (14).

While braided and alternating gravel bar rivers may be treated similarly, straight rivers can be expected to be fundamentally different. They are likely to be more homogeneous in spatial patterns of velocity and depth, consistent with the assumption of a trapezoidal cross-section. Such a cross-section is also likely to lead to stronger correlation between velocity and depth. Straight rivers were not among those included in the data set used in chapter 2. Therefore, to develop a model for the velocity-depth distribution of straight rivers, we used survey data collected from BWG (Swiss Federal Office for Water and Geology) for three stream reaches in Switzerland. Sets of velocity and depth measurements were conducted between 17 and 61 times within each stream reach to account for the effect of changing stage.

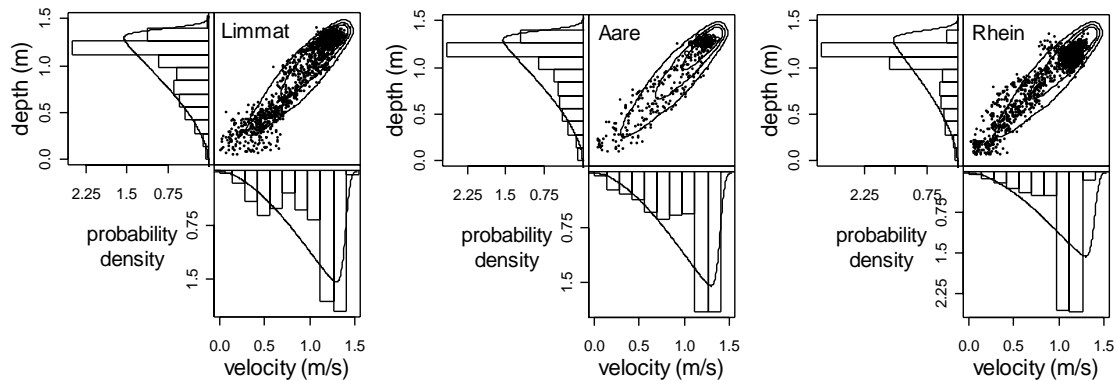


Figure 3.3: Bivariate distribution (joint and marginal densities) for relative velocity and relative depth for straight rivers. Points and histograms represent data, and contour lines and density curves represent modelled distribution. Contour lines indicate the regions containing 25, 75, and 95% of the probability mass. (For details see section 2.3)

We found that for the straight morphology type, the joint distribution of relative velocity ($x=v/v_m$) and relative depth ($y=h/h_m$) can be adequately described by beta-distributed marginals with fixed parameters ($\mu_{x\beta} = 1$, $\mu_{y\beta} = 1$, $\sigma_{x\beta} = 0.291$, $\sigma_{y\beta} = 0.303$, $scale=1.4$) that are correlated with a rank correlation coefficient of 0.94 according to the method of Iman and Conover (1982) (Figure 3.3).

Many published studies have related the occurrence of stream-dwelling organisms to hydraulic units, such as pools, runs, and riffles (e.g. Logan and Brooker, 1983), and this categorization is employed by some ecological models (Fausch et al., 1988). Given a quantitative definition of point hydraulic units in terms of depth and velocity, the relative frequency of each unit can be directly calculated from the predicted bivariate distribution. For example, Jowett (1993) found that pool habitat was associated with values of the Froude number less than 0.18 and a velocity/depth ratio less than 1.24 s^{-1} , riffle habitat with Froude number greater than 0.41 and a velocity/depth ratio greater than 3.20 s^{-1} , and run habitat with intermediate values. We employ these definitions in the model. However such definitions may be site-specific. Therefore, we generally recommend use of the full joint frequency distributions for habitat assessment, as in Kemp et al. (1999).

3.3.4 Riverbed Siltation

Fish and benthic species depend on the interstitial gravel zones to provide cover and egg incubation habitat. Therefore, siltation and clearance of the bed matrix are crucial ecological processes. Additionally, the content of fine particles in the river bed influences water exchange between surface and ground water, thus affecting groundwater regeneration.

Conceptually, we model gravel bed siltation as a process that occurs at low to medium discharges at a rate which depends on hydraulic and bed characteristics. As a result of this process, the percent of fines in the river bed increases and the hydraulic conductivity of the river bed is reduced. Occasionally, high flows flush the river bed, restoring the original structure and gravel-size distribution (Schälchli, 1993, 1995). The temporal progression of the build up of fines between high flows can be calculated as the product of the suspended particle concentration and the volume of water filtered through the gravel bed,

$$\frac{dm_{fines}}{dt} = C_t \frac{dV_A}{dt} = C_t \frac{\Delta h_w \cdot g}{v \cdot \gamma} \quad (15)$$

where m_{fines} is the mass of fines (kg), V_A is the volume of filtered water per unit area ($\text{m}^3 \cdot \text{m}^{-2}$), t is the time since the last flushing event (s), C_t is the concentration of suspended particles ($\text{kg} \cdot \text{m}^{-3}$), Δh_w is the pressure head difference between channel and groundwater (m), ν is kinematic viscosity ($\text{m}^2 \cdot \text{s}^{-1}$), and γ is the infiltration resistance (m^{-1}), all at time t .

According to Schälchli (1995), the resistance γ is itself a function of m_{fines} ,

$$\gamma = r \cdot m_{\text{fines}} + \beta \quad (16)$$

where r is the specific infiltration resistance ($\text{m} \cdot \text{kg}^{-1}$) and β is the infiltration resistance of an unsilted river bed (m^{-1}). Schälchli (1995) gives a formula for estimating the value of r as,

$$r = \frac{e \cdot \theta^{0.5}}{\left(\frac{d_{10}}{d_m}\right)^{3.5} \cdot \text{Re}_f^{1.5} \cdot i^{0.67}} \quad (17)$$

where i is the hydraulic gradient (-), Re_f is the particle Reynold's number (-), d_{10} is 10th percentile of gravel diameter (m) and e is an empirical parameter of Schälchli's formula ($\text{m} \cdot \text{kg}^{-1}$) (Table 3.1). The value of Re_f is calculated as,

$$\text{Re}_f = \frac{d_m \cdot \sqrt{g \cdot (s-1)} \cdot d_m}{\nu} \quad (18)$$

and, β is calculated as,

$$\beta = \frac{L \cdot g}{k_0 \cdot \nu} \quad (19)$$

where L is seepage length (m) ($L = \frac{\Delta h_w}{i}$).

When the deposition and resuspension of particles are in equilibrium, siltation of a river bed stops. Schälchli (1995) gives a formula to estimate the limit of infiltration resistance γ_{max} (m^{-1}) as,

$$\gamma_{\text{max}} = \frac{f \cdot \left(\frac{d_{10}}{d_m}\right)^{1.25} \cdot \text{Re} \cdot i^{2.5} \cdot \left(\frac{C_t}{\rho_w}\right)^{0.75}}{\theta} \quad (20)$$

where ρ_w is water density ($\text{kg} \cdot \text{m}^{-3}$) and f is an empirical parameter (m^{-1}) derived by Schälchli (1995) (Table 3.1).

We use the percentage of fines in the river bed at a particular time as a measure of the degree of gravel bed siltation. This is calculated as,

$$f_{fines} = \frac{m_{fines}}{m_{fines} + m_{coarse}} = \frac{m_{fines}}{m_{fines} + (1 - \phi)H\rho_{sed}} \quad (21)$$

where m_{coarse} is the mass of coarse bed material (kg), ϕ is porosity (-), H is the siltation depth (m) (estimated by Schälchli (1995) as $H=3d_m+0.01$ m), and ρ_{sed} is the gravel density ($\text{kg}\cdot\text{m}^{-3}$).

The magnitude of flow sufficient to clear the river bed can be calculated from comparisons of the dimensionless shear stress (see Eq. 10) with bed stability. A bottom shear stress of sufficient magnitude to initiate bed disturbance and gravel flushing (complete clearance of deposited particles), θ_D , is calculated according to equation (12) derived by Günther (1971). In the interim between floods, bottom shear stress is assumed to not exceed θ_D nor θ_{Cr} so that the river bed is not disrupted.

The water depth associated with a bottom shear stress value of θ_D can be calculated from equation (10) and then related to a critical discharge using Strickler's formula (eq. 3) for single-thread rivers and Zarn's (1997) method for braided rivers (eq. 5 a-h). The frequency of this discharge, together with the siltation rate, determines the temporal extent and severity of siltation.

Because of spatial differences in the bottom shear stress, we apply the siltation equations separately to average conditions in pools and runs. We assume that significant siltation will not occur in riffles due to the very high filter velocities.

3.3.5 Model Implementation

The equations described in the above sections were implemented in Analytica, a commercially available software program for evaluating probability network models (Lumina, 1997). In principle, the IRRM could also be implemented using other software. We chose Analytica because it allows for a wide variety of probability distributions and functional model forms. The major inputs to the model (Figure 3.4) can be determined from historical data for the river system of interest, and the decision variables can be set to values corresponding to current conditions, decision alternatives, or scenarios used for sensitivity analysis. A large sample of realizations is then drawn for each probability distribution in the model using random Latin hypercube sampling. These samples are

propagated to model endpoints, thus conveying the uncertainty in model results. This information can either be considered directly by decision-makers or combined with a model of stakeholder preferences to yield decision theoretic results (Reichert et al., 2007).

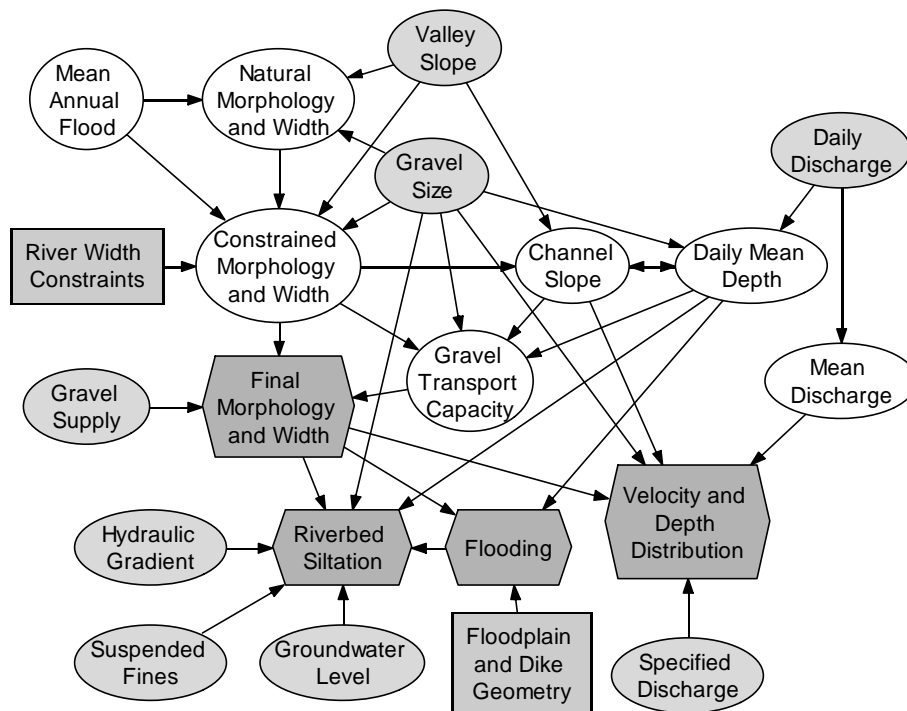


Figure 3.4: Simplified schematic of the hydraulic and morphologic model as implemented in Analytica. Shaded rectangular nodes represent management controls, shaded round nodes represent important site specific input variables, white round nodes represent intermediate variables, and dark shaded hexagonal nodes represent model endpoints. Arrows represent important causal influences between variables, and the double arrow indicates the application of Zarn's iterative approach (1997) for calculating mean depth for braided rivers (For details see sections 2.1 to 2.4).

3.4 A Case Study

3.4.1 Inputs

We use a case study at the Thur River, Switzerland (Figure 3.5), to demonstrate application of the hydraulic and morphologic model. The Thur River lies in the northeast of Switzerland with a total catchment area of 1750 km². Over the past centuries, the Thur River has been channelized and the area of floodplains has been drastically reduced (Frauenlob, 2003). After a series of large floods between 1960 and 1980, authorities realised that the present flood protection level was no longer adequate (Amt für Umwelt, 1999).

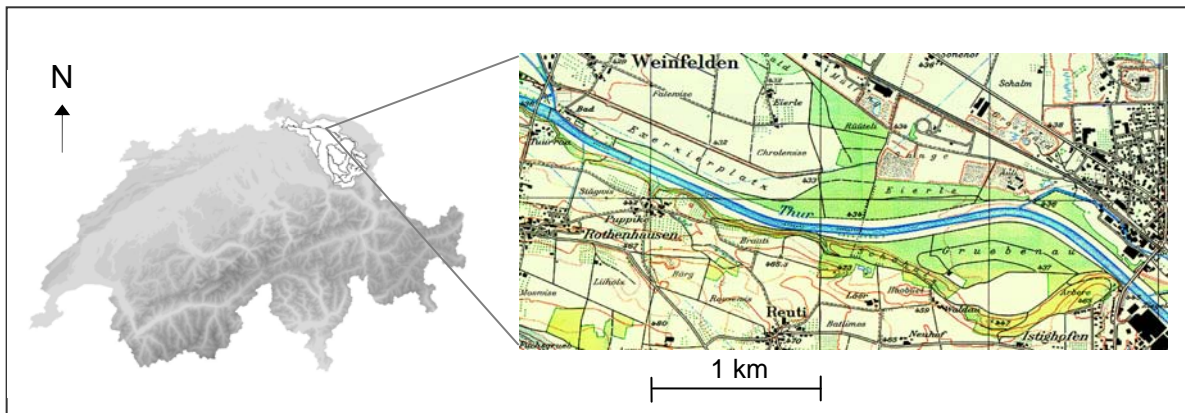


Figure 3.5: Location of the case study site and the Thur River basin in Switzerland. (From Hostmann et al., 2005a) (created with permission of swisstopo (BA067890))

The case study focuses on an intended rehabilitation project at the Thur River between the towns of Weinfelden and Bürglen (Figure 3.5) where the channelized river is approximately 30 m wide with a median discharge of 26 m³/s (Table 3.2). The project area stretches over a length of 4 km and a width of 300 to 1000 m. Dikes are located at the border of the project area, protecting the surrounding towns and villages from a 100-year flood.

We considered two scenarios: (i) present conditions (river width constraints at 30 m and a distance between dikes of 300-1000 m); and (ii) a possible river widening up to 200 m (by reducing floodplain height and returning this area to the river) while maintaining the

present dike width of 300-1000 m (Table 3.2). The distance between dikes includes the width of the floodplains. These two scenarios correspond loosely to the alternatives presented by Hostmann et al. (2005a). For the present state, the model results can be directly compared with current conditions, while for the rehabilitated scenario only model predictions will be available.

Table 3.2: Model inputs for the Thur River between the towns of Bürglen and Weinfelden. For uncertain variables, $T(a, b, c)$ = triangular distribution with minimum at a , mode at b and maximum at c , $N(m_N, s_N)$ = normal distribution with median at m_N and standard deviation of s_N , $LN(m_{LN}, s_{LN})$ = lognormal distribution with median at m_{LN} and geometric standard deviation of s_{LN} and Δh = (daily mean depth - yearly mean depth).

Model input	Value
River width constraints w_{bf} (present state) [m]	30
River width constraints w_{bf} (after rehabilitation) [m]	200
Distance between Dikes [m]	300-1000
Height of Dike [m]	6
Height of Floodplain (present state) [m]	3
Height of Floodplain (after rehabilitation) [m]	1
Slope J [‰]	2.0
Mean Annual Flood Discharge Q_a [m ³ /s]	610
Mean Discharge MQ [m ³ /s]	41
Median discharge Q_{50} [m ³ /s]	26
d_{50} [cm]	3.1
d_{90} [cm]	6.0
Gravel Supply [m ³ /a]	N(15000, 1000)
Porosity ϕ [%]	LN(25, 1.08)
Hydraulic conductivity of unsilted bed material k_0 [m/s]	0.0002
Hydraulic gradient i [-]	T(0.1, 0.5, 0.9)
Pressure head Δh_w [m]	$7 + 0.56 * \Delta h$

Static model inputs are given in Table 3.2. Gravel supply at this section of the Thur River is estimated to be between 14000 and 16000 m³ per year (Schälchli et al 2005). Porosity ϕ (%), hydraulic conductivity of unsilted bed material k_0 (m/s), the hydraulic gradient i (-) and the pressure head Δh_w (m) were estimated from unpublished studies at adjacent Thur reaches and from groundwater maps. For dynamic model inputs, we used

time series data of discharge, suspended particle concentration, and water temperature for five representative years 1990-1994. Discharge was measured daily and ranged from 4 to 596 m³/s, with a median of 23 m³/s. Suspended particle concentration was measured biweekly and daily values were estimated from a log-log regression against discharge. Water temperature was also measured biweekly, and daily values were represented by a sinusoidal curve fitted by Hari et al. (2006). For all uncertain input variables and model parameters (see Table 3.1 and 3.2), 1000 random Latin hypercube samples were drawn and propagated through the model equations.

3.4.2 Results

Under current conditions in the study section of the Thur River, the transport of gravel out of the reach exceeds upstream inputs. Thus a straight, incising river bed is predicted by the model and readily confirmed by observation. If this section were to be free of any width constraints, the logistic regression (Eq. 1) predicts that the natural river form is more likely to be single-threaded (i.e. straight, meandering, or alternating gravel bars with 68% probability) than multi-threaded (i.e. braided with 32% probability). The constrained channel morphology would then depend on the severity of width constraints, as predicted by the pattern diagram of da Silva (1991).

When the width is constrained, points on the da Silva diagram move from upper left to lower right, eventually crossing into more homogeneous forms (Figure 3.6). When uncertainty in the predicted values of (h/d) and (B_f/h) is considered, these predictions can be interpreted probabilistically (Figure 3.7). It is clear that in the present state (30m), the river is predicted to be straight (as it actually is), and as more space is given to the river, the chance that the river produces alternating gravel bars increases. If the width is allowed to be 125m or more, there is a small chance that braids will form. For a 200m constraint, the probability of a braided form is 28%, while the probability of a straight form drops to 16%. The most likely morphology after widening would be alternating gravel bars with a probability of 56%. Beyond 300m, the probabilities of the various morphologies remain nearly constant at their unconstrained values. If the river should be braided, however, the number of braids is expected to increase linearly with width, up to the maximum number given by Equation (6), in this case eleven. With a 200m width constraint between 1 and 6 braids are expected to form.

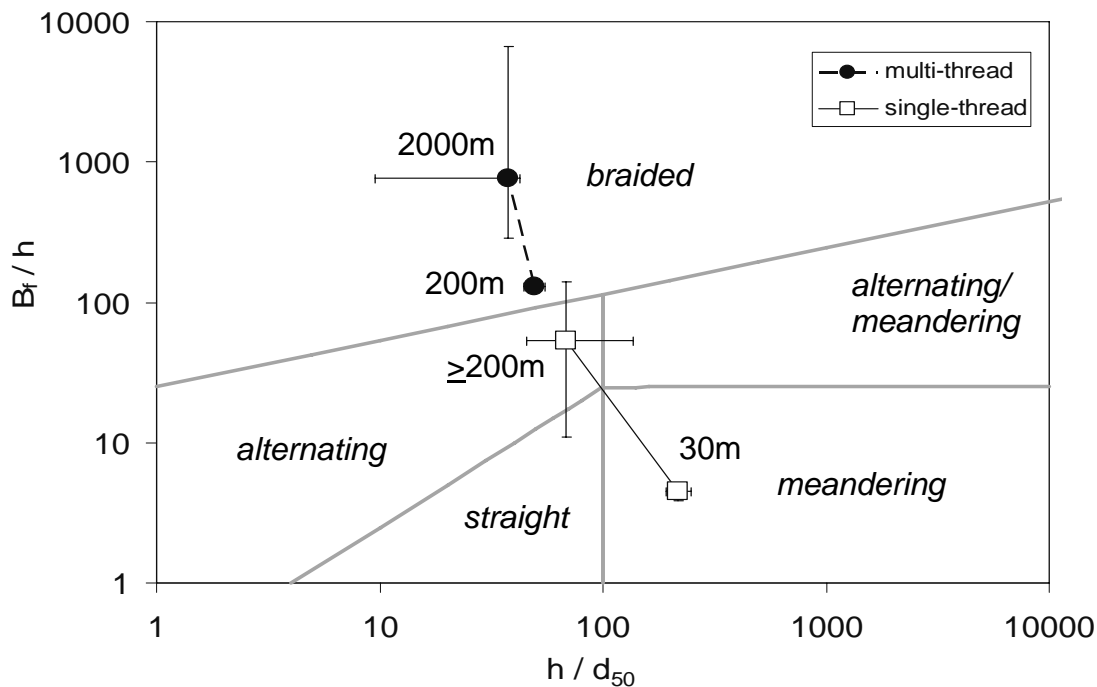


Figure 3.6: Pattern diagram of da Silva (1991) for predicting channel morphology. Position of the present state (30m), and widenings to 200m and 2000m are shown for a channel pattern that is predicted by eq. (1) to be either multi-thread (filled circles) or single-thread (open squares). Error bars indicate the 5th and 95th confidence limits on the axis variables. Rivers classified as meandering are assumed to actually be alternating due to space constraints. Additionally, alternating rivers that are constrained to less than their natural width are assumed to actually be straight. (h = water depth at bankfull discharge, w_{bf} = width at bankfull discharge, d_{50} = median gravel size)

If constrained width is greater than 60 or 70m, then the gravel transport capacity would be reduced sufficiently to yield gravel deposition rather than incising for both the single- and multi-thread river forms (Figure 3.8). Thus, the gravel should not be a limiting factor in the formation of morphology at these widths.

Mean water depth, mean velocity and their spatial distributions can be calculated from the model for any discharge below bankfull. To illustrate the difference in hydraulic conditions between the present state and for the 200m widening scenario, we used the discharge which occurs most frequently (mode, $Q=8\text{m}^3/\text{s}$) and the median discharge ($Q = 26\text{m}^3/\text{s}$) (Table 3.3). For the modal discharge, the two possible morphological outcomes of the widening scenario do not differ considerably from the present state with respect to mean width, depth and velocity, but a substantial increase in the variability of velocity and depth is predicted (Figure 3.9).

Table 3.3: Predicted hydraulic properties for the current state and the two possible morphological outcomes of the widening alternative for the most common discharge $Q=8 \text{ m}^3/\text{s}$ and the median discharge $Q=26 \text{ m}^3/\text{s}$. For both discharges, a significant increase in the variability of hydraulic habitats (pools, runs, riffles) is expected for the two morphological outcomes of the 200m widening scenario compared with the current straight channel.

	Q=8m ³ /s			Q=26m ³ /s		
	Present State (30m)	Widening Alternative (200m)		Present State (30m)	Widening Alternative (200m)	
	Straight	Alternating	Braided	Straight	Alternating	Braided
Mean Width (m)	21	23	58	22	36	89
Mean Depth (m)	0.4	0.5	0.2	0.9	0.7	0.4
Mean Velocity (m/s)	0.9	1.0	0.6	1.4	1.3	0.8
% Pools	0	21	16	0	19	15
% Runs	95	50	49	99	57	53
% Riffles	5	29	35	1	24	32

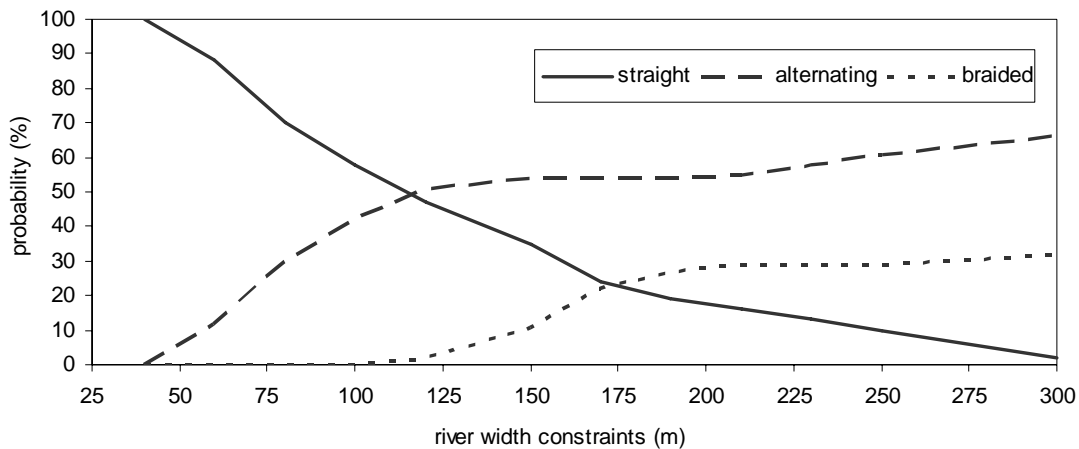


Figure 3.7: Probability of possible river forms as a function of river width constraint for the Thur River between the towns of Bürglen and Weinfeld. For the present state (river width constraint = 30m) a straight river form (solid line) is predicted with near certainty. If the river were to be widened to 200m, there would still be a 16% probability of a straight river form, but the probability of alternating gravel bars (dashed line) would increase to 56%, and the probability of a braided form (dotted line) would be 28%.

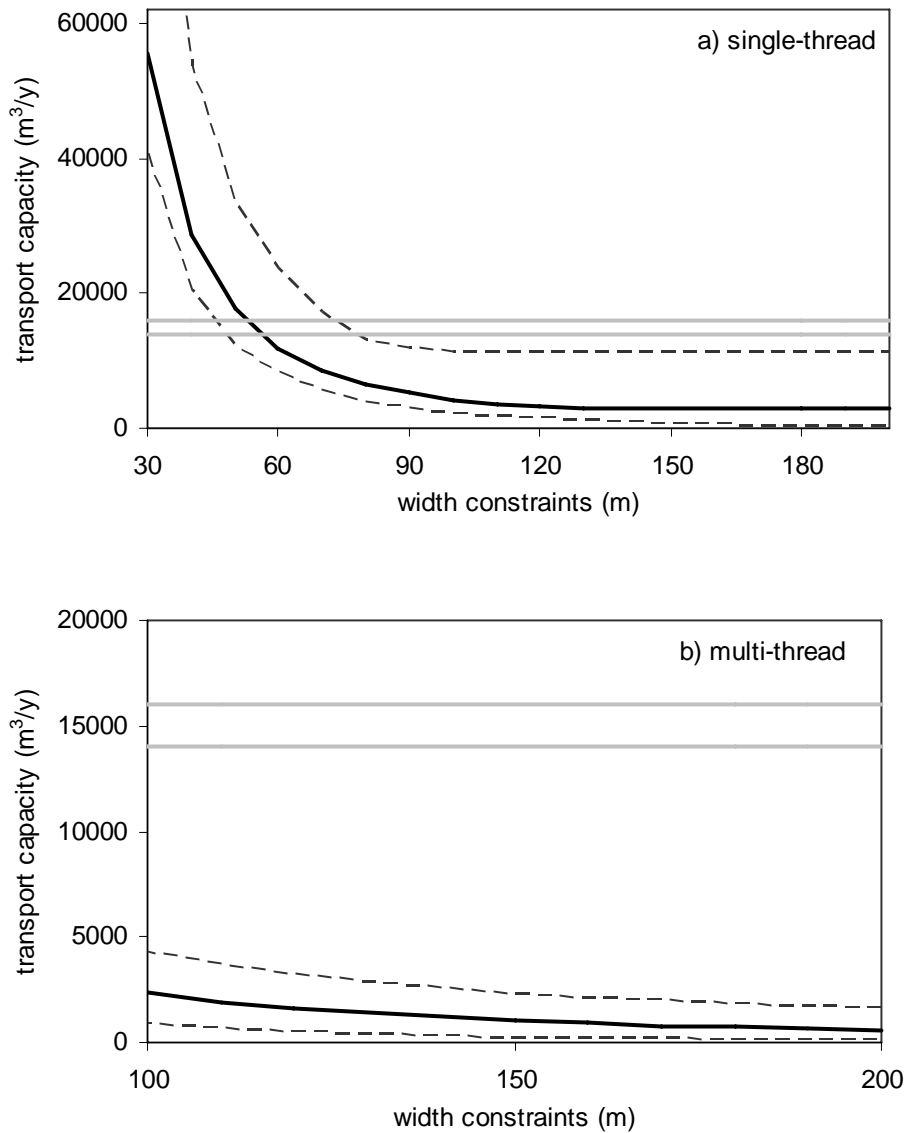


Figure 3.8: Gravel transport capacity as a function of width constraints for the Thur River between Weinfelden and Bürglen. The black solid line represents the median, and the thin dashed lines represent the 5th and 95th percentiles of estimated transport capacity for single- and multi-thread morphology. Gravel supply into this reach was estimated by Schälchli et al (2005) and is shown as minimum and maximum values in horizontal grey solid lines. It can be seen that for width constraints exceeding 60m, a sufficient gravel supply for the formation of gravel bars in single thread rivers can be expected. For braided rivers, gravel supply is always greater than transport capacity (results are not shown for braided rivers for widths less than 100 m, because this river form is not expected to develop under such conditions (see Figure3.7).

The two variables are also expected to vary much more independently from one another, relative to the present straight morphology. This is reflected in the predicted distribution of habitat units (i.e. pools, riffles, runs) (Table 3.3). The current hydraulic conditions are extremely homogenous (pools and riffles are almost absent), while after rehabilitation, whether the river takes on a braided or alternating form, approximately half of the river stretch will consist of either pool or riffle habitat. At the three times higher median discharge, it is apparent that higher flow increases the differences between the present and rehabilitated state with respect to average hydraulic conditions, whereas for all three morphologies, hydraulic variability decreases with increasing discharge (see Table 3.3).

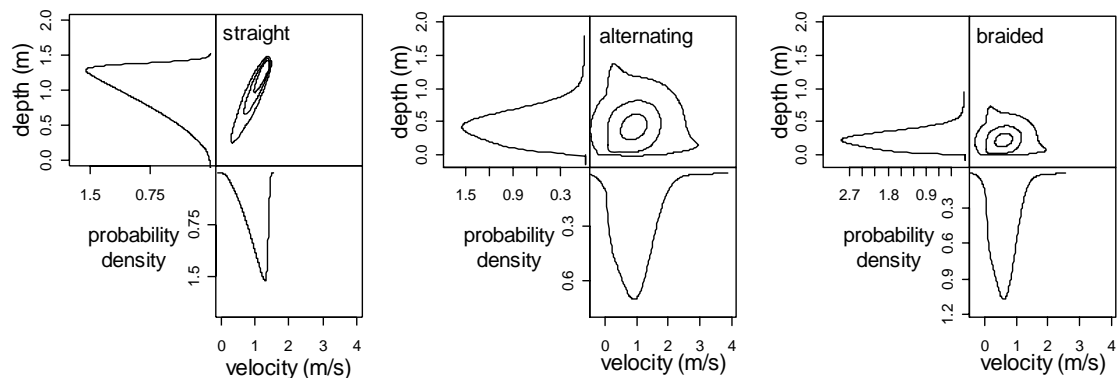


Figure 3.9: Predicted marginal and joint frequency distribution of depth and velocity at $Q = 8 \text{ m}^3/\text{s}$ (modal discharge) for the present state (30m) and for two possible morphological outcomes of the 200m widening scenario. Contour lines indicate the regions containing 25, 75, and 95% of the probability mass. A significant increase in the variability of hydraulic habitats (different combinations of velocities and depths) is predicted for both possible morphological outcomes of widening.

Model predictions indicate that the current, channelized river bed is flushed frequently thus leading to very little siltation (Figure 3.10). The average percent fines is predicted to be 1% (with a 90% predictive interval (PI) of 0 to 8%), a value similar to those actually measured in the field (unpublished data). This is due to the width constraints which cause higher water depths and thus higher dimensionless shear forces for a given discharge compared to a less constrained river. After widening, desiltation will occur less frequently (Figure 3.10b and 3.10c). The reduction of riverbed flushing events leads to a predicted average fine particle content after widening (assuming an alternating gravel bar form) of 5% (90% PI of 0 to 20%) in runs. Pools can be expected to have slightly higher rates of siltation (average fine particle content of 8% (90% PI of 0 to 25%) - see also Figure 3.10c).

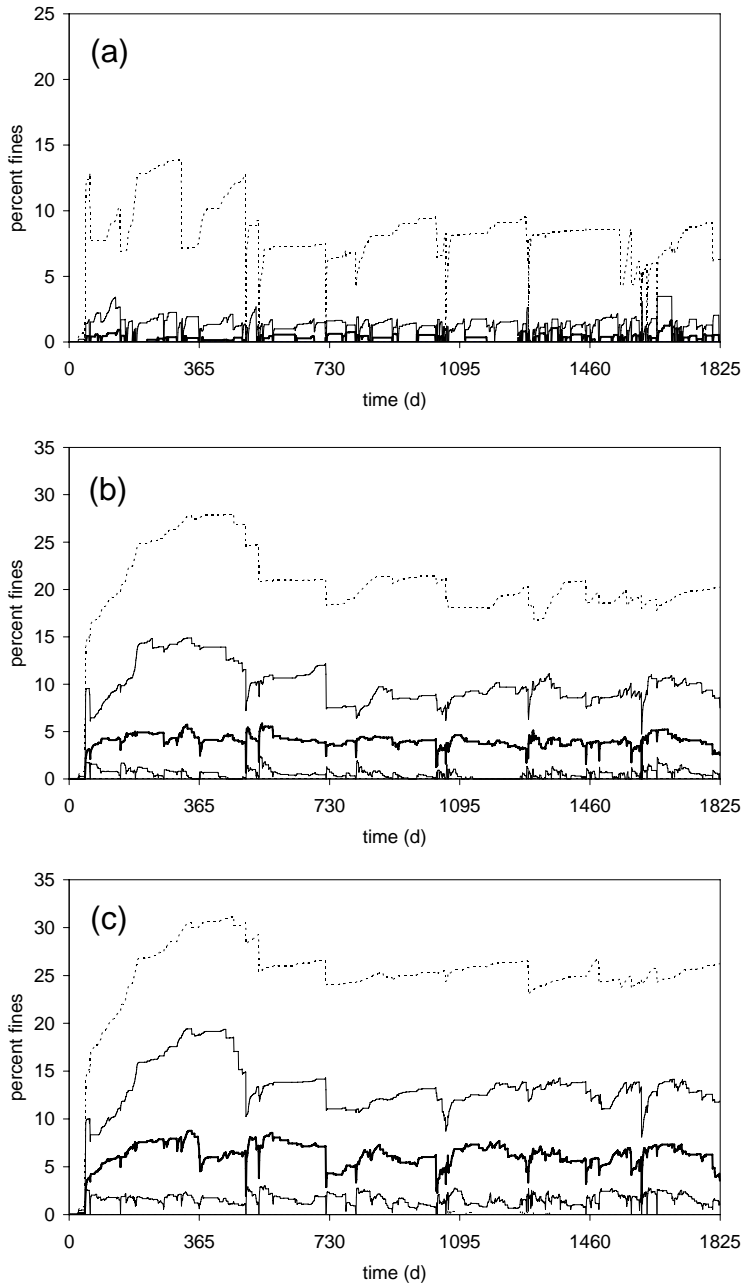


Figure 3.10: Predicted percent fines as a function of time over five representative years (1990-1994) for (a) the runs of the straight channel under current conditions, (b) the runs of the alternating gravel bar channel after 200m widening, and (c) the pools of the alternating gravel bar channel after 200m widening. The heavy solid line represents the median, the thin lines represent the 25th and 75th percentiles, and the dotted lines represent the 5th and 95th percentiles (across 1000 model runs). It is assumed that siltation is absent at time = 0 days.

While siltation conditions appear to worsen on average after widening, it should be kept in mind that a widened river is expected to be much more variable with respect to depth and velocity (see Figure 3.9). Therefore, during high discharges some areas are likely to be more deeply inundated than calculations based on average depths suggest. This will result in some local bed flushing that is not predicted by the model. Additionally, a widened river reach will contain 20 to 30% more riffles than a constrained river, and these can be expected to remain clear of fines due to their hydraulic conditions. Both of these phenomena will result in a mosaic of silted and clean riverbed sections in a widened river, rather than the spatial uniformity expected for a channelized river. From an ecological perspective, this may have important consequences.

Due to generally lower water depths in a widened river reach, the frequency of bed moving floods decreases from one per 33 days for the current conditions to approximately one per year for the 200m widening alternative. For the current conditions of 30m width and a 3m high floodplain, the model predicts that the floodplain will be flooded approximately 3-4 times in a year, as it actually is. If a floodplain height of 1m is chosen after rehabilitation (this is a management option) for both possible morphology types, a mean return period for floodplain flooding of 5 months is predicted for a braided river system and 1 month for an alternating gravel bar river. The difference between the two forms can be explained by the difference in predicted widths at mean annual flood discharge (200m for a braided river and 112m for a river with alternating gravel bars).

3.5 Discussion and Conclusions

A variety of models and data analyses have been reported in the literature to evaluate the primary determinants of river channel pattern, hydraulic and bed characteristics, and functional habitat. However, for river rehabilitation planning, these findings need to be applied simultaneously for predicting the overall outcome of alternative management measures. The model described here is one attempt to combine multiple analyses into a tool that can be used to forecast the features of a river after widening.

Based on the nature of the data used to develop our model, we believe it is appropriate to apply the model to gravel bed rivers with a relatively natural flow regime and mean discharge between 1 and 60 m³/s and slope less than 2%. Application to river sections with artificial constructions, such as weirs or groynes, should be avoided because these

structures will interfere with the development of natural morphological and hydraulic characteristics. However, river rehabilitation often targets the removal of such artificial constructions, thus allowing the use of the model to forecast the rehabilitated state. Because our joint velocity-depth model was derived for low to intermediate flow conditions (survey flows between 5% and 100% of mean discharge), this part of the model should not be applied to flows outside of this range. However, for the purposes of habitat assessment, these low flows are usually of most interest, because they define critical conditions. Therefore, this restriction should not be a practical limitation.

The definitions of pools, runs, and riffles that we employ are likely to be site-specific (see Jowett, 1993, Allen, 1951). Therefore, we recommend that further studies should be performed to better characterize the factors that control the development of these important hydraulic features. Alternately, the use of these features for habitat assessment could be bypassed and velocity-depth patterns be used directly, as by Kemp et al. (1999).

In the literature, many bed load formulae are reported. We chose a modified version of Meyer-Peter & Müller (1948) (see section 2.2) for single-thread rivers and Zarn's method (1997) for multi-thread rivers, since these approaches have been developed for Swiss midland gravel bed rivers which are the focus of our model. Although we attempted to only employ model inputs that are either readily available or easily predictable for modified conditions, estimations of gravel input to a reach may be difficult to obtain. This may be critical, as the success of river rehabilitation is directly affected by the gravel budget within the widened reach. Only if the supply is sufficient will morphological structures such as bars or braids form. Unfortunately, many rivers in Central Europe have lost their natural gravel regime due to upstream gravel retainment or extraction in the catchment area or measures to stabilize the shoreline and bed. Therefore, detailed hydraulic and gravel transport studies are recommended before initiating construction work.

Despite the limitations mentioned above, our case study at the Thur River, Switzerland, shows that our model yields useful information for rehabilitation planning. Since the gravel supply in a 200 m widening exceeds the estimated transport capacity, the channel morphology can be expected to change from the present straight channelized form to a river with alternating gravel bars with a probability of 56% and to a river with multiple braids with a probability of 28%. In either case, the new morphology would have a greatly increased variability of velocity and depth and contain a significant fraction of pools and riffles. Further widening would not significantly augment the likelihood of forming braids, but would probably lead to a greater number of braids should a multi-thread form develop. A widening would likely increase the average riverbed siltation (mean percentage of fines up from 1% to >5%) but would also result in a patchier structure, with zones of different degrees of siltation. The net result with respect to siltation on the aquatic ecosystem is equivocal.

Some of the abiotic endpoints predicted by our model (e.g. channel morphology, depth and velocity variability) are of direct interest to river stakeholders because they determine the recreation potential of the river system (Hostmann et al., 2005b). Moreover, they are of substantial indirect interest because of their influence on the biological status. For example, morphological form, velocity-depth patterns, distribution of habitat units (riffles and pools), and degree of riverbed siltation are all critical determinants of fish and benthic populations. Similarly, morphology and floodplain flooding frequency are fundamentally important controls on bankline vegetation and terrestrial fauna.

To formalize the relations between abiotic and biotic features, our model results can be combined with habitat preference functions to assess the suitability of conditions after rehabilitation for endangered or otherwise desirable species. The results can also be used as inputs for other types of ecological models, such as population or individual-based models, which predict biomass, abundance and/or functional groups of fish, macroinvertebrates, aquatic plants, bankline vegetation or fauna (e.g. Borsuk et al., 2006, Kemp et al, 1999, Lamouroux & Jowett, 2005). We are currently in the process of developing such links within the framework of probability networks (Reichert et al., 2007).

The use of the probability network structure makes it relatively easy to add further components. Submodels of water temperature variation, width variability, and relative bankline length could add utility to the model by allowing prediction of additional important attributes. Representation of the influence of rehabilitation projects on water quality could also improve our link between abiotic and biotic features. Finally, an additional investigation to assess the joint velocity-depth distribution for braided rivers would improve the model accuracy for this type of channel morphology.

An integrative model of the possible outcomes of river rehabilitation can be combined with stakeholder value assessments of those outcomes to provide comprehensive decision support for managers (Reichert et al., 2007). Such an analysis can improve a project's financial and public backing, as well as help guide selection of the most appropriate stream reaches and reach-specific rehabilitation measures. In the long term, repeated application of such a transparent and rational process should benefit both society and the environment.

Acknowledgements

This study was supported by the Rhone-Thur project, which was initiated and is funded by the Swiss Federal Office for Water and Geology (BWG), the Swiss Federal Institute for Environmental Science and Technology (EAWAG) and the Swiss Federal Institute for Forest, Snow and Landscape Research (WSL). For stimulating discussions, comments, advice and for sharing valuable datasets, we thank the many Rhone-Thur project partners, the Laboratory of Hydraulic, Hydrology, and Glaciology (VAW), D. Streit, A. Kohler, B. Sigrist, A. Burri (BWG), P. Requena-Méndez, H.-E. Minor, (VAW), N. Lamouroux, I. Jowett, M. Stewardson, U. Schälchli, P. Julien, and B. Bledsoe.

3.6 References

- Allen K R. 1951. The Horokiwi Stream. *Fisheries bulletin* **10**, New Zealand Marine Department, Wellington, 231 pp.
- Amt für Umwelt, Kanton Thurgau. 1999. *Die Thur - eine unberechenbare Grösse (The Thur River - an Unpredictable River)*. Frauenfeld, Switzerland.
- BUWAL (Swiss Agency for the Environment, Forests and Landscape). 1997. *Umwelt in der Schweiz (The Environment of Switzerland)*. Bern, Switzerland.
- Bledsoe B P and Watson C C. 2001. Logistic analysis of channel pattern thresholds: meandering, braiding, and incising. *Geomorphology* **38**: 281-300.
- Borsuk M E, Stow C A, and Reckhow K H. 2004. A Bayesian network of eutrophication models for synthesis, prediction, and uncertainty analysis. *Ecological Modelling* **173**: 219-239.
- Borsuk M E, Reichert P, Peter A, Schager E, Burkhardt-Holm P. 2006. Assessing the decline of brown trout (*Salmo trutta*) in Swiss rivers using a Bayesian probability network. *Ecological Modelling* **192**: 224-244.
- da Silva A M A F. 1991. *Alternate Bars and Related Alluvial Processes*, Master of Science Thesis, Queen's University, Kingston, Ontario, Canada.
- Fausch K D, Hawkes C L, and Parsons M G. 1988. Models that predict standing crop of stream fish from habitat variables, 1950-85. Gen. Tech. Rep. PNW-GTR-213. Portland, OR, U.S. Department of Agriculture, Forest Service, Pacific Northwest Research Station, 52 pp.

- Frauenlob G. 2003. Ökologisches Potenzial der Thur (Ecological potential of the Thur River). *Natur und Mensch* **5**: 14-21.
- Günther A. 1971. Die kritische mittlere Sohlenschubspannung bei Geschiebemischung unter Berücksichtigung der Deckschichtbildung und der turbulenzbedingten Sohlenschubspannungsschwankung (The critical mean bottom shear stress for varying bed materials regarding the development of armoured layers and fluctuations in the bottom shear stress). *Mitteilung Nr.3 der Versuchsanstalt für Wasserbau, Hydrologie und Glaziologie*, ETH Zürich.
- Hari R E, Livingstone D M, Siber R, Burkhardt-Holm P, Güttinger H. 2006. Consequences of climatic change for water temperature and brown trout populations in Alpine rivers and streams. *Global Change Biology* **12**: 10-26.
- Hostmann M, Borsuk M, Reichert P, Truffer B. 2005a. Stakeholder values in decision support for river rehabilitation. *Large Rivers* **15(1-4) Arch. Hydrobiol. Suppl.** **155/1-4**: 491-505.
- Hostmann M, Bernauer, T., Mosler H-J, Reichert P, Truffer B. 2005b. Multi-attribute value theory as a framework for conflict resolution in river rehabilitation. *Journal of Multi-Criteria Decision Analysis (JMCD)* **13**: 91-102.
- Hunziker R P. 1995. Fraktionsweiser Geschiebetransport (Bed load of different grain size fractions). *Mitteilungen der Versuchsanstalt für Wasserbau, Hydrologie und Glaziologie*, 138, Eidgenössische Technische Hochschule (ETH), Zürich, Switzerland, 209 pp.
- Hunziker R P & Jäggi M N R. 2002. Grain sorting processes. *J. Hydraul. Eng.*, ASCE, **128(12)**, 1060-1068.
- Iman R. L, Conover W. J, 1982. A distribution-free approach to inducing rank correlation among input variables. *Commun. Statist.-Simula. Computa.* **11**: 311-334.
- Jäggi M. 1983. Alternierende Kiesbänke: Untersuchungen über ihr Auftreten, den Zusammenhang mit der Bildung von Sohlenformen im allgemeinen, sowie ihre Auswirkungen auf Ufererosion und Fließwiderstand (Alternating gravel bars: Investigations of occurrence, their general relation to bed forms and their implications for bank erosion and flow resistance. *Mitteilung Nr.62 der Versuchsanstalt für Wasserbau, Hydrologie und Glaziologie*, ETH Zürich.
- Jowett I G. 1993. A method for objectively identifying pool, run, and riffle habitats from physical measurements. *New Zealand Journal of Marine and Freshwater Research* **27**: 241-248.
- Kemp J L, Harper D M, Crosa G A. 1999. Use of 'functional habitats' to link ecology with morphology and hydrology in river rehabilitation. *Aquatic Conservation: Marine and Freshwater Ecosystems* **9**: 159-178.

- Keulegan G H. 1938. Laws of turbulent flow in open channels. *Journal of Research of the National Bureau of Standards* **21** : 707-741.
- Lamouroux N, Souchon Y, and Herouin E. 1995. Predicting velocity frequency distributions in stream reaches. *Water Resources Research* **31**: 2367-2375.
- Lamouroux N. 1998. Depth probability distributions in stream reaches. *Journal of Hydraulic Engineering* **12**: 224-227.
- Lamouroux N & Jowett I. 2005. Generalized instream habitat models. *Canadian Journal of Fish and Aquatic Science* **61**(1): 7-14.
- Logan P & Brooker M P. 1983. The macroinvertebrate faunas of riffles and pools. *Water Research* **17**: 262-270.
- Lumina. 1997. *Analytica for Windows, User's Guide, Version 1.1*, Lumina Decision Systems, Denver, US.
- Meyer-Peter E and Müller R. 1948. Formulas for bedload transport. Proc. IAHR 3rd Congress, Stockholm.
- Pearl J. 1988. *Probabilistic Reasoning in Intelligent Systems*. Morgan Kaufmann, San Mateo, CA.
- Peter A. 1998. Interruption of the river continuum by barriers and the consequences for migratory fish. - In: Jungwirth M, Schmutz S & Weiss S (eds.): *Fish migration and fish bypasses*: 99-112. Fishing News Books, Oxford.
- Peter A, Kienast F, and Nutter S. 2005. The Rhone-Thur River project: a comprehensive river rehabilitation project in Switzerland. *Large Rivers* **15**: 643-656.
- Petts G E. 1989. Perspectives for ecological management of regulated rivers. In: Gore J A & Petts G E (Editors), *Alternatives in Regulated River Management*. CRC Press, Boca Raton, Fla.: 3-24.
- Reichert P, Borsuk M, Hostmann M, Schweizer S, Spörri C, Tockner K and Truffer B. 2007. Concepts of decision support for river rehabilitation. *Environmental Modelling and Software* **22**: 188-201.
- Robertson-Rintoul M S E & Richards K S. 1993. Braided channel pattern and palaeohydrology using an index of total sinuosity. In Best J L & Bristow C S (eds): *Braided Rivers*. Geological Society, special publication No. **75**: 113-118.
- Schälchli U. 1993. Die Kolmation von Fließgewässersohlen: Prozesse und Berechnungsgrundlagen (Siltation of riverbeds: Processes and methods for estimation) Mitteilungen der Versuchsanstalt für Wasserbau, Hydrologie und Glaziologie der ETH Zürich Nr. 124, 273 pp.
- Schälchli U. 1995. Basic equations for siltation of riverbeds. *Journal of Hydraulic Engineering* **121**(3): 274-287.

- Schälchli U, Abbegg J and Hunzinger L. 2005: Geschiebestudie Thur und Einzugsgebiet (Gravel report for the Thur River and its catchment area). Amt für Umwelt, Kantons Zürich, Thurgau, Appenzell and St. Gallen, Switzerland.
- Schöberl F. 1981. Abpflasterungs- und Selbststabilisierungsvermögen erodierender Gerinne (Delamination and self-stabilisation of eroding channels). *Österreichische Wasserwirtschaft Jahrgang* **33**, Heft 7/8: 180-186.
- Schweizer S, Borsuk M, Jowett J, Reichert P. 2007. Predicting joint frequency distributions of depth and velocity for instream habitat assessment. *River Research and Applications*. In press.
- Smart G M & Jäggi M N R. 1983. Sediment transport on steep slopes. *Mitteilungen der Versuchsanstalt für Wasserbau, Hydrologie und Glaziologie*, 64, Eidgenössische Technische Hochschule (ETH), Zürich, Switzerland, 191 pp.
- Smart G M. 1984. Sediment transport formula for steep channels. *J. Hydraul. Eng.*, ASCE, 110(3): 267-276.
- Spörri, C, Borsuk M, Peters I, Reichert P. 2006. The economic impacts of river rehabilitation: a regional input-output analysis. *Ecological Economics*, in press.
- Statzner B, Gore J A, Resh V H. 1988. Hydraulic stream ecology: observed patterns and potential applications. *Journal of the North American Benthological Society* **7**: 307-360.
- Strickler A. 1923. Beiträge zur Frage der Geschwindigkeitsformel und der Rauigkeitszahlen für Ströme, Kanäle und geschlossene Leitungen (Contributions to the formula of flow velocity and to the estimation of flow resistance for rivers, channels and closed conduits). Mitteilung Nr. 16 des Amtes für Wasserwirtschaft; Eidg. Departement des Inneren, Bern.
- Van den Berg J H. 1995. Prediction of alluvial channel pattern of perennial rivers. *Geomorphology* **12**: 259-279.
- Ward J V, Tockner K, Uehlinger U, and Malard F. 2001. Understanding natural patterns and processes in river corridors as the basis for effective river restoration. *Regulated Rivers: Research & Management* **17**: 311-323.
- Wong M & Parker G. (not yet published): Re-analysis and correction of bedload relation of Meyer-Peter and Müller using their own database. *Journal of Hydraulic Engineering*, accepted May 2006.
- Zarn B. 1997. Einfluss der Flussbettbreite auf die Wechselwirkung zwischen Abfluss, Morphologie und Geschiebetransportkapazität (Influence of river width on interactions between discharge, morphology and transport capacity). *Mitteilungen der Versuchsanstalt für Wasserbau, Hydrologie und Glaziologie* **154**, Eidgenössische Technische Hochschule (ETH), Zürich, Switzerland, 209 pp.

4 PREDICTING THE BIOMASS OF PERIPHYTON AND MACROINVERTEBRATE FUNCTIONAL FEEDING GROUPS IN STREAM REACHES

Steffen Schweizer¹, Mark E. Borsuk¹, Urs Uehlinger¹, Stephanie Bouletrêau²
and Peter Reichert¹

¹ *Eawag: Swiss Federal Institute of Aquatic Science and Technology,
8600 Dübendorf, and ETH Zürich, Switzerland*

² *Laboratoire d'Écologie des Hydrosystèmes,
UMR 5177 CNRS-Université Paul Sabatier, Toulouse, France.*

4.1 Abstract

Periphyton and invertebrates are important components of the trophic cascade in running waters due to their ability to produce organic material, decompose detritus, and serve as a food source for organisms at higher trophic levels. River rehabilitation (e.g. local habitat improvement or reach-scale widening of the river bed) often changes the morphological and hydraulic conditions of the river, affecting the development of periphyton and invertebrates. However, few predictive models exist which can support decision-making (e.g. where and how to conduct a rehabilitation activity). To provide such predictions, an integrative model is necessary that represents the cause-effect relations between rehabilitation alternatives and morphological, hydraulic, and ecological consequences. This chapter describes simple statistical periphyton and invertebrate models that can serve as submodels of such an integrative model. For model development and calibration, we used data on periphyton from 8 sites (3 different rivers, total sample size 286) and invertebrates from 2 sites (1 river, sample size 86) to derive a predictive river benthos model. Linear and non-linear regression analyses revealed that periphyton is most strongly influenced by the time since the last bed-moving flood and hydraulic conditions (in particular, flow velocity), whereas invertebrate functional groups are predominantly dependent on seasonality. For total invertebrates, collector-gatherers, and predators, regression models could be developed with R^2 values between 0.52 and 0.71. The representation of scrapers was somewhat less satisfying. Shredders and filterers were significantly less abundant in our data set and were therefore not modelled. Model development and complexity were severely limited by the small number of complete data

sets available. Additional long time series data on periphyton and invertebrate density from different rivers together with values of important variables influencing the benthos community dynamics, would be extremely useful to improve such simple prediction models.

4.2 Introduction

Careful planning of river rehabilitation requires predictions of the expected response of the river morphology and ecosystem to proposed management actions. To produce such predictions, we are developing an integrative river rehabilitation model (IRRM) (Reichert et al. 2007, Schweizer et al. 2007b, Spörri et al. 2007, Borsuk et al. 2006) which represents important cause-effect relations between critical influence factors and river system attributes. Together with a model of the stakeholders' preference structure for different levels of these attributes (Hostmann et al. 2005), the IRRM is intended to provide a comprehensive basis for supporting river rehabilitation decisions (Reichert et al. 2007). The present chapter describes the benthos community submodel for the IRRM.

Periphyton and invertebrates are primary and secondary producers in running waters that dominate the first levels of the trophic pyramid in many small and intermediate size rivers. While algae use radiation and nutrients to produce organic material, invertebrates perform diverse ecological functions and feed on various food bases: scrapers on periphyton; collector-filterers and -gatherers on organic material in the running water and sediment, respectively; shredders primarily on allochthonous inputs of leaves, seeds and small branches from the shoreline vegetation; and predators on other invertebrates. The next higher level of the trophic cascade is composed of fish which feed on macroinvertebrates and some additionally on periphyton (Power et al 1989). In this vein, periphyton and invertebrates exhibit bottom-up control on the complete ecological system of running waters. Furthermore, periphyton and invertebrates (mainly through their effect on periphyton) have a strong influence on oxygen and nutrient concentrations, pH, and the content of organic material, due to their metabolism (Reichert et al. 2001). From the socio-economic perspective, periphyton and macroinvertebrates exert further important influences on the river and its users. Blooms of algae or macrophytes reduce the cross-sectional area of a river and its flow velocity resulting in higher water levels (Bretschneider & Schulz 1985) and increasing the probability and frequency of dike overtopping. Moreover, algal blooms negatively affect the aesthetic value of a river and thus decrease the river's recreation potential. Since invertebrates gather or filter organic material from the river bed and flowing water, they influence water colour, clarity and odour. Moreover, anglers rely on fish abundance which depends partly on the availability

of macroinvertebrate biomass. These relations indicate that successfully predicting the benthos community in a river is essential for understanding the river ecosystem and its response to rehabilitation efforts.

Several previous attempts have been undertaken to model the dynamics of periphyton and macroinvertebrate biomass in river reaches. These attempts can be divided into mechanistic population dynamic models and statistical approaches that empirically relate abundance of functional groups to important external influence factors. Mechanistic models generally give better and more detailed insights into the ongoing processes within a system. However, as these models represent a relatively large number of processes, they tend to be overparameterized, making it difficult to estimate model parameters from empirical data alone. The large data requirement of such models also makes it difficult to have measurements from a sufficient number of sites for a cross-system fitting procedure (e.g. Borsuk et al. 2001). This makes most applications of such models site-specific and leads to a lack of universality that would be required for prediction. Statistical approaches describe less detail of ecosystem function, which reduces their data requirements. For this reason, it is easier to develop a more universal model calibrated using data from several study sites jointly. The smaller data requirements also make it easier to use such models predictively. On the other hand, prediction accuracy is limited by the simpler modelling approach.

One of the pioneers in mechanistic modelling of lotic ecosystems is McIntire (1973) who developed a periphyton model and a hierarchical model for biomass of periphyton and invertebrate functional feeding groups (grazers, shredders, collectors and predators). Power et al (1995) modelled the food-web dynamics in large rivers linking physical and biological processes. They aggregated species of a hypothetical river food web into four functional groups (detritus, vegetation, grazers, predators) intended to represent the dominant resources and consumers in a river food chain. Unfortunately, no comparison between model simulations and measured data are given in these publications. Uehlinger et al. (1996) presented mechanistic periphyton models for the Necker River (Switzerland) describing periphyton growth, detachment, and loss due to floods. These models considered the effects of temperature, light, discharge, periphyton density limitations on growth and detachment rates. Their best model shows a good agreement with measured data. However, the derivation of the model is based on a data set from only one site at the Necker River. Boulêtreau et al (2006) adapted this model to two sites of the Garonne River (France) and introduced an additional term to account for temperature-dependent, self-generated loss due to heterotrophic processes in the biofilm. We have used the datasets of both Uehlinger et al (1996) and Bouletreau et al (2006) in the derivation of the periphyton models presented in this chapter.

Lamouroux et al. (2004) analyzed the relationships between habitat (characterized by hydraulic conditions (Froude Number), substrate size and benthic particulate organic

matter) and the functional structure of invertebrate communities at three spatial scales (microhabitat, stream reach, basin) with a statistical model. They found good correlations for deposit feeders (collector-gatherers who feed on coarse organic matter in the river bed), and fair associations for shredders and scrapers. Yoshimura et al (2006) focused on the prediction of functional ratios of the different feeding groups of macroinvertebrates to relate them to ecosystem attributes. These ratios were found to depend on dissolved oxygen and organic carbon, periphyton cover and organic halogen compounds. Other approaches have used artificial neural networks as a “black box” model structure for describing the dependence of invertebrate abundance on external influence factors (e.g. Gevrey et al 2003, Park et al 2003)

In this article, we develop a statistical model for predicting periphyton and invertebrate biomass in rivers as a function of the major influence factors. In contrast to “black box” statistical approaches, after preliminary linear regression analyses, we develop a nonlinear model formulation that represents the expected response as a mechanistically derived function of the influence factors. This attempts to combine the advantages of a statistical model formulation (minor data requirements, joint evaluation of several data sets) with a simple parameterization of what we expect to be the behaviour of a mechanistic model. We expect that this will lead to more robust behaviour of the model, particularly when extrapolating outside its calibrated range of influence factors. In addition to these statistical approaches, a mechanistic model simulating periphyton and invertebrate functional groups in one of the rivers investigated in this study (the Sihl River) is being developed and reported separately (Schuwirth et al. 2007). This will provide improved understanding of the benthos community dynamics in this river, but will require many more data from other rivers to achieve universal model parameter values. We hope that the parallel development along these two research lines will lead to improved insight into benthic community dynamics and that the relationships discovered with the statistical approach will support the process of improving mechanistic models.

The remainder of this chapter is structured as follows: We begin by describing the study sites and data sources. We then describe our modelling procedures. Next, we present and discuss the results and, finally, draw our conclusions.

4.3 Study Sites and Data

The data used to derive the periphyton models presented in this article were collected by previous studies at the Swiss rivers, Necker (4 sites) and Sihl (2 sites), and the French river, Garonne (2 sites). Since no accompanying invertebrate studies at the sites of the Necker and Garonne were conducted, only invertebrate data from the Sihl River could be used to derive the invertebrate models.

Sihl

The Sihl River is a prealpine Swiss river flowing into the Limmat River in the city of Zürich. Its catchment is predominated by pasture and forest. Since the construction of the Sihl reservoir (Sihlsee) in 1937 for hydropower generation, the flow regime of the Sihl River has been reduced artificially to a constant discharge between 2.5 - 4.0 m³/s, promoting river bed siltation and algal proliferation due to the absence of bed disturbances (Elber et al 1996). Between 1990 and 1992, several artificial floods were released from the Sihlsee to investigate the morphological and ecological responses to attempts at mimicking a more natural flow regime.

In two campaigns (May 1990 - August 1990 and April 1991 - July 1992) (Elber et al 1992, Elber et al 1996), total periphyton biomass as well as invertebrate abundance and total biomass were measured irregularly every 1-4 weeks at two locations at the Sihl River. The first site (“upstream”) is located in a typical flowing reach while the second (“downstream”) is situated in the backwater zone of a weir (at 1.5 km distance from the upstream site), with a lower mean velocity and grain size and a modestly higher water depth (Table 4.1). Figure 4.1, panel A, shows maximum daily discharge and standing biomass (in g ash free dry biomass (AFDM) / m²) over the study period at both sites.

Invertebrates were sampled with a surber sampler (30cm x 30cm) at six locations over the complete wetted river width. Invertebrates were identified to family or genus level and, where reasonable, to species level. In Figure 4.1, panel B, the pattern of total invertebrates (in dry weight / m²) over time is depicted.

Further details on the methods of data collection are described by Elber et al (1992) and Elber et al (1996).

For the Sihl River, further processing of data was necessary to transform abundance data of invertebrates to biomass estimates for the functional feeding groups. The mean specific body mass (mass per individual) of the most important species or higher taxonomic groups was evaluated from the literature. Total biomass was then calculated as the measured abundances multiplied by the corresponding mean specific body masses.

Finally, the biomass estimates of the different taxa were aggregated according to their functional feeding groups (see Schuwirth et al. 2007 for more details).

Necker

The Necker, a prealpine, 6th order river in the eastern part of Switzerland has its sources at an elevation of about 1300 m a.s.l.. About 30% of its catchment area is forested, the remainder is pasture land. Agricultural runoff and inflow of treated sewage have increased the concentrations of inorganic phosphorus and nitrogenous compounds above reported limiting concentrations for the growth of benthic algae (Table 4.1). The flow regime is rather unpredictable, since bed-moving spates may occur at any time of the year (Fig. 4.1, panels C and D).

Necker Downstream

From October 1992 to the beginning of March 1994, periphyton was monitored at two riffles/runs and two pools at the site “Necker Downstream” (Uehlinger et al 1996). Samples were taken every two weeks (Fig. 4.1, panel C) and periphyton biomass was determined as AFDM / m². A more detailed description of the study site and sampling methods are given by Uehlinger et al. (1996).

Necker Aachsäge

Nine sites were sampled at the Necker Aachsäge site (Uehlinger 1991): five in the main channel and four on a partially inundated bar and one in a side channel, which was formed during the investigation. From the end of February 1989 until March 1990 all sites were sampled biweekly (Fig. 4.1, panel D). Periphyton biomass for each morphological type (main channel, inundated bar, side channel) was determined as AFDM/m². Uehlinger (1991) gives a more detailed description of the methods and study sites.

Garonne

The Garonne River is a large river located in southwest France with pebble banks and a mean daily discharge of 150 m³/s at Toulouse, an urban centre with approximately one million inhabitants (Boulêtreau et al 2006). Study sites were located 36 km upstream (site Aouach, 6th order) and 12 km downstream (site Gagnac, 7th order) of Toulouse (Table 4.1). During the low water period (from July to October), the mean discharge is reduced to about 50 m³/s and the river is characterized by a shallow (<1.5m) and wide profile (100m).

Sampling was conducted from July 2001 to December 2001 at weekly intervals and then monthly until November 2002 (Fig. 4.1, panel E). For each study site, a reference point was chosen in a riffle. At this reference point, sampling was performed at each date at three distinct depths of the cross section: 30, 50 and 70 cm. Biomass values (in AFDM / m²) of the three depths were then averaged to provide biomass measurements for each

date at each site. The recorded biomass is not representative of the biomass occurring at all points of the cross section but satisfactorily describes the low depth region where epilithic biofilm typically develops (Améziane et al 2002). A more detailed description of the study sites and sampling methods is given by Boulêtreau et al (2006).

Table 4.1: Summary of site characteristics. (DIN= dissolved inorganic nitrogen = $\sum NO_3-N, NO_2-N, NH_4-N$; SRP = soluble reactive phosphorus)

Parameter/ site name	Necker Aachsäge main channel	Necker Aachsäge side channel	Necker Aachsäge gravel bar	Necker Down- stream	Sihl Up- stream	Sihl Down- stream	Garonne Aouach	Garonne Gagnac
Catchment Area (km ²)	88	88	88	126	na	na	56000	56000
Height a.s.l. (m)	607	607	607	559	485	442	na	na
Mean Discharge (m ³ /s)	3.4	3.4	3.4	4.6	3 ⁺	3 ⁺	113	159
Slope (-)	na	na	na	0.006	na	na	0.005	0.005
Grain Size (m)	0.08	0.08	0.08	0.05	0.22	0.16	0.12	0.12
Mean Velocity (ms ⁻¹)	0.8	0.5	0.5	0.7	0.63*	0.5	1	1
Mean Depth (m)	0.2	0.2	0.1	0.4	0.4	0.5	0.5	0.5
Mean Fr (-)	0.6	0.3	0.4	0.3	0.4	0.2	0.5	0.5
Mean Temperature (Winter) (°C)	2.1	2.1	2.1	2.3	1	1	8.1	8.1
Mean Temperature (Summer) (°C)	14	14	14	15.7	15	15	20.0	20.0
Shading by riparian vegetation (%)	35%	0%	5%	0%	0%	0%	na	na
DIN (mg l ⁻¹)	1.22	1.22	1.22	1.28	0.82	0.82	0.74	1.59
SRP (µg l ⁻¹)	38	38	38	25	50	50	9	85
Number of samples	29	29	29	46	43	43	33	34

+ Artificial flow regime

* The reported value of 0.8 m/s had to be reduced to guarantee compatibility with the downstream site with approximately the same width and discharge.

na – data not available

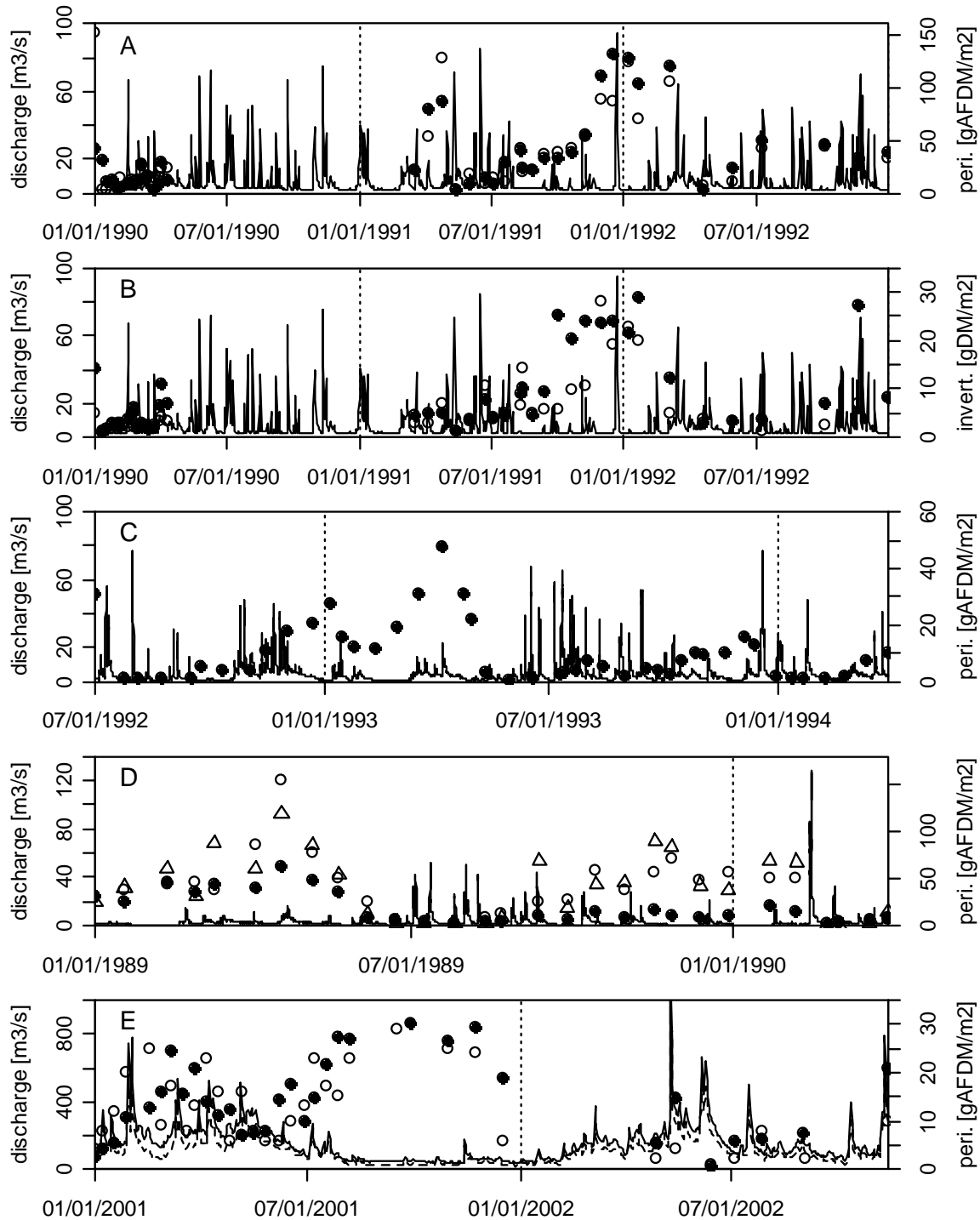


Figure 4.1: Discharge time series (solid and dashed lines) and measured functional group biomass (markers) for the study sites. Periphyton (AFDM; panel A) and benthic invertebrate biomass (panel B) for the upstream (solid circles) and downstream (circles) sites of the River Sihl. Periphyton biomass for the sites “Downstream” (panel C) and “Aachsäge” (panel D; solid circles: main channels; circles: gravel bar; and side channel: triangles) at the Necker River, and for the the sites “Auouach” (solid circles) and “Gagnac” (circles) at the Garonne River (panel E). The solid line in panel E represents the discharge at Auouach, the dashed line the discharge at Gagnac.

4.4 Modelling Methods

The goal of our modelling effort was to obtain parsimonious statistical models that consider the most important factors influencing the biomass of the functional groups. Such models cannot describe all relevant processes in detail, but they should also not be a “black-box” model formulation, unrelated to known system behaviour. To derive such models, we used a four-step approach: (i) the important influence factors for the functional groups were identified based on the analysis of scatterplots and systematic linear regressions of combinations of influence factors and their transformations, (ii) a nonlinear model was formulated that considers the most important influence factors identified with the linear model but that can be expected to have a more robust behaviour when applied to different rivers and for extrapolations beyond the range of influence factors, (iii) the sensitivity of model fits to the values of parameters that could not be fitted was performed, and (iv) a model selection procedure was carried out by jointly fitting a series of submodels of this nonlinear model to the data of as many sites as possible. For the selected model, an uncertainty analysis with respect to model results was performed.

Table 4.2 summarizes the variables considered as potential predictive influence factors in the river benthos model.

4.4.1 Preliminary Analysis of the Significance of Influence Factors

In the linear regression approach, all linear models based on one, two or three influence factors or their square root, inverse, log or square transformations were systematically considered to find the model that provides the best fit to the data. This led to a ranking of the most important factors influencing the biomass of each functional group.

Table 4.2: Summary of influence factors used to derive models for periphyton and invertebrates. DIN = Dissolved inorganic nitrogen (ΣNO_3-N , NO_2-N , NH_4-N) SRP = Soluble reactive phosphorus

Influence Factor	Units	Minimum	Mean	Maximum
Julian Day	(-)	1 (1 st January)	169 (18 th June)	365 (31 st December)
Month	(-)	1 (January)	7 (July)	12 (December)
Season	(-)	Spring	Summer/Fall	Winter
Time since last flood with bed movement	(d)	0	95	411
Time since last minor flood (exceeding twice the mean discharge)	(d)	0	8	35
Temperature of the last 14 or 30 days	(°C)	0.3	10.7	24.5
Seasonal Temperature	(°C)	1.0	10.8	20.0
Mean Discharge	(m ³ /s)	3.0	34.6	159.0
Flow Velocity	(m/s)	0.5	0.7	1.0
Water Depth	(m)	0.1	0.4	0.5
Froude N ^o	(-)	0.3	0.4	0.6
Median Grain Size	(m)	0.05	0.12	0.22
DIN	(mg/l)	0.7	1.1	1.6
SRP	(µg/l)	9	42	85
Catchment Area	(km ²)	88		56000

4.4.2 Formulation of Nonlinear Model

As described in the Results section, time since the last bed-moving flood was found to be the most significant influence factor, particularly for periphyton. Therefore, the nonlinear model must provide a reasonable phenomenological description of the development of periphyton after bed movement. As the linear models indicate, a proportional increase in periphyton biomass with time after the flood already provides a good description of observations. However, due to the increasing instability of a benthic biofilm with increasing thickness, this cannot be an adequate description for long times after the flood. For this reason, we seek a model formulation that describes linear growth of biomass with time immediately after a flood, but reaches saturation over time. If k_B is the slope of the initial increase, B_{max} is the biomass saturation value, Δt_{flood} is the time after the last bed-moving flood, and B denotes current biomass, then

$$B = \frac{B_{max} \cdot k_B \cdot \Delta t_{flood}}{B_{max} + k_B \cdot \Delta t_{flood}}$$

is such a process formulation. We generalized this approach by adding limiting effects with increasing water depth and flow velocity and decreasing gravel size, by allowing for nonlinearity of the increase as a function of the time since the last bed-moving flood, and by adding a seasonal dependence. This led to the following model formulation:

$$B = \frac{\overline{B_{\max}} \cdot \overline{k_B} \cdot \Delta t_{\text{flood}}^b}{\overline{B_{\max}} + \overline{k_B} \cdot \Delta t_{\text{flood}}} l(h, v, d_{50}, \Delta t_{\text{jul}}) \quad (1)$$

where

$$l(h, v, d_{50}, \Delta t_{\text{jul}}) = \exp(-\gamma h) \cdot \exp(-\delta v) \cdot \frac{d_{50}}{k_{d_{50}} + d_{50}} \max \left(1 + \alpha \cos \left(2\pi \cdot \frac{\Delta t_{\text{jul}} - \Delta t_{\text{jul}}^{\max}}{1y} \right), 0 \right) \quad (2)$$

describes the limiting effect of mean water depth, h (m), mean flow velocity v (ms⁻¹), and median gravel grain size, d_{50} (m), as well as seasonal variation (through the time within the year, Δt_{jul} (Julian days)). The model parameters in equations (1) and (2) have the following interpretations: $\overline{k_B}$ is the maximum (with respect to h , v , and d_{50}) and mean (with respect to seasonality) coefficient describing benthic biomass growth after a flood (g/m²/d^b), $\overline{B_{\max}}$ is the maximum (with respect to h , v , and d_{50}) and mean (with respect to seasonality) asymptotic biomass after long times after the last flood occurred (g/m²), b is the exponent of Δt_{flood} (-), $\Delta t_{\text{jul}}^{\max}$ is the time within the year (Julian Days) at which standing crop would be maximum for constant values of the other influence factors, $k_{d_{50}}$ is the grain size with half saturation for $\overline{k_B}$ and $\overline{B_{\max}}$ (m), α is the relative amplitude of the seasonal variation (relative to the mean) (-), and γ (m⁻¹) and δ (m⁻¹s) are the parameters describing limitation by water depth and flow velocity (1y = 1 year).

For short times after the last flood, this model behaves as:

$$B \approx \overline{k_B} \cdot \Delta t_{\text{flood}}^b \cdot l(h, v, d_{50}, \Delta t_{\text{jul}}) \quad \text{for } \Delta t_{\text{flood}} \ll \left(\overline{B_{\max}} / \overline{k_B} \right)^{1/b} \quad (3a)$$

Long after the last flood, this model asymptotically approaches a biomass that depends only on the limiting factors h , v , and d_{50} , and on the season (through Δt_{jul}):

$$B \approx \overline{B_{\max}} \cdot l(h, v, d_{50}, \Delta t_{\text{jul}}) \quad \text{for } \Delta t_{\text{flood}} \gg \left(\overline{B_{\max}} / \overline{k_B} \right)^{1/b} \quad (3b)$$

This general model was used to describe the behaviour of all functional groups in the river, despite the smaller importance of time since the last flood for invertebrates compared to periphyton.

4.4.3 Parameter Estimation

The model given by the equations (1) and (2) has a more realistic asymptotic behaviour than the linear models. On the other hand, because of the larger number of parameters it can be expected to have worse identifiability. The most obvious example of the trade-off between a realistic formulation of asymptotic behaviour and identifiability is the dependence of biomass on time since the last flood. Increase after the flood is characterized by the parameter $\overline{k_B}$, asymptotic biomass by $\overline{B_{\max}}$. If a data set does not contain measurements of biomass for long times after a flood, $\overline{B_{\max}}$ is not identifiable. Nevertheless, a model that includes this saturation effect is more realistic when applied to times long after a flood if we use a realistic estimate for $\overline{B_{\max}}$ from the literature.

To account for model structure uncertainty and measurement error, the deterministic model was extended by a random error term. Because of the heteroscedasticity of the error in original biomass density units (larger error for larger values of functional group biomass density), the error was assumed to be additive to Box-Cox transformed model results (Box and Cox, 1964, 1982) rather than to the predicted biomasses directly. This transformation of biomass, B , is given by the following equation

$$g(B) = \begin{cases} \frac{(B + \lambda_2)^{\lambda_1} - 1}{\lambda_1} & \lambda_1 \neq 0 \\ \ln(B + \lambda_2) & \lambda_1 = 0 \end{cases} \quad (4)$$

where λ_1 (-) and λ_2 (g/m^2) are parameters that can be adjusted to improve the fit of the empirical distribution of the residuals to that generated by the model. As a function of the model parameters, $\boldsymbol{\theta} = (\overline{k_B}, \overline{B_{\max}}, b, \gamma, \delta, k_{d50}, \alpha, \Delta t_{\text{jul}}^{\max})$, external influence factors, $\mathbf{x} = (\Delta t_{\text{flood}}, h, v, d_{50}, \Delta t_{\text{jul}})$, and the error term, E (g/m^2) ^{λ_1} , the probabilistic predictions of biomass B^{prob} (g/m^2) are then given by

$$B^{\text{prob}}(\boldsymbol{\theta}, \mathbf{x}) = g^{-1}(g(B(\boldsymbol{\theta}, \mathbf{x})) + E) \quad (5)$$

where $B^{\text{prob}}(\boldsymbol{\theta}, \mathbf{x})$ is the deterministic function given by equations (1) and (2). With appropriate adjustments of the parameters λ_1 and λ_2 of the Box-Cox transformation, the residuals of transformed model results and data could be shown to approximately follow a normal distribution with constant variance. Therefore, maximum likelihood parameter estimation could be performed by applying the unweighted least-squares regression function “nls” of the statistics and graphics package R (<http://www.r-project.org>).

4.4.4 Sensitivity Analysis

Due to identifiability problems, some parameters had to be kept at a fixed value that could not be estimated from the data. Other parameters were then estimated for different values of such parameters to evaluate the sensitivity of the parameter estimates on the values of fixed parameters.

4.4.5 Model Structure Selection

Setting α , γ or δ equal to zero, or b equal to unity, leads to simplified submodels that do not consider seasonality of the dynamics, dependence on mean water depth and flow velocity, or nonlinearity in recovery after a flood, respectively. By analyzing the loss in the quality of fit when setting one of these parameters to zero (α , γ or δ) or unity (b), we obtained an assessment of the importance of the corresponding influence factor in describing the data. Together with an assessment of the estimated parameter values, this trade-off between simplicity and quality of fit was used to select the final model for each functional group.

4.4.6 Uncertainty Analysis

Prediction uncertainty of the finally selected models was estimated by propagating the uncertainty in the estimated parameters as well as a 20% uncertainty in the parameters not included in the statistical fit, and adding the error term accounting for model structure and measurement error. A multivariate normal distribution was used to describe parameter uncertainty. This distribution was truncated to avoid negative values of the parameters for which negative values do not have a reasonable interpretation (k_B , B_{\max} , b , k_{d50}). Monte Carlo simulation was used to get a sample from the distribution of model results. As the probabilistic model predictions, B^{prob} , are given by equation (5), this required a five step procedure: (i) a random sample was drawn from the multivariate parameter distribution, (ii) this sample was propagated through the model to the results, (iii) these results were transformed using the Box-Cox transformation, (iv) the normally distributed error term was added, and (v) the results were transformed back to original units by applying the inverse Box-Cox transformation.

4.5 Results

In this section, we present the results of the modelling approach discussed in the previous section as applied to the data sets of periphyton from the Sihl, Necker and Garonne rivers and to the data sets of total invertebrates and their dominant functional groups (scrapers, collector-gatherers, and predators) from the Sihl River. While the model is not explicitly dynamic, the daily model predictions can be calculated from daily data of the influence factors. This is a convenient way of representing model results and comparing them with measured data. Still it has to be kept in mind that the linear and nonlinear regression relationships are calculated based on average depth, velocity and grain size, and that only time since the last flood and seasonality (in Julian Days) provide the dynamics of the predictions.

The shape of the empirical distribution of the residuals was critically analyzed after performing the fits. Without applying the Box-Cox transformation (see equations 4 and 5) there was strong heteroscedasticity of the residuals with a much larger variance for large values of the observations than for small ones. We obtained best results when setting $\lambda_1 = 0.3$ for all modelled functional groups and $\lambda_2 = 1 \text{ gAFDM/m}^2$ for periphyton, $\lambda_2 = 1 \text{ gDM/m}^2$ for total invertebrates, and $\lambda_2 = 0.1 \text{ gDM/m}^2$ for the functional groups of invertebrates. (Because it represents a sort of “offset parameter”, it is expected that the value of λ_2 will vary according to the range of values of each measured variable). These values led to the elimination of heteroscedasticity for periphyton and collector-gatherers, and to a significant reduction in heteroscedasticity for scrapers and predators. Also, normal quantile-quantile plots showed significantly less deviation from normality.

Table 4.3 shows the results of the fits performed for sensitivity analysis and model structure selection for all functional groups. For each functional group, parameter estimates are shown for a base model (model x.1), for models with modified values of the parameters that were not estimated (models x.2 and x.3; to analyze the sensitivity of parameter estimates and fit quality to the selected values), and for simplified models that omit one or several influence factors (models x.4 to x.9; for model structure selection). In addition to the parameter estimates, for each fit, the number of fitted parameters, n , and the correlation coefficient between measurement and predictions, R^2 , are given. This comparison of fit results allows us to make an assessment for the degree in quality of fit we lose by omitting an influence factor from the analysis. To avoid identifiability problems, best estimates of the saturation biomass, $\overline{B_{\max}}$, and the half-saturation gravel diameter, k_{d50} , were specified in all base models. The lack of data after long periods without floods and the small spread in gravel size across the sites did not allow us to estimate these parameters. Nevertheless, we decided to include these influence factors to make the model more robust when applied outside its calibration range. The value of k_{d50} was selected according to Biggs & Price (1987), the saturation biomass, $\overline{B_{\max}}$, was

chosen based on survey data of Austrian rivers (Yoshimura et al 2006). As many fewer data were available for invertebrates, a simpler base model had to be chosen. This was done by setting the parameter of the velocity dependence term, δ , to zero for all invertebrate data analyses (preliminary fits with inclusion of this parameter led to unsatisfying parameter estimates). In Table 4.3, the model finally selected (see below for rationale), is indicated by a bold model identifier in the second column. The parameter estimates, including standard deviations and correlation coefficients, for these models are given in the appendix.

Table 4.3: Parameter estimates of base model (x.1), of models used for sensitivity analysis of fixed parameters (x.2 and x.3), and for simplified models used for model structure selection (x.4 to x.9 (see text for additional explanation)). The values of fitted parameters are indicated in bold; fixed parameter values are in standard style; and parameter values that were fixed to yield omission of a term are in italics. n is the number of fitted model parameters. Finally selected models are indicated with bold model indentifiers in the second column.

	model	$\overline{B_{\max}}$	$\overline{k_B}$	k_{d50}	$\Delta t_{\text{jul}}^{\max}$	α	γ	δ	b	n	R^2
periphyton	1.1	1500	22.6	0.2	220.0	0.056	0.34	2.96	0.89	6	0.595
	1.2	3000	31.9	0.2	235.9	0.097	0.40	3.36	0.82	6	0.611
	1.3	1500	28.3	0.4	129.8	0.016	0.55	2.46	0.94	6	0.577
	1.4	1500	23.8	0.2	<i>250</i>	<i>0</i>	0.29	2.97	0.87	4	0.594
	1.5	1500	21.8	0.2	218.5	0.047	<i>0</i>	3.11	0.89	5	0.594
	1.6	1500	26.4	0.2	125.8	0.100	3.24	<i>0</i>	0.50	5	0.382
	1.7	1500	16.8	0.2	219.3	0.079	0.35	3.07	<i>1</i>	5	0.593
	1.8	1500	16.5	0.2	<i>250</i>	<i>0</i>	<i>0</i>	3.22	<i>1</i>	2	0.590
	1.9	1500	17.0	0.2	<i>250</i>	<i>0</i>	0.27	3.10	<i>1</i>	3	0.591
total invertebrates	2.1	150	4.47	0.2	257.9	0.781	1.85	<i>0</i>	0.63	5	0.726
	2.2	300	5.73	0.2	257.1	0.788	2.40	<i>0</i>	0.59	5	0.732
	2.3	150	5.05	0.4	257.9	0.780	1.11	<i>0</i>	0.64	5	0.727
	2.4	150	9.11	0.2	<i>250</i>	<i>0</i>	2.65	<i>0</i>	0.54	3	0.356
	2.5	150	2.26	0.2	257.1	0.788	<i>0</i>	<i>0</i>	0.57	4	0.713
	2.6	150	3.57	0.2	255.1	0.793	3.53	<i>0</i>	<i>1</i>	4	0.693
	2.7	150	0.45	0.2	243.8	0.887	<i>0</i>	<i>0</i>	<i>1</i>	3	0.607
scrapers	3.1	25	5.45	0.2	250.9	0.878	5.02	<i>0</i>	0.58	5	0.304
	3.2	50	7.55	0.2	249.9	0.884	5.77	<i>0</i>	0.44	5	0.303
	3.3	25	5.91	0.4	251.0	0.877	4.15	<i>0</i>	0.61	5	0.306
	3.4	25	9.67	0.2	<i>250</i>	<i>0</i>	5.93	<i>0</i>	0.96	3	0.055
	3.5	25	0.84	0.2	250.5	0.887	<i>0</i>	<i>0</i>	0.27	4	0.261
	3.6	25	5.22	0.2	253.6	0.862	5.77	<i>0</i>	<i>1</i>	4	0.296
	3.7	25	0.06	0.2	230.5	0.969	<i>0</i>	<i>0</i>	<i>1</i>	3	-0.031
Collect.-gatherers	4.1	100	0.80	0.2	248.5	0.770	-0.61	<i>0</i>	0.61	5	0.637
	4.2	200	0.86	0.2	248.3	0.772	-0.45	<i>0</i>	0.60	5	0.639
	4.3	100	0.96	0.4	248.3	0.770	-1.20	<i>0</i>	0.62	5	0.641
	4.4	100	1.57	0.2	<i>250</i>	<i>0</i>	-0.25	<i>0</i>	0.47	3	0.338
	4.5	100	1.01	0.2	248.6	0.768	<i>0</i>	<i>0</i>	0.62	4	0.636
	4.6	100	1.20	0.2	243.0	0.808	2.90	<i>0</i>	<i>1</i>	4	0.560
	4.7	100	0.26	0.2	237.5	0.867	<i>0</i>	<i>0</i>	<i>1</i>	3	0.535
predators	5.1	30	1.64	0.2	277.8	0.816	4.16	<i>0</i>	0.70	5	0.578
	5.2	60	2.60	0.2	276.4	0.823	5.47	<i>0</i>	0.69	5	0.602
	5.3	30	1.78	0.4	278.0	0.814	3.27	<i>0</i>	0.70	5	0.569
	5.4	30	2.15	0.2	<i>250</i>	<i>0</i>	4.79	<i>0</i>	0.68	3	0.286
	5.5	30	0.28	0.2	271.8	0.843	<i>0</i>	<i>0</i>	0.59	4	0.515
	5.6	30	0.98	0.2	274.9	0.826	4.81	<i>0</i>	<i>1</i>	4	0.565
	5.7	30	0.06	0.2	258.8	0.919	<i>0</i>	<i>0</i>	<i>1</i>	3	0.476

Periphyton

The linear regression analyses revealed that the influence factor “time since last bed-moving flood” (Δt_{flood}) was by far the most significant predictor for estimating periphyton biomass, followed by water temperature and photosynthetically active radiation (PAR) over the last 14 days. Apparently, the concentrations of dissolved inorganic nitrogen (DIN) and soluble reactive phosphorus (SRP) were sufficiently high to avoid nutrient limitation of periphyton growth.

The structure of the periphyton model (equations 1 and 2) directly formulates the dependence on the time since the last flood. The influence of radiation and temperature on periphyton growth and standing crop are included indirectly by the term describing the seasonal effects.

The Swiss rivers (Necker, Sihl) differ from the French river (Garonne) with respect to size (mean discharge, depth) (Table 4.1) and frequency of disturbance (Fig. 4.1). Thus, the data from the more stable (in terms of frequency of disturbance) Garonne River provide some information on the saturation biomass, $\overline{B_{\text{max}}}$, while the data from the more flood prone Swiss rivers are better able to provide information on the coefficient describing the increase of biomass after a flood, $\overline{k_B}$. Nevertheless, the estimates of $\overline{B_{\text{max}}}$ for different choices of the model structure varied over so wide ranges, that we cannot rely on these estimates. Data from only one river that also differs considerably from the other rivers in the values of other influence factors seem not to be sufficient to provide a reliable estimate of this parameter.

The models 1.2 and 1.3 (when compared to model 1.1) in Table 4.3 show that even drastic changes of the values of the fixed parameters $\overline{B_{\text{max}}}$ and k_{d50} did not strongly affect the quality of the fit (compare the values of R^2 between these models). With the exception of the parameters $\Delta t_{\text{jul}}^{\text{max}}$ and α , the values of the estimated parameters do not change very strongly when the fixed parameters are changed. This is an indication that $\Delta t_{\text{jul}}^{\text{max}}$ and α are poorly identifiable. This is confirmed by the very small values of α for all fits which indicate a minor seasonal component and thus provide the cause for the poor identifiability.

The models 1.4 to 1.7 in Table 4.3 demonstrate the effect of omitting the seasonal dependence ($\alpha = 0$, making $\Delta t_{\text{jul}}^{\text{max}}$ irrelevant), the effect of water depth ($\gamma = 0$), the effect of flow velocity ($\delta = 0$), and the nonlinearity of increase after a flood ($b = 1$). The results (R^2) clearly show that omission of seasonality (model 1.4), omission of depth dependence (model 1.5) and omission of nonlinearity of increase after a flood (model 1.7) only leads to a minor decrease in the quality of the fit. On the other hand, consideration of velocity dependence seems to be important (model 1.6 leads to a considerable drop in R^2). Model 1.8 demonstrates that even the combined omission of the three less relevant influence factors does not lead to a significant drop in R^2 . Adding depth dependence in model 1.9 did not improve the fit significantly. For this reason, model 1.8 with only two fitted

parameters is obviously the best compromise between model complexity and quality of fit. Figure 4.2 illustrates the behaviour of model 1.8 as compared to measured data from all sites.

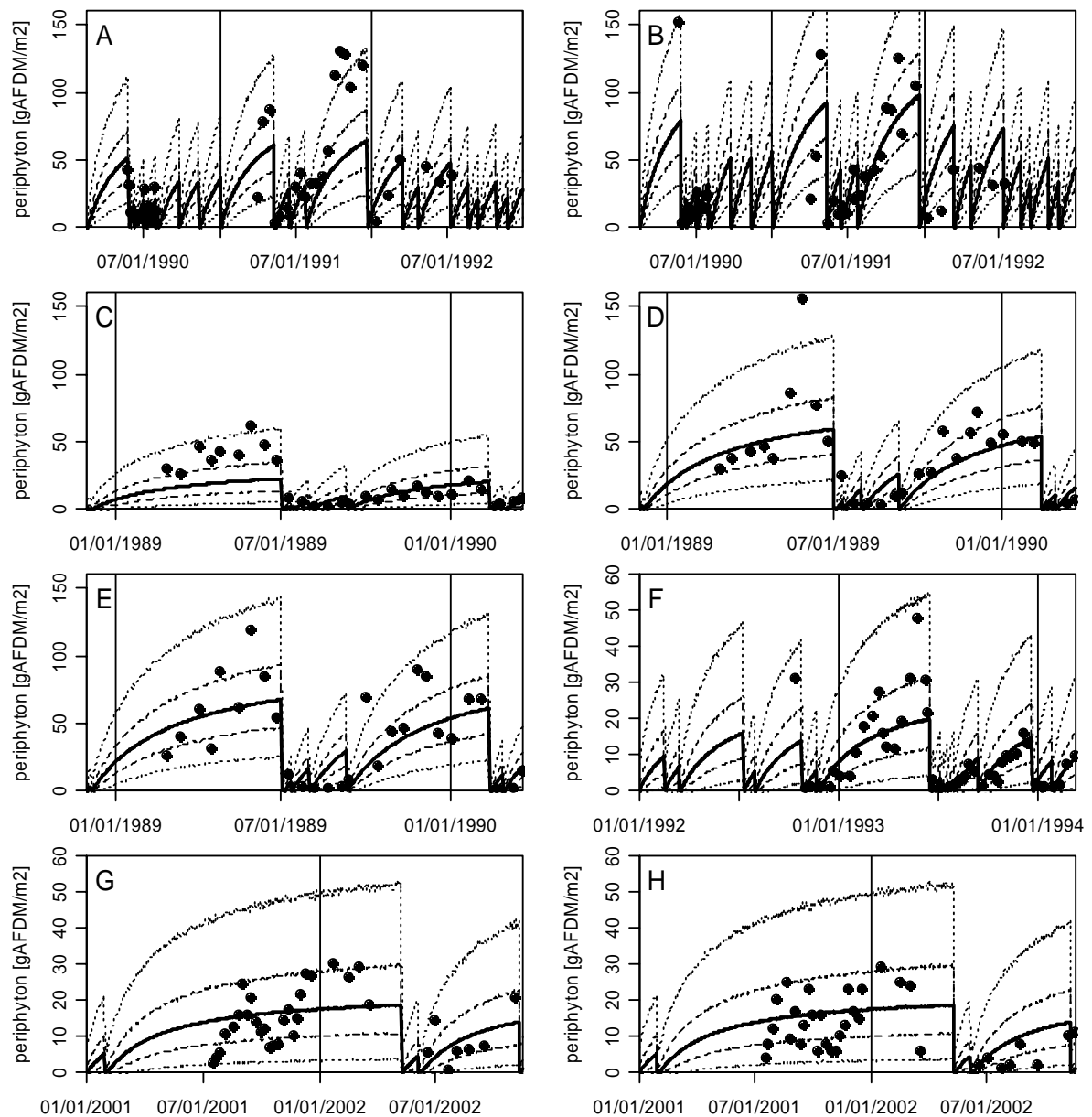


Figure 4.2: Time series of results of model 1.8 and measured periphyton biomass (solid circles) for all study sites. The solid lines represent the best estimates, the dashed lines bound the 50% and the outer dotted lines the 90% uncertainty intervals of the predictive distributions and the symbols represent measured data. A: Sihl upstream site. B: Sihl downstream site. C: Necker Aachsäge main channel. D: Necker Aachsäge gravel bar. E: Necker Aachsäge side channel. F: Necker downstream site. G: Garonne Gagnac. H: Garonne Auach.

Invertebrates

Exploratory linear regression models for total invertebrate, collector-gatherer, and predator biomass performed fairly well, with R^2 values exceeding 0.6. However, the results of linear regression models for scraper biomass were significantly worse ($R^2 = 0.38$). Linear regression results for shredder and collector-filterer biomass were even worse ($R^2 = 0.19$ and 0.32 respectively). Due to the low biomass of these last two functional groups (< 6 % of total biomass), they were not included in the further model development.

As mentioned before, due to the lack of data from several rivers, we had to choose a simplified base model for invertebrates. From the model used for periphyton (equations 1 and 2) we omitted the velocity dependence term by setting $\delta = 0$ because including this term did not lead to reasonable parameter estimates. Starting from this base model, we performed a similar sensitivity analysis and model selection procedure as for periphyton (see Table 4.3). The values of $\overline{B_{\max}}$ and k_{d50} were again chosen according to typical values found in Yoshimura et al (2006) and Biggs & Price (1987).

As expected for parameters that are poorly identifiable because of their low influence on model results (in contrast to parameters that are poorly identifiable because of strong correlations), a change in the values of $\overline{B_{\max}}$ and k_{d50} had only a small effect on parameter estimates and a very small effect on the performance of the fit (compare the R^2 values of the models x.2 and x.3 with x.1 for $x = 2, 3, 4$ and 5 in Table 4.3).

The models x.4 to x.6 in Table 4.3 ($x = 2, 3, 4$ and 5) demonstrate the effect of omitting the seasonal dependence ($\alpha = 0$, making $\Delta t_{\text{jul}}^{\max}$ irrelevant), the effect of water depth ($\gamma = 0$), and the nonlinearity of increase after a flood ($b = 1$). The results (R^2) clearly show that omission of seasonality (models x.4) leads to a drastic reduction in R^2 for all functional groups of invertebrates. On the other hand, omission of depth dependence (models x.5) or nonlinearity of increase after a flood (models x.6) led to similarly good fits (inclusion of depth dependence was better for scrapers and predators, inclusion of nonlinearity of increase was better for total invertebrates and collector-gatherers). Omission of both effects (models x.7) did not lead to satisfying behaviour. As the estimated parameter values for depth dependence did not seem realistic and estimation of depth dependence seems to be critical from just two sites of the same river with only small differences in depth, we selected the models x.5 that interpreted the data with the nonlinear increase term after floods.

Figure 4.3 illustrates the results of the models x.5 ($x = 2, 3, 4$ and 5) compared to the measured data from both sites.

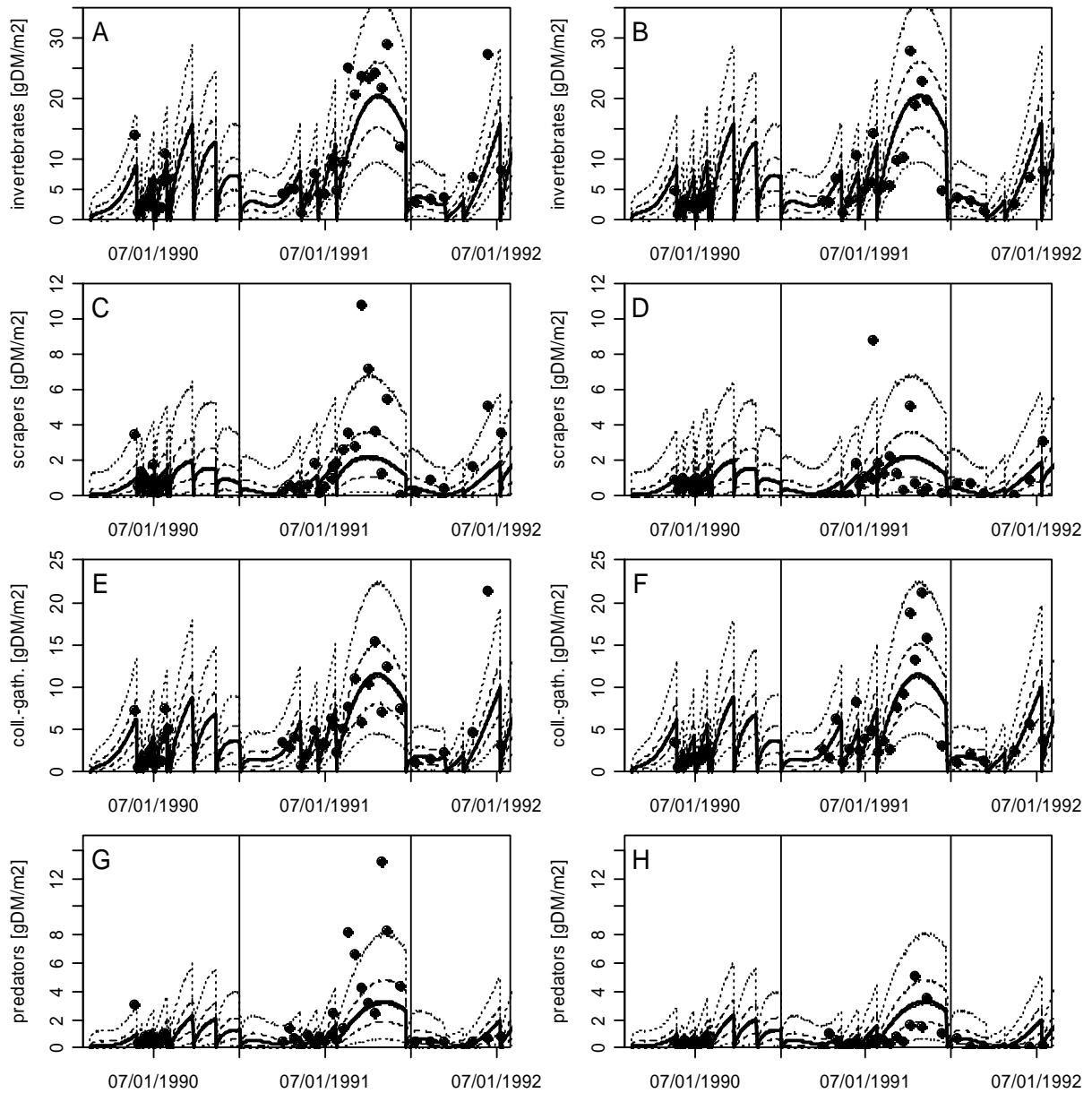


Figure 4.3: Time series of results of invertebrate models and data from the Sihl River. The solid lines represent the best estimates, the dashed lines bound the 50% and the outer dotted lines the 90% uncertainty intervals of the predictive distributions and the solid circles represent measured data. Left column: upstream site. Right column: downstream site. Top row (panels A and B): model 2.5 for total invertebrate biomass density. Second row (panels C and D): model 3.5 for scraper biomass density. Third row (panels E and F): model 4.5 for collector-gatherer biomass density. Bottom row (panels G and H): model 5.5 for predator biomass density.

4.6 Discussion

The nonlinear regression models presented in the previous section differ in accuracy (R^2), complexity and the number of data points used to derive the models. The algae models are based on data sampled from eight sites located in three rivers ($n=286$) while the derivation of the invertebrate models relied on data from only two sites at one river (Sihl) ($n=86$). The results of the periphyton model fit the data surprisingly well (see Figure 4.2). Only two parameters were fitted for a joint calibration to all eight data sets. This strongly supports the chosen model structure. On the other hand, four parameters had to be fitted for each of the four models of total invertebrates, scrapers, collector-gatherers, and predators at only two sites at the same river (see Figure 4.3). This leads to a much weaker confidence in the predictive capabilities of these models. The poorer performance of the scraper model as compared to the other models is reflected by wider 90% prediction uncertainty bands that extend nearly down to zero over the complete simulation period.

The quality of fit quantified by R^2 values was only slightly higher for the best non-linear regression models as compared the best linear regression models. This shows that we cannot considerably improve the quality of the fit with the nonlinear dependence formulation. The reason for formulating nonlinear models was to avoid unreasonable extrapolation behaviour of the linear models. Extrapolating the linear models can lead to negative or arbitrarily large predictions. Both of these behaviours are excluded by our formulation of the nonlinear models.

The low variation in grain size across sites precluded estimation of the model parameter k_{d50} characterizing decrease of biomass densities with decreasing grain size. Therefore, this parameter was estimated from the literature to be 0.2 m (Biggs & Price 1987, Quinn & Hickey 1990). Additionally, the maximum biomass density achieved under non-limiting conditions for long times after a flood, $\overline{B_{\max}}$, was difficult to fit, since longer periods without flood disturbances did not occur during the sampling period with the exception of the Garonne river. Therefore, this parameter also had to be chosen based on the literature (Yoshimura et al., 2006).

The model structure selection process based on the remaining parameters describing the increase in biomass density after a flood, seasonal variation, and dependence on flow velocity and water depth led to very different results for periphyton than for invertebrates. For periphyton it led to the exclusion of a significant seasonal variation, a linear initial increase of biomass with time after a flood, and a significant dependence on flow velocity. On the other hand, seasonality is a dominant explaining variable for invertebrate biomass density and there seems to be a strong nonlinearity of increase in time after a flood.

The absence of a strong seasonal variation of periphyton density seems to be a surprising result, as the seasonal component in our simple model mainly represents the effect of light and temperature on algal biomass. However, this finding is in agreement with earlier results of a mechanistic model (Uehlinger et al. 1996). It seems that adaptation of chlorophyll content and species composition of the benthic periphyton biofilm can compensate for most of the light and temperature dependence observed for individual species. The dependence on flow velocity may still contain some confounding with water depth and it would be very interesting to separate those two effects. However, more data from sites with considerable differences in flow velocity and water depth would be required to do this.

Due to their immobility, periphyton are more susceptible to floods compared to invertebrates which can move to more stable refuges (e.g. river bed interstitial, side braids, low-velocity areas around stable boulders) during high stage (Quinn & Hickey 1990). The regression analysis indicates that for periphyton, the best predictor is “time since the last bed-moving flood” (Δt_{flood}), while invertebrates (and most of their functional feeding groups) are more strongly controlled by seasonal effects. This is reflected in the nonlinear invertebrate models by the value of the parameter b smaller than unity that describes a faster recovery from the flood-induced depletion of invertebrates as compared to the linear recovery of periphyton (compare Figs. 4.2 and 4.3). In contrast to periphyton, invertebrates can have a more complicated life cycle (larvae, imago, adults) with possibly varying food and habitat preferences. This makes it more difficult to get good predictions for invertebrates with a simple non-linear regression model. This is also a significant problem for more complicated dynamic functional group models (Schuwirth et al. 2007). In our simple nonlinear regression approach, the life stages of invertebrates are aggregated into the seasonal effect described by the model.

The relationships found with the nonlinear regression approach can stimulate formulation of detailed mechanistic models of the benthos community such as those of Boulétreau et al (2006) and Schuwirth et al (2007). The dominance of time since the last flood as an explaining variable for periphyton suggests the necessity of a careful formulation of flood-induced detachment processes and subsequent recovery by growth. Unless light, low temperatures and nutrients are significantly limiting (which is not the case for the sites studied in this chapter), these factors seem to be of minor importance for a simple periphyton model for Swiss midland rivers. Nevertheless, these factors must be kept in mind when designing a model to be applied to different climatic regimes and with smaller nutrient loads or higher turbidity. For the invertebrate models, at least seasonally varying or temperature dependent growth rates should be formulated, and the model should contain a higher relative colonization rate after floods than the periphyton model.

The ratio of primary to secondary producer biomass estimated by the model can be compared to values predicted by theoretical concepts (e.g., Vannote et al 1980) and used for the evaluation of an expected ecosystem state. Moreover, the estimated biomass of the functional feeding groups can illuminate dominant pathways of nutrient cycling in a particular river reach (Yoshimura et al 2006, Merritt et al 1999, Klemm et al 2003, Böhmer et al 2000). For example, to assess habitat stability, Yoshimura et al (2006) propose to calculate the ratio of the more flood susceptible scrapers and collector-filterers to shredders and collector-gatherers. They recommend using abundances, but similar results can be expected when biomasses are used instead. Functional feeding groups emphasize the multiple linkages that exist between food resources and the ability of invertebrates to successfully acquire these resources (Cummins et al. 1981, Merritt et al. 1999, Barbour et al. 2001). Thus, function-based metrics are more directly related to ecosystem integrity than solely taxonomic composition (Yoshimura et al. 2006).

Our proposed models have the potential to support decision-making in the context of river rehabilitation, since periphyton and invertebrates play a key role in river ecology by serving as food for fish and controlling decomposition. Predictions of the response of these organisms to management actions can help to guide the selection of the most appropriate stream reaches and site-specific rehabilitation measures. While grain size and seasonal effects are usually not changed by rehabilitation measures, the hydraulic conditions (velocity, depth) usually are. In the previous chapters 2 and 3 (and Schweizer et al 2007a, 2007b) we developed a relatively simple hydraulic-morphological model to predict the hydraulic conditions after measures such as river widening. The major hydraulic responses of widening are an increased wetted perimeter, a lower mean water depth and flow velocity, and a higher spatial variability of depth and velocity. The simple benthic community models discussed in this chapter would predict a higher periphyton biomass density due to the decreasing flow velocity. In addition, due to the increased wetted perimeter, there will be more habitat area available per unit river length for both periphyton and invertebrates.

4.7 Summary and Conclusions

Simple nonlinear regression models were developed for describing the biomass of periphyton and benthic invertebrate functional feeding groups in rivers as a function of time since the last bed-moving flood, mean water depth, grain size, mean flow velocity, and season (time within the year). The models were calibrated using periphyton data from 8 sites in 3 rivers and invertebrate feeding group data from 2 sites in one river. The statistical approach made it much easier to derive relationships between biomass densities

of functional groups of the benthos community across different rivers and sites than would have been possible with mechanistic models. The results of sensitivity analyses, the model structure selection process, and comparisons of model results with data lead to the following conclusions:

- Considering the diversity of data sets and the simplicity of the models, the models lead to a remarkably good agreement with time series of measurements. Due to the larger data set available, this is particularly true for the periphyton model.
- The major influence factors for periphyton were identified to be time since the last bed-moving flood and mean flow velocity. No significant seasonal effects could be identified. In contrast to this result, seasonally varying influence factors or seasonal effects of changing life stages were identified to be important factors influencing total invertebrate and invertebrate functional feeding group biomass. Recovery after flood-induced disturbance events was identified to be significantly faster for invertebrates than for periphyton.
- The small number and simple nature of the considered influence factors makes the model an easily applicable tool for predicting the effect of rehabilitation measures on the benthic community.
- The model was derived with as many data sets as were available. Nevertheless a better support by data from additional rivers is necessary to test and improve its universality.

The suggested simple benthic community models seem to be useful for roughly estimating the effect of river rehabilitation measures on the benthic community. Furthermore, they support the development of more detailed mechanistic model of benthic community dynamics. More and longer data sets of rivers of different characteristics would be extremely useful for improving the development of both model types.

Acknowledgements

This study was supported by the Rhone-Thur project, which was initiated and is funded by the Swiss Federal Office for Water and Geology (BWG) (now BAFU), the Swiss Federal Institute for Environmental Science and Technology (Eawag) and the Swiss Federal Institute for Forest, Snow and Landscape Research (WSL). For stimulating discussions, comments, helpful advices and for sharing valuable datasets, we thank the Rhone-Thur project partners (P. Baumann, K. Tockner) and N. Lamouroux, C. Robinson, C. Yoshimura, S. Boulêtreau, D. Arscott, M. Scarsbrook, V. Acuña, H.-L. Morf, J. Hürlimann, F. Elber, K. Niederberger, P. Burgherr and E. Meyer.

4.8 References

- Améziane T, Garabétian F, Dalger D, Sauvage S, Dauta A and Capblancq J. 2002. Epilithic biomass in a large gravel-bed river (the Garonne, France): a manifestation of eutrophication? *River Research and Applications* **18**: 343-354.
- Barbour M T, Geristen J, Snyder B D, Stribling J B. 2001. Rapid bioassessment protocols for use in streams and wadeable rivers: periphyton, benthic macroinvertebrates, and fish. EPA, Washington DC, 1-339.
- Biggs B J F & Price G M. 1987. A survey of filamentous algal proliferations in New Zealand rivers. *New Zealand Journal of Marine and Freshwater Research* **21**: 175-181.
- Böhmer J, Rawer-Jost C and Kappus B. 2000. Ökologische Fließgewässerbewertung. Biologische Grundlagen und Verfahren - Schwerpunkt Makrozoobenthos. In: *Handbuch Angewandte Limnologie*.
- Borsuk M. E., Stow, C. A., Higdon, D. and Reckhow, K. H. 2001. A Bayesian hierarchical model to predict benthic oxygen demand from organic matter loading in estuaries and coastal zones. *Ecological Modelling* **143**: 165-181.
- Borsuk M E, Reichert P, Peter A, Schager E, Burkhardt-Holm P. 2006. Assessing the decline of brown trout (*Salmo trutta*) in Swiss rivers using a Bayesian probability network. *Ecological Modelling* **192**: 224-244.
- Boulêtreau S, Garabétian F, Sauvage S and Sanchez-Pérez J-M. 2006. Assessing the importance of a self-generated detachment process in river biofilm models. *Freshwater Biology* **51(5)**: 901-912.
- Box G.E.P., Cox, D.R. 1964. An analysis of transformations. *Journal of the Royal Statistical Society Series B*, 211-252.
- Box G.E.P., Cox, D.R., 1982. An analysis of transformations revisited, rebutted. *Journal of the American Statistical Association* **77(377)**, 209-210.
- Bretschneider H & Schulz A. 1985. Anwendung von Fließformeln bei naturnahem Gewässerausbau. *Schriftenreihe des deutschen Verbandes für Wasserwirtschaft und Kulturbau e.V. Heft 2*. Verlag Paul Parey, Hamburg, Berlin.
- Cummins K W, Klug M J, Ward G M, Spengler G L, Speaker R W, Ovink R W, Mahan D C and Petersen R C. 1981. Trends in particulate organic matter fluxes, community processes and macroinvertebrate functional feeding groups along a Great Lakes Drainage Basin river continuum. *Verh. Internat. Verein. Limnol.* **21**: 841-849.

- Elber F, Hürlimann J and Niederberger K. 1992. Biologische Begleitung der Schwallversuche vom Sommer 1990 in der Sihl. *Wasser, Energie, Luft* **84** (3/4): 42-50.
- Elber F, Hürlimann J and Niederberger K. 1996. Algenmonitoring als Grundlage für das Abflussmanagement in der Sihl. *Wasser, Energie, Luft* **88** (3/4): 55-62.
- Gevrey M, Dimopoulos I and Lek S. 2003. Review and comparison of methods to study the contribution of variables in artificial neural network models. *Ecological Modelling* **160**: 249-264.
- Hostmann M, Borsuk M, Reichert P, Truffer B. 2005. Stakeholder values in decision support for river rehabilitation. *Large Rivers* **15**(1-4) *Arch. Hydrobiol. Suppl.* **155**/1-4: 491-505.
- Klemm D J, Blocksom K A, Fulk F A, Herlihy A T, Hughes R M, Kaufmann P R, Peck D V, Stoddard J L, Thoeny W T and Griffith M B. 2003. Development and evaluation of a macroinvertebrate biotic integrity index (MBII) for regionally assessing Mid-Atlantic Highlands streams. *Environmental Management* **31**: 656-669.
- Lamouroux N, Doledec S, Gayraud S. 2004. Biological traits of stream macroinvertebrate community: effects of microhabitat, reach, and basin filters. *J. N. Am. Benthol. Soc.* **23**(3): 449-466.
- McIntire C D. 1973. Periphyton dynamics in laboratory streams: a simulation model and its implications. *Ecological Monographs* **43**: 399-420.
- Merritt R W, Higgins M J, Cummins K W and Vandeneeden B. 1999. The Kissimmee River-Riparian Marsh Ecosystem, Florida. Seasonal differences in invertebrate functional feeding group relationships. In *Invertebrates in Freshwater Wetlands of North America: Ecology and Management*. Edited by Darold P Batzer D P, Rader R B, and Wissinger S A, John Wiley & Sons, Inc.
- Park Y-S, Céréghino R, Compin A and Lek S. 2003. Applications of artificial neural networks for patterning and predicting aquatic insect species richness in running waters. *Ecological Modelling* **160**: 265-280.
- Power M E, Dudley T L, Cooper S D. 1989. Grazing catfish, fishing birds, and attached algae in a Panamanian stream. *Environmental Biology of Fishes* **26**: 285-294.
- Power M E, Sun A, Parker G, Dietrich W E, and Wootton J T. 1995. Hydraulic food-chain models. An approach to the study of food-web dynamics in large rivers. *Bioscience* **45**: 159-167.
- Quinn J M & Hickey C W. 1990. Magnitude of effects of substrate particle size, recent flooding, and catchment development on benthic invertebrates in 88 New Zealand rivers. *New Zealand Journal of Marine and Freshwater Research* **24**: 411-427.

- Reichert P, Borchardt D, Henze M, Rauch W, Shanahan P, Somlyódy L and Vanrolleghem P. 2001. River Water Quality Model no.1 (RWQM1): II. Biochemical process equations. *Water Science and Technology* **43**(5): 11-30.
- Reichert P, Borsuk M, Hostmann M, Schweizer S, Spörri C, Tockner K and Truffer B. 2007. Concepts of decision support for river rehabilitation. *Environmental Modelling and Software* **22**: 188-201.
- Schuwirth N, Kühni M, Schweizer S, Uehlinger U and Reichert P. 2007. A mechanistic model of benthos community dynamics in the River Sihl, Switzerland. *Submitted to Freshwater Biology*.
- Schweizer S, Borsuk M, Jowett I, Reichert P. 2007a. Predicting joint frequency distributions of depth and velocity for instream habitat assessment. *River Research and Applications*, in press.
- Schweizer S, Borsuk M, Reichert P. 2007b. Predicting the hydraulic and morphological consequences of river rehabilitation. *River Research and Applications*, in press.
- Spörri C, Borsuk M, Peters I and Reichert P. 2007. The economic impacts of river rehabilitation: a regional input-output analysis. *Ecological Economics*, in press.
- Uehlinger U. 1991. Spatial and temporal variability of the periphyton biomass in a prealpine river (Necker, Switzerland). *Arch. Hydrobiol.* **123**(2): 219-237.
- Uehlinger U, Bühner H and Reichert P. 1996. Periphyton dynamics in a floodplain prealpine river: evaluation of significant processes by modelling. *Freshwater Biology* **36**: 249-263.
- Vannote R L, Minshall G W, Cummins K W, Sedell J R and Cushing C E. 1980. The river continuum concept. *Can. J. Fish. Aquat. Sci.* **37**: 130-137.
- Yoshimura C, Tockner K, Omura T and Moog O. 2006. Species diversity and functional assessment of macroinvertebrate communities in Austrian rivers. *Limnology* **7** (2): 63-74.

4.9 Appendix

Uncertainty of model parameters and correlation between model parameters ($sd =$ standard error, for abbreviation of model parameters see chapter 4.4.2). The standard deviations of the error term in equation (5) were $1.63 \text{ (gAFDM/m}^2\text{)}^{0.3}$ for periphyton, $0.75 \text{ (gDM/m}^2\text{)}^{0.3}$ for total invertebrates, $0.94 \text{ (gDM/m}^2\text{)}^{0.3}$ for scrapers, $0.81 \text{ (gDM/m}^2\text{)}^{0.3}$ for collector-gatherers, and $0.75 \text{ (gDM/m}^2\text{)}^{0.3}$ for predators.

		Estimate	sd	Coefficient of correlation r							
				$\overline{B_{\max}}$	$\overline{k_B}$	k_{d50}	$\Delta t_{\text{jul}}^{\max}$	α	γ	δ	b
Periphyton Model 1.8	B_{\max}	1500	300	1	0	0	-	-	-	0	-
	k_B	16.5	2.2	0	1	0	-	-	-	0.84	-
	k_{d50}	0.2	0.04	0	0	1	-	-	-	0	-
	$\Delta t_{\text{jul}}^{\max}$	0	-	-	-	-	-	-	-	-	-
	α	0	-	-	-	-	-	-	-	-	-
	γ	0	-	-	-	-	-	-	-	-	-
	δ	3.22	0.11	0	0.84	0	-	-	-	1	-
	b	1	-	-	-	-	-	-	-	-	-
Total invertebrates Model 2.5	B_{\max}	150	30	1	0	0	0	0	-	-	0
	k_B	2.26	0.52	0	1	0	0.55	-0.31	-	-	-0.96
	k_{d50}	0.2	0.04	0	0	1	0	0	-	-	0
	$\Delta t_{\text{jul}}^{\max}$	257.1	6.2	0	0.55	0	1	-0.33	-	-	-0.46
	α	0.79	0.06	0	-0.31	0	-0.33	1	-	-	0.29
	γ	0	-	-	-	-	-	-	-	-	-
	δ	0	-	-	-	-	-	-	-	-	-
	b	0.57	0.06	0	-0.96	0	-0.46	0.29	-	-	1
Scrapers Model 3.5	B_{\max}	25	5	1	0	0	0	0	-	-	0
	k_B	0.84	0.33	0	1	0	0.55	-0.30	-	-	-0.93
	k_{d50}	0.2	0.04	0	0	1	0	0	-	-	0
	$\Delta t_{\text{jul}}^{\max}$	250.5	11.5	0	0.55	0	1	-0.28	-	-	-0.41
	α	0.89	0.13	0	-0.30	0	-0.28	1	-	-	0.26
	γ	0	-	-	-	-	-	-	-	-	-
	δ	0	-	-	-	-	-	-	-	-	-
	b	0.27	0.11	0	-0.93	0	-0.41	0.26	-	-	1
Collector-Gatherers Model 4.5	B_{\max}	100	20	1	0	0	0	0	-	-	0
	k_B	1.01	0.25	0	1	0	0.51	-0.34	-	-	-0.95
	k_{d50}	0.2	0.04	0	0	1	0	0	-	-	0
	$\Delta t_{\text{jul}}^{\max}$	248.6	7.2	0	0.51	0	1	-0.30	-	-	-0.41
	α	0.77	0.07	0	-0.34	0	-0.30	1	-	-	0.32
	γ	0	-	-	-	-	-	-	-	-	-
	δ	0	-	-	-	-	-	-	-	-	-

	b	0.62	0.07	0	-0.95	0	-0.41	0.32	-	-	1
Predators Model 5.5	B_{\max}	30	6	1	0	0	0	0	-	-	0
	k_B	0.28	0.12	0	1	0	0.58	-0.22	-	-	-0.96
	k_{d50}	0.2	0.04	0	0	1	0	0	-	-	0
	$\Delta t_{\text{jul}}^{\max}$	271.8	9.9	0	0.58	0	1	-0.28	-	-	-0.50
	α	0.84	0.08	0	-0.22	0	-0.28	1	-	-	0.22
	γ	0	-	-	-	-	-	-	-	-	-
	δ	0	-	-	-	-	-	-	-	-	-
	b	0.59	0.11	0	-0.96	0	-0.50	0.22	-	-	1

- = model parameter not estimated

5 GENERAL DISCUSSION

A variety of models and data analyses have been reported in the literature to evaluate the primary determinants of river channel pattern, hydraulic and bed characteristics, functional habitat and of the benthic development. However, for river rehabilitation planning, these findings need to be applied simultaneously for predicting the overall outcome of alternative management measures. The hydraulic-morphological model and the benthic model described here are an attempt to combine multiple analyses into a tool that can be used to forecast the features of a river after widening. These two models are part (submodels) of the Integrative River Rehabilitation Model (IRRM), which can be used to support decision-making in river rehabilitation projects.

5.1 The hydraulic-morphological submodel

This submodel consists of four modules predicting:

- channel morphology
- frequency of floods (bed moving spates, floodplain flooding, dike overtopping)
- bivariate velocity-depth distribution
- siltation of the riverbed

To predict the channel morphology after a widening, the approaches from Bledsoe & Watson (2001) (distinguishing between multi- and single-thread rivers), Da Silva (1991) (distinguishing straight, meandering, alternating gravel bars and braided for width constraints) and our own data analysis (calculation of natural width) are combined (Fig 3.2).

In the literature, many bed load formulae are reported. A modified version of Meyer-Peter & Müller (1948) for single-thread rivers and Zarn's method (1997) for multi-thread rivers have been chosen, since these approaches have been developed for Swiss midland gravel bed rivers which are the focus of the IRRM. Although it was attempted to only employ model inputs that are either readily available or easily predictable for modified conditions, estimations of gravel input to a reach may be difficult to obtain. This may be critical, as the success of river rehabilitation is directly affected by the gravel budget within the widened reach. Only if the supply is sufficient will morphological structures such as bars or braids form. Unfortunately, many rivers in Central Europe have lost their natural gravel regime due to upstream gravel retainment or extraction in the catchment

area or measures to stabilize the shoreline and bed. Therefore, detailed hydraulic and gravel transport studies are recommended before initiating construction work.

The frequencies of extreme events (bed moving floods, floodplain flooding, dike overtopping) have a strong influence on aquatic and terrestrial flora and fauna and on society. A simplified geometry can be assumed for such high stages, and for both single- and multi-threaded rivers formulae to estimate water depth exist (Strickler (1923), Zarn (1997)) which can be used to calculate the frequency of floodplain flooding and of dike overtopping. The bed stability can be estimated with the formula of Günther (1971) and related to a critical water depth. This way, also the ecologically important frequency of bed moving floods can be predicted.

The temporal development of river bed siltation can be approximated with the approach from Schälchli (1993, 1995) combined with the frequency of bed moving floods when the river bed is cleared from fine particles.

The results of the joint frequency distribution of velocity and depth (chapter 2) can be predicted for a wide variety of stream reaches using a simple mixture of two end-member distributions (one bivariate normal distribution and one bivariate log-normal distribution) with fixed parameters. This finding suggests that there is some degree of “universality” in the two extreme distributions, at least for the type of gravel bed rivers examined in this study. The skewed shape of the bivariate log-normal distribution leads to a visually negative relationship between the two variables, as anticipated by Stewardson and McMahon (2002). As also expected by Stewardson and McMahon (2002), the relative contribution of each end-member distribution, indicated by the value of the mixing factor s_{mix} , spans the range from 0 to 1, with most river reaches having some contribution of each distributional form.

A higher reach mean Froude number leads in Lamouroux’s (pure) velocity model (1995) and in this joint velocity-depth model to a more symmetric/normal distributional shape. Additionally, the mixture parameter s_{mix} responds to relative roughness consistently in the two approaches: a shift from a symmetric to a skewed shape with increasing relative roughness. This is because a stream bed with larger roughness elements will produce more spatial variation in velocity and depth than one with lower roughness. A third predictor of s_{mix} is the square root of relative survey discharge, $(q/MQ)^{0.5}$ (where q = survey discharge and MQ = mean discharge). The distributional response to this variable is as anticipated by Stewardson and McMahon (2002) - an increasingly centered shape with increasing discharge. This is because for a fixed streambed and channel geometry, increases in discharge will tend to smooth out variations between riffles and pools. Changes in discharge also have an indirect effect, by influencing the stage and therefore

the relative importance of roughness elements. Consequently, with increasing discharge, the influence of roughness elements on flow pattern will decrease and the variability in velocity and depth will be reduced. The explicit representation of the direct and indirect influences of flow on spatial patterns of velocity and depth may make this module useful for assessing the biological effects of variations in discharge.

While these results are qualitatively similar to those of previous studies, the representation of velocity and depth jointly, rather than independently, is a significant advancement. Not only does this lead to a more realistic description of hydraulic conditions, but it should also lead to improved ecological assessments. Both living and non-living elements of streams are clearly influenced by these two variables simultaneously, and methods for analyzing survey data are beginning to reflect this (e.g., Kemp et al. 1999, Jowett 2003). Using “occurrence matrices” to identify the depth and velocity combinations at which various meso-habitats are most likely to be found, Kemp et al. (1999) distinguished some distinct sets of conditions. For example, cobbles, mosses, and submerged fine-leaved macrophytes were most often found in the fastest water at low depths. Silt, submerged broad-leaved macrophytes, and floating leaved macrophytes were found in the slowest water at high depths. Marginal plants were associated with the slowest and shallowest water. These findings could not be addressed by a model that considers velocity and depth independently.

The interactions between velocity and depth in determining habitat quality and preferences are also beginning to be explicitly considered in predictive ecological models (e.g., Schneider 2001). This should be the most comprehensive and appropriate use of these module results and I hope that these findings can stimulate such efforts. However, many other published studies have related the occurrence of stream-dwelling organisms to hydraulic units, such as pools, runs, and riffles (e.g., Logan and Brooker 1983, Pridmore and Roper 1985), and this categorization continues to be employed by some ecological models (Fausch et al. 1988). It is shown in chapter 2 how the joint frequency distributions of velocity and depth are compatible with such approaches. However, it should be kept in mind that classification of pool, run, and riffle habitats may be river-specific and with different threshold definitions. Jowett (1993) found that the velocity:depth ratio was nearly as good a discriminant between the hydraulic units as the Froude number. Allen (1951) also used the Froude number and the velocity:depth ratio, but with lower threshold values than Jowett (1993). In any case, the definition that is deemed most appropriate for a studied reach can be used as the boundaries for integrating the joint density function to yield the relative frequencies of each hydraulic unit.

Other researchers have attempted to capture the interactive effects of velocity and depth on instream fauna by using dimensionless transformations that combine the two variables. The Froude number and boundary Reynold's number are common choices (Orth and Maughan 1983, Quinn and Hickey 1994, Brooks et al. 2005). The predicted

joint distribution can easily be transformed to distributions on these derived quantities or another option is to predict a joint distribution of Fr and Re directly, using a method similar to the one presented here. However, as velocity and depth are the fundamental quantities that are measured in the field and directly experienced by aquatic organisms, I feel that their use as response variables is more convenient and direct. Additionally, I believe that full consideration of the joint distribution is the most informative way forward for modelling and data analysis. Each of the other approaches loses some information content, as is apparent through consideration of the results of Kemp et al. (1999), described above. While the particular habitat containing cobbles, mosses, and submerged fine-leaved macrophytes could be classified as “riffles” and that containing silt, submerged broad-leaved macrophytes, and floating leaved macrophytes could be classified as “pools” (with high and low Froude numbers, respectively), the distinct habitat of marginal plants (slow and shallow) would not be identified by a system only using pools, runs, and riffles. Therefore, we encourage more studies of the type of Kemp et al. (1999) and Jowett (2003), which consider depth, velocity, and their interaction explicitly.

One purpose in undertaking the present study was to provide support for reach-scale river rehabilitation decisions of the type described by Hostmann et al. (2005a). These include conversion of an entire river reach from a channelized form to a natural form by relieving lateral width constraints and/or restoring natural flow and gravel input patterns. In terms of the notation employed here, greater ecological benefits can be expected when the value of s_{mix} is predicted to be relatively high. This is an indication of diverse velocity-depth pairs (see Figure 2.2), and a relatively high proportion of pools and riffles relative to runs, although the exact combination of hydraulic units will also depend on the reach average Froude number (see Figure 2.6). Channelized rivers are predominated by runs (chapter 3.3.3, and Tab.3.3) and can be described with beta-distributed marginals with fixed parameters that are correlated with a rank correlation coefficient according to the method of Iman and Conover (1982) (Figure 3.3). However, a common goal of rehabilitation is to increase diversity by creating pools and riffles. Although the values of s_{mix} and Fr for a re-naturalized river reach (i.e. without width constraints) will be primarily determined by the discharge regime, valley topography, gravel balance and river bed composition (all of which may not be affected by most rehabilitation measures), river managers can influence these parameters through appropriate gravel entrainment, discharge regulation strategies and obviously through the proper choice of width constraints.

Based on the nature of the data used to develop this model, the hydraulic-morphological submodel should be appropriate for application to gravel bed rivers with a relatively natural flow regime and mean discharge between 1 and 60 m³/s and slope less than 2%. Application to river sections with artificial constructions, such as weirs or groynes,

should be avoided because these structures will interfere with the development of natural morphological and hydraulic characteristics. However, river rehabilitation often targets the removal of such artificial constructions, thus allowing the use of the model to forecast the rehabilitated state. Because the joint velocity-depth module was derived for low to intermediate flow conditions (survey flows between 5% and 100% of mean discharge), this part of the submodel should not be applied to flows outside of this range. However, for the purposes of habitat assessment, these low flows are usually of most interest, because they define critical conditions. Therefore, this restriction should not be a practical limitation.

Despite the limitations mentioned above, the case study at the Thur River, Switzerland, shows that the hydraulic-morphological submodel yields useful information for rehabilitation planning. Since the gravel supply in a 200 m widening exceeds the estimated transport capacity, the channel morphology can be expected to change from the present straight channelized form to a river with alternating gravel bars with a probability of 56% and to a river with multiple braids with a probability of 28%. In either case, the new morphology would have a greatly increased variability of velocity and depth and contain a significant fraction of pools and riffles. Further widening would not significantly augment the likelihood of forming braids, but would probably lead to a greater number of braids should a multi-thread form develop. A widening would likely increase the average riverbed siltation (mean percentage of fines up from 1% to 8%) but would also result in a patchier structure, with zones of different degrees of siltation. The net result with respect to siltation on the aquatic ecosystem is equivocal.

Some of the abiotic endpoints predicted by the hydraulic-morphological submodel (e.g. channel morphology, depth and velocity variability) are of direct interest to river stakeholders because they determine the recreational potential of the river system (Hostmann et al., 2005b). Moreover, they are of substantial indirect interest because of their influence on the biological status. For example, morphological form, velocity-depth patterns, distribution of habitat units (riffles and pools), frequency of bed moving floods and degree of riverbed siltation are all critical determinants of fish and benthic populations. Similarly, morphology and floodplain flooding frequency are fundamentally important controls on bankline vegetation and terrestrial fauna.

To formalize the relations between abiotic and biotic features, the hydraulic-morphological submodel results can be combined with habitat preference functions to assess the suitability of conditions after rehabilitation for endangered or otherwise desirable species. The results can also be used as inputs for other types of ecological models, such as population or individual-based models, which predict biomass, abundance and/or functional groups of fish, macroinvertebrates, aquatic plants, bankline

vegetation or fauna (e.g. Borsuk et al., 2006, Kemp et al, 1999, Lamouroux & Jowett, 2005). The research group SIAM from Eawag is currently in the process of developing such links within the framework of probability networks to complete the IRRM (Reichert et al., 2006).

5.2 The benthic submodel

The benthic regression models presented in chapter 4 differ in accuracy (R^2), precision and in the number of data used to derive the models. Generally, due to limitations in the sampling programs, the algae models are based on data collected from eight sites located in three rivers ($n=286$) while the invertebrate models have been developed by applying data from solely two sites situated at one river (Sihl River) ($n=86$). With an increased number of data points used for regression computations, the R^2 can be expected to decrease since the model's deviation from the data points can be expected to increase more rapidly than the variance of the data points itself. However, models based on more data and from varying sources (e.g. different river reaches), should be more robust and widely applicable. This applies in particular for ecological models. Thus, the periphyton models presented herein can be regarded as more broadly supported compared to the invertebrate models. Indeed, the models predicting total invertebrate biomass perform better than the periphyton model, while the models predicting the biomass of each functional feeding group perform similar or worse than the algal model. For both primary (periphyton) and secondary producers (total invertebrates) good relationships could be found, with R^2 exceeding 0.6 for algae and 0.7 for total invertebrate biomass (Table 4.3).

The results of the periphyton model fit the data surprisingly well (see Figure 4.2). Only two parameters were fitted for a joint calibration to all eight data sets. This strongly supports the chosen model structure. On the other hand, four parameters had to be fitted for each of the four models of total invertebrates, scrapers, collector-gatherers, and predators at only two sites at the same river (see Figure 4.3). This leads to a much weaker confidence in the predictive capabilities of these models. The poorer performance of the scraper model as compared to the other models is reflected by wider 90% prediction uncertainty bands that extend nearly down to zero over the complete simulation period.

The quality of fit quantified by R^2 values was only slightly higher for the best non-linear regression models as compared the best linear regression models. This shows that we cannot considerably improve the quality of the fit with the nonlinear dependence formulation. The reason for formulating nonlinear models was to avoid unreasonable

extrapolation behaviour of the linear models. Extrapolating the linear models can lead to negative or arbitrarily large predictions. Both of these behaviours are excluded by our formulation of the nonlinear models.

The low variation in grain size across sites precluded estimation of the model parameter k_{d50} characterizing decrease of biomass densities with decreasing grain size. Therefore, this parameter was estimated from the literature to be 0.2 m (Biggs & Price 1987, Quinn & Hickey 1990). Additionally, the maximum biomass density achieved under non-limiting conditions for long times after a flood, $\overline{B_{\max}}$, was difficult to fit, since longer periods without flood disturbances did not occur during the sampling period with the exception of the Garonne river. Therefore, this parameter also had to be chosen based on the literature (Yoshimura et al., 2006).

The model structure selection process based on the remaining parameters describing the increase in biomass density after a flood, seasonal variation, and dependence on flow velocity and water depth led to very different results for periphyton than for invertebrates. For periphyton it led to the exclusion of a significant seasonal variation, a linear initial increase of biomass with time after a flood, and a significant dependence on flow velocity. On the other hand, seasonality is a dominant explaining variable for invertebrate biomass density and there seems to be a strong nonlinearity of increase in time after a flood.

The absence of a strong seasonal variation of periphyton density seems to be a surprising result, as the seasonal component in our simple model mainly represents the effect of light and temperature on algal biomass. However, this finding is in agreement with earlier results of a mechanistic model (Uehlinger et al., 1996). It seems that adaptation of chlorophyll content and species composition of the benthic periphyton biofilm can compensate for most of the light and temperature dependence observed for individual species. The dependence on flow velocity may still contain some confounding with water depth and it would be very interesting to separate those two effects. However, more data from sites with considerable differences in flow velocity and water depth would be required to do this.

Due to their immobility, periphyton are more susceptible to floods compared to invertebrates which can move to more stable refuges (e.g. river bed interstitial, side braids, low-velocity areas around stable boulders) during high stage (Quinn & Hickey 1990). The regression analysis indicates that for periphyton, the best predictor is “time since the last bed-moving flood” (Δt_{flood}), while invertebrates (and most of their functional feeding groups) are more strongly controlled by seasonal effects. This is reflected in the nonlinear invertebrate models by the value of the parameter b smaller than unity that describes a faster recovery from the flood-induced depletion of invertebrates as compared to the linear recovery of periphyton (compare Figs. 4.2 and 4.3). In contrast to periphyton, invertebrates can have a more complicated life cycle

(larvae, imago, adults) with possibly varying food and habitat preferences. This makes it more difficult to get good predictions for invertebrates with a simple non-linear regression model. This is also a significant problem for more complicated dynamic functional group models (Schuwirth et al., 2007). In our simple nonlinear regression approach, the life stages of invertebrates are aggregated into the seasonal effect described by the model.

The relationships found with the nonlinear regression approach can stimulate formulation of detailed mechanistic models of the benthos community such as those of Boulêtreau et al (2006) and Schuwirth et al (2007). The dominance of time since the last flood as an explaining variable for periphyton suggests the necessity of a careful formulation of flood-induced detachment processes and subsequent recovery by growth. Unless light, low temperatures and nutrients are significantly limiting (which is not the case for the sites studied in this chapter), these factors seem to be of minor importance for a simple periphyton model for Swiss midland rivers. Nevertheless, these factors must be kept in mind when designing a model to be applied to different climatic regimes and with smaller nutrient loads or higher turbidity. For the invertebrate models, at least seasonally varying or temperature dependent growth rates should be formulated, and the model should contain a higher relative colonization rate after floods than the periphyton model.

The ratio of primary to secondary producer biomass estimated by the model can be compared to values predicted by theoretical concepts (e.g., Vannote et al 1980) and used for the evaluation of an expected ecosystem state. Moreover, the estimated biomass of the functional feeding groups can illuminate dominant pathways of nutrient cycling in a particular river reach (Yoshimura et al 2006, Merritt et al 1999, Klemm et al 2003, Böhmer et al 2000). For example, to assess habitat stability, Yoshimura et al (2006) propose to calculate the ratio of the more flood susceptible scrapers and collector-filterers to shredders and collector-gatherers. They recommend using abundances, but similar results can be expected when biomasses are used instead. Functional feeding groups emphasize the multiple linkages that exist between food resources and the ability of invertebrates to successfully acquire these resources (Cummins et al. 1981, Merritt et al. 1999, Barbour et al. 2001). Thus, function-based metrics are more directly related to ecosystem integrity than solely taxonomic composition (Yoshimura et al. 2006).

Our proposed models have the potential to support decision-making in the context of river rehabilitation, since periphyton and invertebrates play a key role in river ecology by serving as food for fish and controlling decomposition. Predictions of the response of these organisms to management actions can help to guide the selection of the most appropriate stream reaches and site-specific rehabilitation measures. While grain size and seasonal effects are usually not changed by rehabilitation measures, the hydraulic conditions (velocity, depth) usually are. In the previous chapters 2 and 3 (and Schweizer et al 2007a, 2007b) we developed a relatively simple hydraulic-morphological model to

predict the hydraulic conditions after measures such as river widening. The major hydraulic responses of widening are an increased wetted perimeter, a lower mean water depth and flow velocity, and a higher spatial variability of depth and velocity. The simple benthic community models discussed in this chapter would predict a higher periphyton biomass density due to the decreasing flow velocity. In addition, due to the increased wetted perimeter, there will be more habitat area available per unit river length for both periphyton and invertebrates.

Since the derivation of the models is based on only a few river sites, the application of the models to other river sections can be critical, not least due to the high variability of benthic organisms. Thus, application of the models should be limited to rivers of similar size and character (Table 4.1 and 4.2) in the temperate climate zone. River reaches affected severely by hydro-peaking or with artificial bed constructions (e.g. channelized river reaches without a natural interstitial) should be excluded from model application. In addition, for rivers with nutrient concentrations below critical thresholds for growth or with completely shaded or siltated river beds, the models presented here are not suitable.

While grain size and seasonal effects are usually independent from rehabilitation measures, the hydraulic conditions (velocity, depth, Froude Number) may change after a project has been conducted. Many rehabilitation measures aim to increase the hydraulic variability to support a higher habitat and species diversity. To approximate the required inputs to the benthic models (hydraulic conditions) for more rigorous measures (e.g. widening of a river bed) the hydraulic-morphological sub-model of the IRRM can be used. In the other direction, the results of this benthic submodel can be applied as model inputs for other ecological submodels. For example, predicted total invertebrate biomass can serve as an input to the fish model (e.g., Borsuk et al 2005).

5.3 The IRRM

The integrative river rehabilitation model IRRM can be combined with stakeholder value assessments of model outcomes to provide comprehensive decision support for managers (Reichert et al., 2006). Such an analysis can improve a project's financial and public backing, as well as help guide selection of the most appropriate stream reaches and reach-specific rehabilitation measures. In the long term, repeated application of such a transparent and rational process should benefit both society and the environment.

In the relatively new field of river rehabilitation many studies focusing on a particular system (e.g., hydraulics, morphology, riparian and aquatic fauna and flora) have been conducted but an approach to link these different systems to an overall picture has been lacking. The IRRM is the first attempt to fill this gap with the aim to give new insights how the different systems function and interact, and where further studies are required for an improved understanding. Additionally, the IRRM can be used for a particular river rehabilitation planning and can support decision-making in this vein. The development of the IRRM has involved interdisciplinary communication among experts and has been accomplished iteratively answering the questions:

- What are the meaningful model outputs?
- What are the key factors necessary to predict these outputs and what are the relevant cause-effect relations?
- How change these key factors with a rehabilitation measure (e.g., for a changed channel geometry)?
- How do these different factors interact?
- What are the appropriate spatial and temporal scales?
- And how can the uncertainty in model inputs and structure be determined and propagated through the model?

This time consuming process together with the complex nature of river ecosystems are the principal causes of the prolonged development of the IRRM.

However, the development of a comprehensive hydraulic-morphological model considering all relevant factors controlling the different aquatic and terrestrial communities is an important achievement in river rehabilitation. To improve the utility of the IRRM, I recommend to conduct further studies, in particular to measure repeatedly the main abiotic (morphology, bivariate velocity-depth distribution, grain size, siltation, frequency of floodplain flooding and bed moving spates, fine and coarse organic material, ...) and biotic (biomass of periphyton and of the functional feeding groups of invertebrates, fish abundances and diversity, and of the terrestrial ecosystems) conditions before and after a rehabilitation measure.

5.4 Future Research Questions

The use of the probability network structure makes it relatively easy to add further components. Submodels of water temperature variation, width and grain size variability, of relative bankline length and of the terrestrial vegetation could add utility to the model by allowing prediction of additional important attributes. Representation of the influence of rehabilitation projects on water quality could also improve the link between abiotic and biotic features.

An additional investigation to assess the joint velocity-depth distribution for braided rivers would improve the model accuracy for this type of channel morphology.

Further biologic studies on more river sites which include sampling of periphyton, invertebrates and their influence factors over a longer period (at least one year) could improve ecological understanding and increase the robustness and generality of the benthic submodel.

Finally, it should be stated that a model can never represent all processes going on in the very complex nature. Therefore, a model has to be adjusted, calibrated and eventually restructured iteratively. Since, in the near future, many projects to rehabilitate river reaches in Central Europe will be conducted, there is an opportunity to accomplish comprehensive studies (before and after a measure) to learn more about the multifaceted field of river ecology and rehabilitation, and use these results to calibrate the IRRM. The additional costs of such studies should not be regarded as a misuse of public money since the new insights and findings will improve subsequent measures and can help to reduce projects' costs in the future, in particular to select the optimum width for a widening.

5.5 References

- Allen K R. 1951. The Horokiwi Stream. *Fisheries bulletin* **10**, New Zealand Marine Department, Wellington, 231 pp.
- Barbour M T, Geristen J, Snyder B D, Stribling J B. 2001. Rapid bioassessment protocols for use in streams and wadeable rivers: periphyton, benthic macroinvertebrates, and fish. EPA, Washington DC, 1-339.
- Biggs B J F & Price G M. 1987. A survey of filamentous algal proliferations in New Zealand rivers. *New Zealand Journal of Marine and Freshwater Research* **21**: 175-181.
- Bledsoe B P and Watson C C. 2001. Logistic analysis of channel pattern thresholds: meandering, braiding, and incising. *Geomorphology* **38**: 281-300.
- Böhmer J, Rawer-Jost C and Kappus B. 2000. Ökologische Fließgewässerbewertung. Biologische Grundlagen und Verfahren - Schwerpunkt Makrozoobenthos. In: Handbuch Angewandte Limnologie.
- Borsuk M E, Reichert P, Peter A, Schager E, Burkhardt-Holm P. 2005. Assessing the decline of brown trout (*Salmo trutta*) in Swiss rivers using a Bayesian probability network. *Ecological Modelling*, In press.
- Borsuk M E, Reichert P, Peter A, Schager E, Burkhardt-Holm P. 2006. Assessing the decline of brown trout (*Salmo trutta*) in Swiss rivers using a Bayesian probability network. *Ecological Modelling* **192**: 224-244.
- Boulêtreau S, Garabétian F, Sauvage S and Sanchez-Pérez J-M. 2006. Assessing the importance of a self-generated detachment process in river biofilm models. *Freshwater Biology* **51(5)**: 901-912.
- Brooks A J, Haeusler T, Reinfelds I, and Williams S. 2005. Hydraulic microhabitats and the distribution of macroinvertebrate assemblages in riffles. *Freshwater Biology* **50**: 331-344.
- Cummins K W, Klug M J, Ward G M, Spengler G L, Speaker R W, Ovink R W, Mahan D C and Petersen R C. 1981. Trends in particulate organic matter fluxes, community processes and macroinvertebrate functional feeding groups along a Great Lakes Drainage Basin river continuum. *Verh. Internat. Verein. Limnol.* **21**: 841-849.
- da Silva A M A F. 1991. *Alternate Bars and Related Alluvial Processes*, Master of Science Thesis, Queen's University, Kingston, Ontario, Canada.
- Fausch K D, Hawkes C L, and Parsons M G. 1988. Models that predict standing crop of stream fish from habitat variables, 1950-85. *Gen. Tech. Rep. PNW-GTR-213*. Portland, OR, U.S. Department of Agriculture, Forest Service, Pacific Northwest Research Station. 52 pp.

- Günther A. 1971. Die kritische mittlere Sohlenschubspannung bei Geschiebemischung unter Berücksichtigung der Deckschichtbildung und der turbulenzbedingten Sohlenschubspannungsschwankung (The critical mean bottom shear stress for varying bed materials regarding the development of armoured layers and fluctuations in the bottom shear stress.. Mitteilung Nr.3 der Versuchsanstalt für Wasserbau, Hydrologie und Glaziologie, ETH Zürich.
- Hostmann M, Borsuk M, Reichert P, Truffer B. 2005a. Stakeholder values in decision support for river rehabilitation. *Large Rivers* **15**(1-4) *Arch. Hydrobiol. Suppl.* **155**/1-4, 491-505.
- Hostmann M, Bernauer, T, Mosler H-J, Reichert P, Truffer B. 2005b. Multi-attribute value theory as a framework for conflict resolution in river rehabilitation. *Journal of Multi-Criteria Decision Analysis (JMCA)* **13**: 91-102.
- Iman R. L, Conover W. J, 1982. A distribution-free approach to inducing rank correlation among input variables. *Commun. Statist.-Simula. Computa.* **11**: 311-334.
- Jowett I G. 1993. A method for objectively identifying pool, run, and riffle habitats from physical measurements. *New Zealand Journal of Marine and Freshwater Research* **27**: 241-248.
- Jowett I G. 2003. Hydraulic constraints on habitat suitability for benthic invertebrates in gravel-bed rivers. *River Research and Applications* **19**: 495-507.
- Kemp J L, Harper D M, Crosa G A. 1999. Use of 'functional habitats' to link ecology with morphology and hydrology in river rehabilitation. *Aquatic Conservation: Marine and Freshwater Ecosystems* **9**: 159-178.
- Klemm D J, Blocksom K A, Fulk F A, Herlihy A T, Hughes R M, Kaufmann P R, Peck D V, Stoddard J L, Thoeny W T and Griffith M B. 2003. Development and evaluation of a macroinvertebrate biotic integrity index (MBII) for regionally assessing Mid-Atlantic Highlands streams. *Environmental Management* **31**: 656-669.
- Lamouroux N, Souchon Y, and Herouin E. 1995. Predicting velocity frequency distributions in stream reaches. *Water Resources Research* **31**: 2367-2375.
- Lamouroux N & Jowett I. 2005. Generalized instream habitat models. *Canadian Journal of Fish and Aquatic Science* **61**(1): 7-14.
- Logan P and Brooker M P. 1983. The macroinvertebrate faunas of riffles and pools. *Water Research* **17**: 262-270.
- Merritt R W, Higgins M J, Cummins K W and Vandeneeden B. 1999. The Kissimmee River-Riparian Marsh Ecosystem, Florida. Seasonal differences in invertebrate functional feeding group relationships. In *Invertebrates in Freshwater Wetlands of North America: Ecology and Management*. Edited by Darold P Batzer D P, Rader R B, and Wissinger S A, John Wiley & Sons, Inc.

- Meyer-Peter E and Müller R. 1948. Formulas for bedload transport. Proc. IAHR 3rd Congress, Stockholm.
- Orth D J and Maughan O E. 1983. Microhabitat preferences of benthic fauna in a woodland stream. *Hydrobiologia* **106**: 157-168.
- Pridmore R D and Roper D S. 1985. Comparison of the macroinvertebrate faunas of runs and riffles in three New Zealand streams. *New Zealand Journal of Marine and Freshwater Research* **19**: 283-291.
- Quinn J M & Hickey C W. 1990. Magnitude of effects of substrate particle size, recent flooding, and catchment development on benthic invertebrates in 88 New Zealand rivers. *New Zealand Journal of Marine and Freshwater Research* **24**: 411-427.
- Quinn J M and Hickey C W. 1994. Hydraulic parameters and benthic invertebrate distributions in two gravel-bed New Zealand rivers. *Freshwater Biology* **32**: 489-500.
- Reichert P, Borsuk M, Hostmann M, Schweizer S, Spörri C, Tockner K and Truffer B. 2006. Concepts of decision support for river rehabilitation. *Environmental Modelling and Software*. In press.
- Schälchli U. 1993. Die Kolmation von Fließgewässersohlen: Prozesse und Berechnungsgrundlagen (Siltation of riverbeds: Processes and methods for estimation.) Mitteilungen der Versuchsanstalt für Wasserbau, Hydrologie und Glaziologie der ETH Zürich Nr. 124, 273 pp.
- Schälchli U. 1995. Basic equations for siltation of riverbeds. *Journal of Hydraulic Engineering* **121**(3): 274-287.
- Schneider M. 2001. *Habitat- und Abflussmodellierung für Fließgewässer mit unscharfen Berechnungsansätzen. Weiterentwicklung des Simulationsmodells CASiMiR*. Ph.D., 146 pp., Institut für Wasserbau, Universität Stuttgart, Mitteilungen 106.
- Schuwirth N, Kühni M, Schweizer S, Uehlinger U and Reichert P. 2007. A mechanistic model of benthos community dynamics in the River Sihl, Switzerland. *Submitted to Freshwater Biology*.
- Stewardson M J and McMahon T A. 2002. A stochastic model of hydraulic variations within stream channels. *Water Resources Research* **38**: 1-14.
- Strickler A. 1923. Beiträge zur Frage der Geschwindigkeitsformel und der Rauigkeitszahlen für Ströme, Kanäle und geschlossene Leitungen (Contributions to the formula of flow velocity and to the estimation of flow resistance for rivers, channels and closed conduits). Mitteilung Nr. 16 des Amtes für Wasserwirtschaft; Eidg. Departement des Inneren, Bern.
- Uehlinger U, Bühner H and Reichert P. 1996. Periphyton dynamics in a floodplain prealpine river: evaluation of significant processes by modelling. *Freshwater Biology* **36**: 249-263.

- Vannote R L, Minshall G W, Cummins K W, Sedell J R and Cushing C E. 1980. The river continuum concept. *Can. J. Fish. Aquat. Sci.* **37**: 130-137.
- Yoshimura C, Tockner K, Omura T and Moog O. 2006. Species diversity and functional assessment of macroinvertebrates in Austrian rivers. *Limnology* **7** (in print).
- Zarn B. 1997. Einfluss der Flussbettbreite auf die Wechselwirkung zwischen Abfluss, Morphologie und Geschiebetransportkapazität (Influence of river width on interactions between discharge, morphology and transport capacity). *Mitteilungen der Versuchsanstalt für Wasserbau, Hydrologie und Glaziologie*, 154, Eidgenössische Technische Hochschule (ETH), Zürich, Switzerland, 209 pp.

Acknowledgements

First, I want to thank my supervisors Peter Reichert and Mark Borsuk for their excellent support in the last 4 years. I am thankful for the many (and partly “long-term”) interesting discussions and for their exceptional support in statistics, mathematics, programming and modelling. Finally, I really appreciate their fairness and kindness in the daily work.

This thesis was only possible thanks to the financial support of the Rhone-Thur Project. Additionally, I could benefit from many interesting discussions with many project members. In particular I want to thank Peter Baumann, Armin Peter, Felix Kienast, Klement Tockner, and Christian Glenz.

I would like to mention all my colleagues from Eawag who helped to create an enjoyable working atmosphere with interesting discussions, in particular all colleagues from the research group siam. Moreover, I want to thank Martin Kühni (who introduced me into the aquatic (magic) world of invertebrates and algae), Christian Spörri and Lorenzo Tomassini (who were always very helpful and supportive for complex model implementations and mathematical questions), Nele Schuwirth (for the daily support on the Benthos model in the office), Markus Hostmann (for his general and daily support in the office) and Olaf Cirpka (who provided valuable information and data on ground water related topics).

The development of the hydraulic-morphological sub-model is based on many findings and discussions with members of the VAW (Versuchsanstalt für Wasserbau, Hydrologie und Glaziologie der ETH Zürich). Particular gratitude is extended to Hans-Erwin Minor, Christian Marty and Patricia Requena Mendez.

Additionally, I am very grateful for the very instructive discussions with Ulrich Schälchli on river bed siltation, hydraulics and gravel transport within a catchment.

Also, I am very thankful to Nicolas Lamouroux, Mike Stewardson and Ian Jowett for a couple of interesting and productive discussions about river hydraulics. In particular I want to show gratitude to Ian Jowett who allowed us to apply his huge dataset on velocity and depth which was the basis for the development of the bivariate velocity-depth model.

For valuable datasets on periphyton and very helpful discussions I want to thank Urs Uehlinger very much. Chihiro Yoshimura, Nicolas Lamouroux, Stéphanie Boulêtreau, Peter Baumann, Mike Scarsbrook, Fredy Elber, Joachim Hürlimann, Klemens Niederberger, Christopher Robinson, David Arscott and Vicenç Acuña Salazar provided

further comprehensive datasets on periphyton and invertebrates. Many thanks for their additional work.

Further, I want to thank Peter Baumann for fruitful discussions about the overall structure of the Benthos model. I could learn a lot in all discussions with him.

For careful checking the text and formats of my dissertation I am very thankful to Elisabeth Böttcher.

Last but not least, I am very grateful to my family and my friends for their great (and often underestimated) support for never stopping to motivate me.